bushfire CRC

REPORT NO. A.11.10

IMPROVED METHODS FOR ASSESSMENT AND PREDICTION OF GRASSLAND CURING

SATELLITE BASED CURING METHODS AND MAPPING

FINAL REPORT: PROJECT A1.4

Glenn J. Newnham[1,5], Ian F. Grant[2,5], Danielle N. Martin[3,5], Stuart A.J Anderson[4*,5]

1. CSIRO Ecosystem Sciences and CSIRO Climate Adaptation Flagship, Private Bag 10, Clayton South VIC 3169, Australia.

2. Bureau of Meteorology, GPO Box 1289, Melbourne VIC 3001, Australia.

3. School of Mathematical and Geospatial Sciences, RMIT University, Melbourne, Australia. 4. Scion, PO Box 29237, Christchurch 8540, New Zealand.

5. Bushfire Cooperative Research Centre, 340 Albert Street, Melbourne VIC 3002, Australia

* Present address: Ministry of Agriculture and Forestry, PO Box 1340, Rotorua 3040, New Zealand

© BUSHFIRE CRC LTD 2010

© Bushfire Cooperative Research Centre 2010.

No part of this publication must be reproduced, stored in a retrieval system or transmitted in any form without prior written permission from the copyright owner, except under the conditions permitted under the Australian Copyright Act 1968 and subsequent amendments.

November 2010

bushfire CRC

REPORT NO. A.11.10

IMPROVED METHODS FOR ASSESSMENT AND PREDICTION OF GRASSLAND CURING

SATELLITE BASED CURING METHODS AND MAPPING

FINAL REPORT: PROJECT A1.4

Glenn J. Newnham[1,5], Ian F. Grant[2,5], Danielle N. Martin[3,5], Stuart A.J Anderson[4*,5]

1. CSIRO Ecosystem Sciences and CSIRO Climate Adaptation Flagship, Private Bag 10, Clayton South VIC 3169, Australia.

2. Bureau of Meteorology, GPO Box 1289, Melbourne VIC 3001, Australia.

3. School of Mathematical and Geospatial Sciences, RMIT University, Melbourne, Australia. 4. Scion, PO Box 29237, Christchurch 8540, New Zealand.

5. Bushfire Cooperative Research Centre, 340 Albert Street, Melbourne VIC 3002, Australia

* Present address: Ministry of Agriculture and Forestry, PO Box 1340, Rotorua 3040, New Zealand

© BUSHFIRE CRC LTD 2010

CONTENTS

ACKNOWLEDGEMENTS	**3**
EXECUTIVE SUMMARY	**4**
1. INTRODUCTION	**5**
2. BACKGROUND	**7**
2.1 Summary of relevant satellite sensors	7
2.2 Satellite mapping of grass curing	8
2.3 The existing satellite curing product	10
3. PROJECT METHODOLOGY	**11**
3.1 Field data collection methods	11
3.2 Satellite data characteristics	13
4 NDVI TIME SERIES METHODS	**18**
4.1 NDVI characteristics for project sites	20
4.2 Static algorithms	21
4.3 Time series normalisation	23
4.4 NDVI time series summary	30
5. SPECTRAL METHODS	**32**
5.1 Review of spectral approaches	32
5.2 Field spectrometry and curing	33
5.3 Site homogeneity at the MODIS scale	34
5.4 Relationship between multispectral MODIS data and curing	37
5.5 Final Australian curing models	45
6. NEW ZEALAND CURING DATA ANALYSIS	**47**
6.1 New Zealand field collection sites	47
6.2 Application of Australian models	49
6.3 Calculation of New Zealand coefficients	52
6.4 New Zealand model summary	55
7. PILOT TRIAL DESIGN	**57**
7.1 User consultation	57
7.2 Base data	58
7.3 Processing steps	59
7.4 Curing model summary	60
8. PILOT TRIAL RESULTS	**61**
8.1 Southern Australian pilot trial	61
8.2 New Zealand pilot trial	66
8.3 General summary of feedback	68
9. CONCLUSIONS	**69**
9.1 Legacy dataset	70
9.2 Comparison of satellite models	70
9.3 Operational curing map system	72
9.4 Future development	74
9.5 Impact on applications	75
9.6 Summary of Recommendations	76
REFERENCES	**77**
APPENDIX A - FORMULAE FOR VEGETATION INDICES	**80**
APPENDIX B - FIELD ASSESSMENT METHODOLOGY	**82**

ACKNOWLEDGEMENTS

This project was conducted as part of Bushfire Cooperative Research Centre (CRC) Project A1.4, "Improved methods for assessment and prediction of grassland curing". The authors would like to thank the CRC for the financial support of this project and the guidance, encouragement and support we received from the centre staff. We would also like to thank Jim Gould, as manager of Bushfire CRC Program A, who provided strong guidance and organisational support through much of the project.

The project also received substantial in-kind and direct financial support from the authors' home institutions; the Commonwealth Scientific and Industrial Research Organisation (CSIRO) through the Climate Adaptation Flagship and the Division of Ecosystem Sciences, the Bureau of Meteorology, Scion New Zealand and RMIT University through the Department of Mathematics and Geospatial Sciences. Danielle Martin's Ph.D. thesis, which forms part of the work reported here was co-supervised by Professor Simon Jones whose guidance we have all greatly appreciated. We also thank Dr. Elizabeth Botha, who played a significant role in the early phases of this project, including the development of field sampling methods and coordination of field sampling activities which have underpinned much of the work reported here.

The authors would also like to recognise the work of Mr Matt Paget and Dr Edward King from CSIRO Marine and Atmospheric Research in preparing the MODIS data used in the study. Considerable time and effort was invested in the development of a new and dedicated parallel system that produced New Zealand MODIS mosaics specifically for this project. Their contribution is ongoing with provision of data to the existing pilot curing map system.

This project would not have been possible without the support of the many Australasian Fire and Emergency Service Authorities Council (AFAC) member organisations and their representatives on the Rural Land Managers Group (RLMG). The RLMG received regular updates on the project through Queensland Fire and Rescue Service Assistant Commissioner Steve Rothwell. We thank him specifically and the broader RLMG for supporting the project through the provision of resources which allowed feedback throughout the project, but critically during the duration of the curing map pilot trials.

The project received particularly strong and sustained guidance from two members of the fire research community: Lachie McCaw from the Western Australian Department of Environment and Conservation (DEC) and Mark Garvey from the Victorian Country Fire Authority (CFA) for which we are very grateful. We also thank Grant Pearce from Scion for the substantial contribution he made through his review of this report. More broadly the authors would like to extend their thanks to the many other staff and volunteers from the research organisations and state-based fire agencies across Australia and New Zealand who helped to guide the project and to build the database of field measurements which allowed this research to be carried out.

EXECUTIVE SUMMARY

The degree of grassland curing (the proportion of cured and/or dead material in a grassland fuel complex) has a significant effect on the ease of ignition, rate of spread and difficulty of suppression of grassfires. There is a critical need for accurate curing information as an input to Australian and New Zealand fire behaviour models and fire danger rating systems. Curing is currently assessed by networks of agency personnel using visual estimates which are spatially sparse, subjective and of limited accuracy. Satellite based curing maps have been produced for south-eastern Australia and Western Australia for several years, but these are based on research restricted to Victorian grasslands, in which curing was estimated visually or indirectly. The component of Project A1.4 reported here has developed satellite-based approaches to the mapping of curing that can provide timely, spatially explicit, objective curing maps covering all of Australia and New Zealand.

The research was based on an extensive dataset of objective curing measurements collected over up to four seasons at 39 sites across Australia and 16 sites in New Zealand, with considerable support from fire agency personnel. The research focused on estimating curing with data from the recent MODIS satellite instrument, as a prototype of future satellite systems that will replace the AVHRR instrument on which current satellite curing maps are based. The project investigated multispectral and temporal approaches to minimising the influence of variations in the relative proportions of grass, evergreen vegetation and soil. Both approaches showed a modest performance benefit in curing estimation over the field dataset. However, the advantages of these methods are expected to be more apparent in regions with more mixed vegetation cover proportions than the project field sites.

The performance of four candidate methods to map curing over the landscape was evaluated through agency feedback during a pilot trail conducted in southern Australia and New Zealand over the 2009/2010 curing season. On the basis of results at the project field sites and agency feedback, methods to map curing using MODIS satellite data are recommended for Australia and New Zealand. Compared to visual estimates, these satellite methods showed greater accuracy at the project field sites, and provide a basis for efficient, objective and spatially continuous curing maps.

The project has surveyed end users on their requirements of an operational system in terms of map format, spatial resolution, frequency, timeliness and delivery mechanism. Given the urgent need for objective and spatially continuous curing information, it is recommended that a system to produce and distribute MODIS curing maps be set up within an agency experienced in the distribution of national scale satellite products. This will enable a more extensive evaluation by end users of their utility in an operational setting in upcoming fire seasons and allow any shortfalls not exposed by the field dataset to be addressed. The potential of the other methods identified by the project to provide alternative curing estimates should be borne in mind during this wider evaluation, particularly in semi-arid or wooded regions where only limited qualitative validation has been available.

1. INTRODUCTION

Grassland curing refers to the dying or senescence of plant material caused by seasonal weather patterns, species-specific phenological cycles and plant succession. Curing has a significant impact on fire behaviour in grasslands, particularly the probability of ignition and the subsequent rate of spread (Cheney and Sullivan, 2008; Luke and McArthur, 1978; McArthur, 1966). The degree of curing represents the proportion of dead material in a grassland fuel complex, expressed as a percentage (Cheney and Sullivan, 2008). Australian and New Zealand fire management agencies rely on estimates of the degree of curing as an input to their fire danger rating systems (Alexander, 2008; Anderson, 2005; Cheney and Sullivan, 2008). These systems underpin a range of fire management decisions and strategies, including fire prevention and public protection measures, suppression strategies and readiness levels, and planning for prescribed burning operations. These decisions can have significant economic and social impacts, and need to be based on the most accurate and scientifically sound curing data available.

The timing of the onset of curing, the degree of curing reached in any given year and the duration of high curing levels varies according to seasonal weather conditions. Periodic rainfall that occurs during the curing process can result in new grass growth from seed germination, lowering the overall degree of curing across a grassland area. Annual grasses lose their ability to draw moisture from the soil as curing progresses and once curing reaches 60%, the curing process is irreversible and will not be delayed by rain. The curing process in perennial grasses is more variable, since seed production is not essential and growth cycles are highly dependant on rainfall and soil moisture (Cheney and Sullivan, 2008). Unlike annual grasses, not all perennial grasses die during a season, and some green material is usually present unless extended drought conditions prevail (Luke and McArthur, 1978). The timing and degree of curing can be significantly accelerated by even one day of strong, hot, dry winds (Cheney and Sullivan, 2008), and can increase by as much as 20% in two weeks (pers. comm. R. McRae, ACT Emergency Services Agency).

The landscape does not necessarily cure uniformly, with drier ridges tending to cure more quickly than moister low areas and creek lines. The vertical structure of curing throughout a grass canopy can take a variety of forms, depending on the weather and land management history. In the absence of frequent grazing, a dead sward from the previous season can underlie the current season's growth in the form of a litter layer. Conversely, rain in perennial grasses may produce new green shoots under a more cured upper layer. An assessment of the state of curing of a sward should take into account the state of the grass through its full height range (Luke and McArthur, 1978).

The degree of curing is used as an input to the Australian McArthur Mk 4 Grassland Fire Danger Meter (Cheney and Sullivan, 2008) and the rate of fire spread model (Cheney et al., 1998), where it is regarded as a surrogate for live fuel moisture content (Cheney and Sullivan, 2008). Moisture associated with dead grassland fuels is treated separately and is largely related to atmospheric conditions, in particular relative humidity. The degree of curing is also an input for grassland fire danger rating and fire spread prediction in the Canadian Forest Fire Danger Rating System (Stocks et al., 1989; Wotton et al., 2009), which has been implemented in a number of countries including New Zealand (Alexander, 2008; Anderson, 2005; Wotton et al., 2009). Fires will generally not spread in grasslands that are less than 50% cured, due to insufficient dead fuel to carry fire. The Australian rate of fire spread model for grasslands therefore assumes no fire spread for curing values below 50% (Alexander, 2008; Cheney et al., 1998). However, recent revisions to the Canadian grassland fire spread models allow very limited spread at curing values below 50% (Wotton et al., 2009). There is a rapid increase in fire spread rate as curing progresses from 75% to 90% (Cheney et al., 1998; Cheney and Sullivan, 2008). Fully cured grasslands can be highly flammable, allowing wildfires to grow and spread rapidly under hot and dry conditions.

Given the flammable nature of grasslands and the importance of the curing input into fire danger rating systems, it is important that fire management agencies have access to timely and accurate assessments of the degree of curing. Currently curing is most commonly assessed by visual estimation. However, it is widely perceived that visual estimates vary significantly in their accuracy and are generally both spatially and temporally sparse. The Bureau of Meteorology distributes satellite-based maps of grassland curing for south-eastern Australia. However, the underpinning algorithm was developed and validated at only a limited number of grassland sites in Victoria and needed to be extended to consider other grassland types and regions across Australia. Furthermore, recent developments in satellite remote sensing have resulted in the availability of higher precision data products at higher spatial resolution in a greater number of spectral bands compared to those available when the Victorian work was conducted in the 1980s, which warrant investigation for potential improvements.

The remote sensing component of the Bushfire CRC Project A1.4 aimed to develop satellite-based methods for the timely assessment of grassland curing across Australia and New Zealand. This research makes the use of emerging satellite data products, which will ensure the relevance of the work into the future. In particular the research addresses the question of how multispectral measurements from satellite instruments such as AVHRR and MODIS may be best processed to quantitatively estimate the degree of grassland curing, and the accuracy of these curing estimates.

The steps in the approach taken were:

1. The compilation of an extensive dataset of field curing measurements collected across Australia and New Zealand over several seasons;
2. Field-based spectrometry at a limited number of sites in order to better understand changes in the reflectance spectrum of grasslands due to curing;
3. Comparison of spectral approaches such as vegetation indices to estimating curing from multispectral data on a single date;
4. Examination of satellite time series analysis techniques to optimise the utility of spectral techniques, evaluated using NDVI as a single reference index;
5. Evaluation of the synthesis of the recommended spectral approach with the recommended temporal approach;
6. Surveying users on their needs for the presentation and delivery of curing data products;
7. Establishment of a pilot system for the delivery of curing maps to state agencies, based on a number of test algorithms;
8. Gathering of feedback from end users of the curing data concerning the delivery mechanism, data format and accuracy at the regional scale;
9. Summary of feedback and the development of recommendations for an operational mapping system for grassland curing.

The following report deals with each of these steps in the project. However, it should be noted that different aspects of the work have often been conducted by researchers residing in different institutions and this report is an attempt to synthesise this work in a coherent manner and draw conclusions from the body of work as a whole.

2. BACKGROUND

2.1 SUMMARY OF RELEVANT SATELLITE SENSORS

Earth observation satellites carry one or more sensors designed to detect energy reflected by or emitted from the earth. The majority of these satellites are in either low polar orbits that enable measurements of the whole globe or in high geostationary orbits that enable constant surveillance from a single point over the equator.

Earth observation satellites are categorised as either operational or research satellites. Operational satellites support routine, operational services such as weather forecasting. They typically employ mature demonstrated instruments and are planned as a series to minimise disruption of the data stream, with the failure of a critical instrument motivating the launch of the next satellite in the series. Research satellites are intended to supply data for a rapidly expanding array of developing applications. They typically incorporate instruments based on novel technology or measurement concepts, and are generally not replaced after failure. Nevertheless, data from research satellites is often used to support operational services, for as long as the data stream exists.

Wide-swath imagers on polar orbiting satellites in low-Earth orbit have the advantage that they can measure every point on the globe in daylight at least once each day. They do this by continuously scanning a swath around 2000 km wide which is centred on their roughly north-south orbital track. On each day, reflected and emitted energy for the whole of Australia is thus recorded by two or three swaths.

The workhorse polar-orbiting operational sensor is currently the Advanced Very High Resolution Radiometer (AVHRR). This sensor has been carried on the Polar Orbiting Environmental Satellite (POES) series of satellites operated by the US National Oceanic and Atmospheric Administration (NOAA) since 1978. The last NOAA satellite was launched on 6 February 2009, with a planned lifetime of at least two years. An AVHRR will also be carried by the European MetOp satellites from 2006 to 2019. While the AVHRR was designed for the measurement of sea surface temperature and the imaging of clouds for meteorology, it has been used extensively for measurement of the terrestrial surface, such as the assessment of vegetation characteristics.

By far the most common way to monitor vegetation status with AVHRR has been with the Normalised Difference Vegetation Index (NDVI) calculated from the red (band 1) and near-infrared (band 2) brightness or reflectance, R_1 and R_2 respectively:

$$NDVI = \frac{R_2 - R_1}{R_2 + R_1}. \qquad (2.1)$$

The AVHRR sensor will be succeeded by the Visible/Infrared Imager/Radiometer Suite (VIIRS) as the operational imager. The VIIRS will be carried by a series of US operational satellites, starting with the NPP satellite in 2011 and followed by the satellites of the Joint Polar Satellite System (JPSS).

The Moderate Resolution Imaging Spectroradiometer (MODIS) is a sensor which has been operating on the US research satellites Terra and Aqua, since 1999 and 2002 respectively. Those satellites form part of NASA's Earth Observing System (EOS). Despite being a research sensor, data from MODIS has been successfully incorporated into many operational applications. MODIS is conceptually similar to AVHRR in design, but has many more spectral bands, finer spatial resolution, more accurate calibration, less sensitivity to atmospheric contamination of land

observations, and better cloud detection. The two MODIS instruments have worked reliably for nine and six years respectively and are expected to operate for several more years.

MODIS is a very well characterised instrument that has internationally standardised software to process the data to robustly validated data products. Near real-time MODIS data has been received and processed for many years by several Australian agencies, notably Geoscience Australia. The Bureau of Meteorology also began reception and processing of MODIS data in near real-time in late 2010. An important feature of MODIS is that it is an excellent prototype for VIIRS due to the similar sensing geometry, spectral bands, and the processing methods planned to be employed. These characteristics all make MODIS a strong candidate on which to base the development of a new grassland curing product for Australia, particularly to ensure that the research is relevant as VIIRS supersedes AVHRR as the main operational sensor for terrestrial broadscale remote sensing applications.

Note that while an imager on a geostationary meteorological satellite gives hourly coverage of nearly half of the globe, the geostationary satellites currently operating over the region of Australia (Japan's MTSAT-1R and China's FY-2C) have only a single spectral band in the visible/infrared region, which severely limits their usefulness for curing estimation. Recent imagers that view other parts of the globe, such as the SEVIRI imager on Europe's Meteosat Second Generation series of satellites, have much more comprehensive multispectral capabilities. When similar capabilities become available in the Australian region, such as Japan's planned MTSAT follow-on satellite from 2015, they should be considered for potential inclusion in any satellite based grassland curing mapping system.

2.2 SATELLITE MAPPING OF GRASS CURING

The assessment of grassland curing from satellites has been the subject of past research throughout Australia (Allan et al., 2003; Barber, 1979; Barber, 1989; Dilley et al., 2004; Hosking, 1990; Millie and Adams, 1999; Paltridge and Barber, 1988; Paltridge and Mitchell, 1990), mainly in Victoria, and also in New Zealand (Pairman et al., 1995; 1996). The methods developed have generally been based on visual estimates of curing, or curing inferred from gravimetric determination of the fuel moisture content (FMC) of field samples.

2.2.1 Victoria

The estimation of curing in Victoria from AVHRR satellite data evolved through a series of studies conducted by the Victorian CFA and CSIRO from the late 1980s to the early 2000s. Paltridge and Barber (1988) used FMC measurements from several field sites across Victoria to develop a state-wide relationship to predict FMC from a modified AVHRR NDVI defined by:

$$NDVI_{1.2} = \frac{R_2 - 1.2R_1}{R_2 + R_1}, \qquad (2.2)$$

where R_1 and R_2 are the top of atmosphere reflectance in AVHRR bands 1 and 2. The index was based on their observation that R_2 / R_1 =1.2 for non-vegetated land, and designed with the intention that $NDVI_{1.2}$ = 0 for bare ground or fully cured grass. They concluded that $NDVI_{1.2}$ = 0.5 for full cover, fully green vegetation. They further concluded that $NDVI_{1.2}$ was proportional to the vegetation cover fraction, that the cover fraction was constant through a curing season, and that the grass was fully green at the start of each season. This leads to FMC being

proportional to the value of $NDVI_{1.2}$ normalised by the full greenness value of $NDVI_{1.2}$, taken from the start of the season, with the constant of proportionality derived from the field measurements of FMC.

Barber (1990) derived a relationship between FMC and curing from earlier published data. Barber (1990) then combined this with the relationship between $NDVI_{1.2}$ and FMC of Paltridge and Barber (1988) to arrive at a relationship between $NDVI_{1.2}$ and curing. This relationship was the basis of the initial AVHRR curing mapping system developed by CSIRO, which was subsequently transferred to the Bureau of Meteorology.

Dilley et al. (2004) found that the relationship between NDVI and FMC differed markedly between three grassland sites in Victoria, and that the differences were accentuated by converting FMC to curing with the relation of Barber (1990). They derived a direct non-linear relationship between NDVI and curing, using visual estimates of curing. The CSIRO/Bureau mapping system was revised to use this relationship.

As an aside, Paltridge and Mitchell (1990) developed a linear relationship based solely on the relationship between FMC and the reflectance in AVHRR band 1, after atmospheric correction and angular normalisation. Gravimetric FMC field data for this study was collected at a limited number of Victorian sites, and the results were not used for routine mapping.

In summary, the methods used to estimate curing in Victoria from AVHRR date have been based on either FMC measurements converted to curing by a fixed relationship, or more recently on visual curing estimates.

2.2.2 Other regions

Chladil and Nunez (1995) found a strong correlation between AVHRR NDVI and curing inferred from the time series of Soil Dryness Index in south-eastern Tasmania, and concluded that NDVI could be used to map the spatial distribution of curing, at least on a regional scale. They suggested that in a cloudy environment, the use of NDVI to monitor the state of grassland fuel was problematic due to long periods without satellite data, but might be exploited by combining NDVI with point curing values estimated by other means, such as ground-based estimates.

A study in New Zealand (Pairman et al., 1996) compared visual curing estimates with AVHRR NDVI values over two seasons. While a weak linear relationship was found, the range of NDVI variation attributable to curing was small. The satellite data used was compromised by the uncorrected effects of satellite view angle, extreme sun angles during a period of reliance on aging satellites, and frequent cloud.

Allan et al. (2003) investigated satellite assessment of curing in the Northern Territory. They compared visual estimates of curing with NDVI normalised to its long-term minimum and maximum, derived from both AVHRR and SPOT data, using sampling at 25 sites over two seasons. They found strong relationships, which were linear at black soil sites, and curvilinear at red soil sites. The relationships were stronger for individual sites and for individual years than when grouped. The change in relationship between years for an individual site was significant.

2.3 THE EXISTING SATELLITE CURING PRODUCT

Currently the Bureau of Meteorology distributes grassland curing maps for south-eastern Australia which are derived from NOAA/AVHRR data, using the (Dilley et al., 2004) algorithm developed by the CSIRO and Victoria's CFA. CSIRO implemented the algorithm in a software system that performs end-to-end processing from raw AVHRR data to the final curing product. This system was originally developed to use the Barber (1990) algorithm, and handed over to the Bureau in 2001 which commenced running it operationally in the 2002/03 season. Subsequently the system was revised to use the Dilley et al. (2004) algorithm, and in 2007 the Bureau fixed an anomaly in the algorithm implementation with minimal impact on the results. Since then the only changes have been updates to satellite-specific calibration parameters as new NOAA satellites have come into operation.

The system output is in the form of image files in GIF format for two rectangular regions: one encompassing Victoria (Figure 2.1) and one covering south-eastern South Australia. Each day, for each of the two regions, the system uses the most overhead afternoon NOAA orbit received at the Bureau's antenna at Crib Point near Melbourne. These images are processed into GIF-format files that colour codes six levels of curing, with cloud, sea and forest areas separately masked. Each image file is accompanied by a text file that describes the image contents, including the georeferencing of the image grid. However, georeferencing is not embedded in the image and currently requires manual intervention when importing into standard GIS software. The curing images are produced within about two hours of the pass and presented to the Bureau's Victorian Regional Office for subjective confirmation of quality and forwarding to fire agencies.

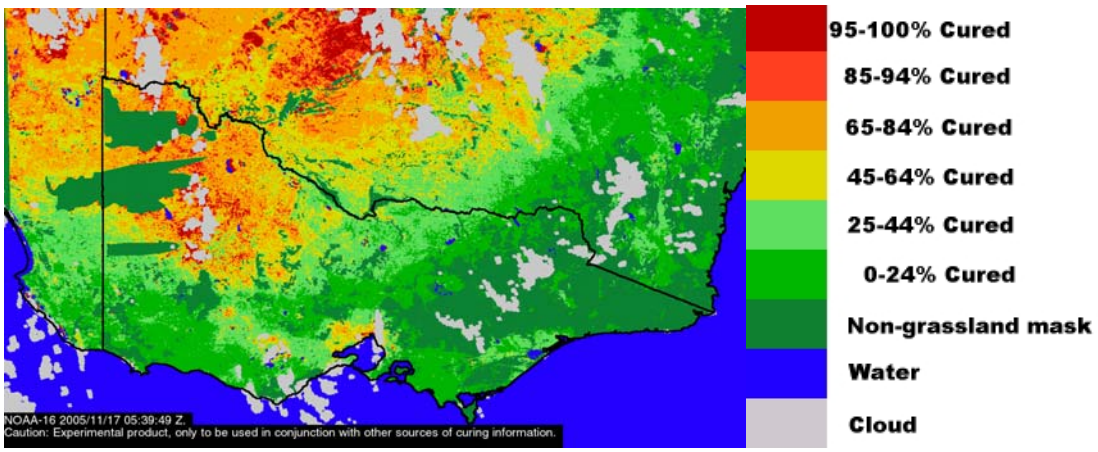

Figure 2.1: Example grassland curing map covering Victoria derived from AVHRR data collected and processes by the Bureau of Meteorology.

3. PROJECT METHODOLOGY

As stated in the previous section, the Bureau of Meteorology currently provides regularly updated maps of curing for the south east of Australia. These estimates are based on an algorithm developed initially by CSIRO and the Victorian CFA in the 1980s and more recently revised by Dilley et al. (2004). Although this data product provides useful information on the relative spatial distribution of curing, the algorithm is likely to be unsuitable for extrapolation over all of Australia and New Zealand due to factors like the significant variations that exist in grassland species types and biomass density and soil background reflectance.

The satellite observational component of the Project A1.4 was designed specifically to address the need for a more generic algorithm that can objectively assess curing over all grassland and soil types found in Australia and New Zealand. The goal for the project was to achieve an absolute accuracy of 10% in curing, substantially improving on visual estimates, over all of the Australia and New Zealand test sites. The ultimate goal is to develop a system that can provide this information in regularly updated spatial products that can be readily integrated into existing grassland fire danger rating systems.

3.1 FIELD DATA COLLECTION METHODS

The collection of field data on grassland curing was a major focus of Project A1.4. Major effort was invested in compiling a database of curing values from a range of grasslands across Australia and New Zealand, with significant in-kind support from end user agencies. This main field data collection program ran for four summers from the 2005/2006 to the end of the 2008/2009 summer season. Data for at least one curing season was collected at 39 sites across Australia and 16 sites in New Zealand that are reasonably uniform at the scale of a MODIS 500-m pixel. Although only 25 sites in Australia and 12 in New Zealand were sampled on more than 5 dates during this period.

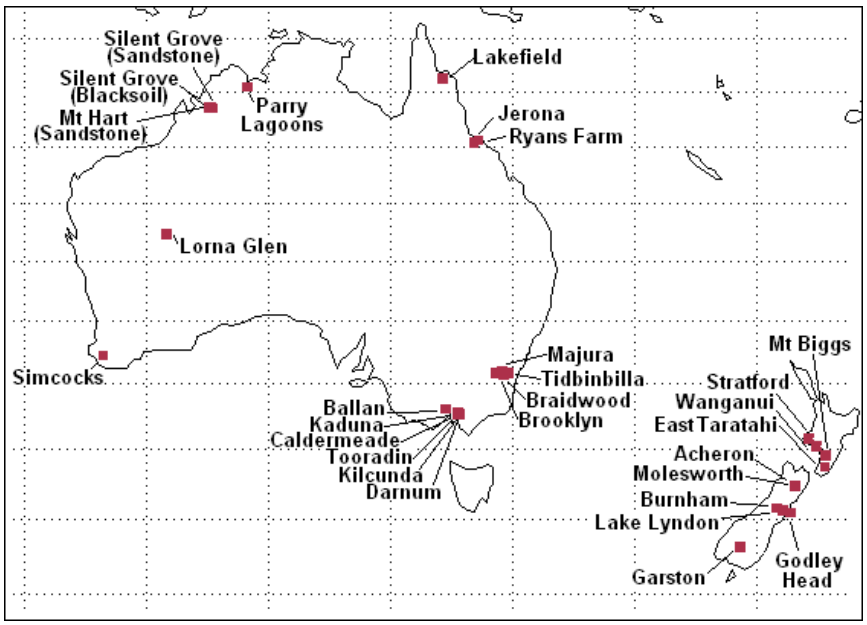

Figure 3.1: Location of field sites across Australia and New Zealand where curing measurements were recorded.

The project required an accurate, objective and repeatable method to collect ground-based curing data for use in the development and validation of a satellite-based curing mapping system. In order to collect enough data for robust analysis over an extensive range of sites across Australia and New Zealand, the field method also had to be inexpensive and easily carried out by fire agency personnel with limited training. While a trained and experienced observer may be capable of achieving high accuracy in their estimates, visual assessments are subjective and have been shown to vary by as much as 50% between observers (Anderson and Pearce, 2003; Millie and Adams, 1999). This is inadequate for the training and validation of a satellite-based product. Destructive sampling, while probably the most accurate method, requires tedious and labour-intensive sorting of samples in a laboratory, and so was also not deemed suitable for large-scale field data collection required.

Several alternative field methods were developed and assessed during the early phase of the project. These results are reported in Anderson et al. (2005). Their recommendation was for the use of a modified Levy Rod method (Levy and Madden, 1933) as it balances efficiency with the need for an accurate and objective measurement technique. The method was initially developed for measuring the species composition of grasslands, and was adapted to the measurement of curing specifically to address the needs of this project.

The adaptation of the Levy Rod method uses a steel pole of approximately 5 mm diameter, driven vertically into the ground at sample points along a transect. Touches of vegetation on the pole are classified as dead or live and separately tallied and converted to a curing percentage. Samples are typically taken every 2 metres along two 20-metre transects at right angles. Anderson et al. (2005) found that the Levy estimates of curing are generally within ±10% of the values from destructive sampling. They also found that visual estimates of curing are accurate to only ±25%, compared to destructive sampling, and show great variability between observers.

This adaption of the Levy Rod method was used to collect 580 sets of curing measurements at the sites shown in Figure 3.1. These measurements have been used as the primary calibration and validation data for the development of satellite-based curing algorithms. A subset of these Levy Rod measurements (134 measurements) also included concurrent destructive and visual observations. As destructive measurements are generally considered to be the most accurate method for quantifying curing, these were used to assess the relative accuracy of the Levy Rod and visual techniques (Figure 3.2). The analysis showed that the Levy Rod method produced a root mean square error (RMSE) in estimates of 13%, while visual estimates produced a RMSE of 20%. Possibly more concerning is the mean error, which indicates bias in the measurements. Here the Levy Rod was shown to overestimate curing by a marginal 2%. However, the visual estimates were shown to underestimate curing, relative to destructive curing assessments, by 11%.

Given these results, we might assume that any satellite-based estimates validated on the basis of Levy Rod data can at best achieve an RMSE of 13%, since there is an inherent variance in the calibration data that cannot be accounted for. Further, it might be assumed that broad scale validation of satellite maps based on visual assessments may inappropriately determine that the maps overestimated curing, simply due to the bias in these measurements.

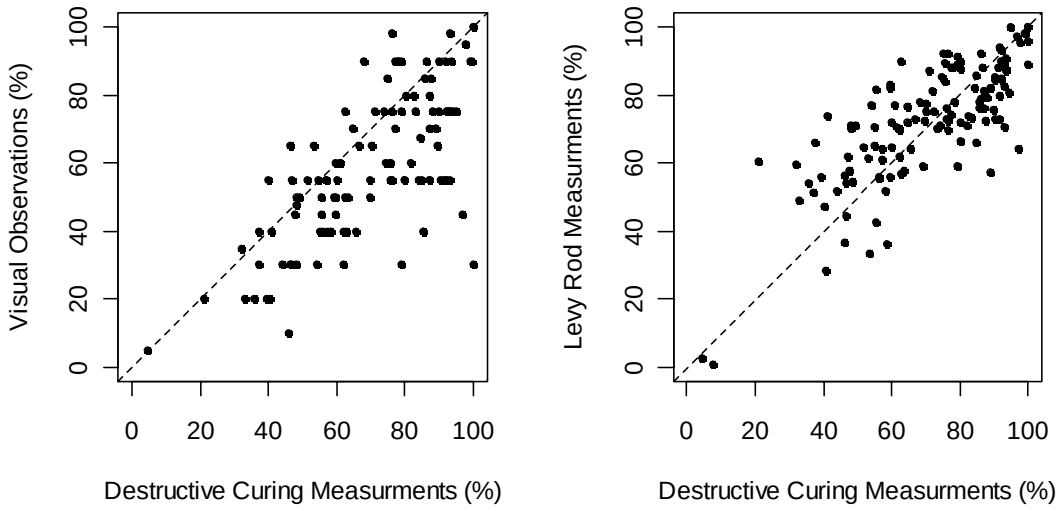

Figure 3.2: Relationship between destructive measurements and concurrent visual assessments, and destructive measurements and concurrent Levy rod measurements. The dashed line indicates the line of equivalence.

3.2 SATELLITE DATA CHARACTERISTICS

MODIS has 36 spectral bands, seven of which were designed for land measurement and are in the visible and shortwave infrared regions of the spectrum. Characteristics of these bands are listed in Table 3.1, while their locations in the electromagnetic spectrum, relative to a typical vegetation spectrum, are shown in Figure 3.3. Two of the MODIS land bands measure red and near-infrared radiance at 250 m spatial resolution and are very similar to the filter functions used by the AVHRR for deriving the NDVI. The remaining five land bands are sensitive to a variety of terrestrial characteristics, and have a lower spatial resolution at 500 m. MODIS gives at least daily coverage poleward of 30° latitude, and nearly daily closer to the equator.

Table 3.1: MODIS surface reflectance bands

Band	Spectral region	Wavelength (nm)	Spatial Resolution (m)
1	Red	645	250
2	Near Infrared – NIR	857	250
3	Blue	466	500
4	Green	554	500
5	Near Infrared – NIR	1242	500
6	Short Wave Infrared – SWIR	1629	500
7	Short Wave Infrared – SWIR	2114	500

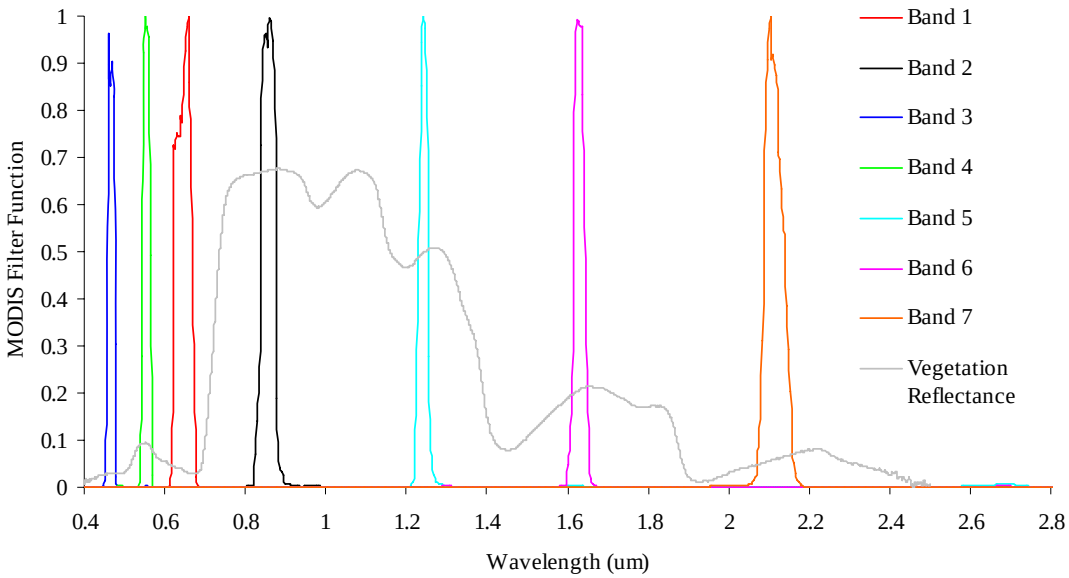

Figure 3.3: Spectral response functions for MODIS land bands, superimposed on a typical reflectance spectrum for green vegetation.

NASA has developed software for MODIS data which produces a sequence of successively more highly processed data products for diverse biogeophysical parameters. The objectives of this project required that the satellite data be processed to a state that enables data to be compared directly over space and time. NASA has developed several standard data products that aim to provide this, each taking a different approach and with their own advantages and drawbacks. Three MODIS products were investigated for inclusion in the curing analysis:

- MOD09 8-day composites of surface reflectance at 500m spatial resolution, referred to here after as MOD09;
- MOD13 16-day composite Vegetation Indices at 500m spatial resolution, referred to here after as MOD13;;
- MCD43A4 16-day Nadir BRDF-Adjusted Reflectance surface reflectance at 500m, referred to here after as MCD43;.

Both MOD13 and MCD43 are derived from MOD09 surface reflectance values that have been corrected for atmospheric effects, including Rayleigh scattering, water vapour, ozone and aerosol. For any particular orbit, some regions may be obscured by cloud, so some compositing of data from orbits over several days is desirable for spatial completeness. Furthermore, from orbit to orbit the spatial resolution at a particular location can vary, and the apparent surface reflectance can vary due to changes in the directions of the sun and the spacecraft view. These directional, or angular, effects are sometimes referred to as bidirectional reflectance distribution function (BRDF) effects. Each of the above three MODIS products combines MOD09 individual orbit data (swath data) over multiple days to minimise the angular effects and resolution changes, but use different method in this compositing process.

Analysis of the variation between these products showed a very high correlation (Figure 3.4, Figure 3.5 and Figure 3.6), well within the limits of accuracy of the field measurements (±13%). It was concluded that the higher temporal resolution of 8 days for MOD09 (when compared to 16 days for MOD13 and MCD43) outweighed any potential benefit in terms of increased surface precision in NDVI. The MOD09 product also provided added flexibility to develop and test new spectral indices from the seven reflectance land bands relative to MOD13, which only includes the NDVI and EVI.

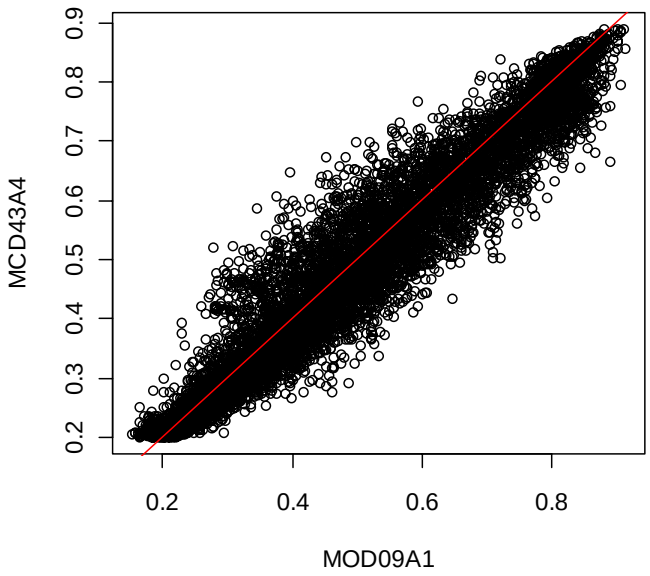

Figure 3.4: Comparison of MOD09 derived NDVI and MCD43 BRDF adjusted NDVI for all Australian sites in the study over the period 2000 to 2009. Correlation is 0.924 with mean residuals of 0.05.

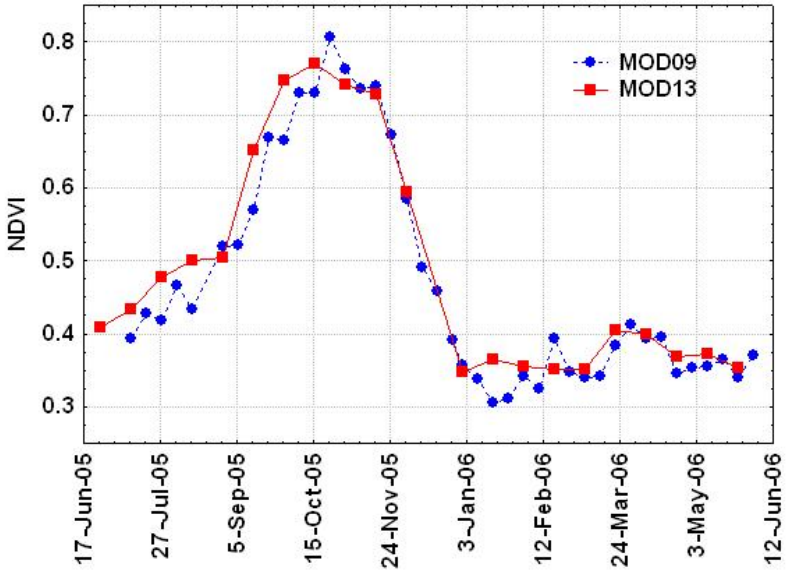

Figure 3.5: Comparison of NDVI time series derived from MOD09 and MOD13 at Majura (ACT) over the 2005-2006 curing season.

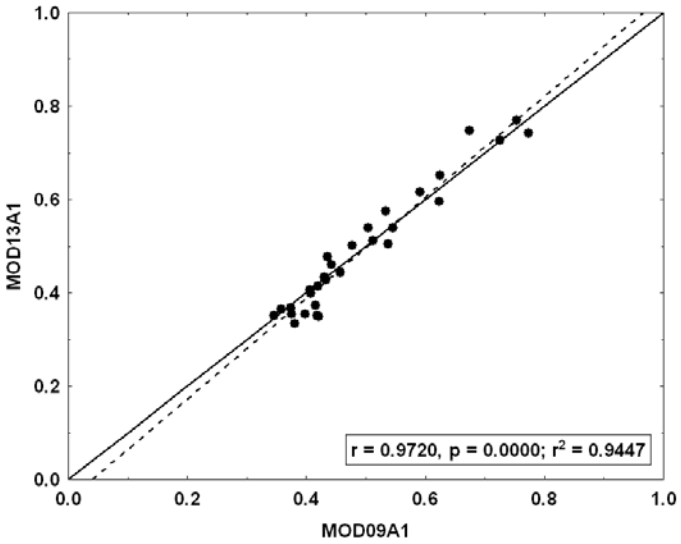

Figure 3.6: MOD09 NDVI against MOD13 NDVI at Majura (ACT), July 2005 to November 2006.

No direct broadcast of satellite data for the whole Australian and New Zealand land mass was available during the study. CSIRO, as a service to Australian researchers, provides an archive of several MODIS products for the seventeen MODIS image tiles that cover continental Australia in a reprojected and mosaiced format. This archive is updated as soon as new data is available from the U.S. via the Land Process Distributed Active Archive Centre (LPDAAC) and details of the processing performed locally by CSIRO are given by Paget and King (2008). CSIRO also agreed to provide a parallel service for the MOD09 tiles covering New Zealand.

The full time series of MOD09 data were extracted for spatial windows (5 by 5 pixels) centred on the geographic locations corresponding to all project field measurement sites. This data includes composited surface reflectance images in the seven MODIS land bands, four angles describing the sun and view directions, the date of the observation selected for the composite, and flags indicating the quality and state (clear, cloud, cloud shadow, etc.). While compositing tends to select cloud-free observations, cloud contamination remains for a small fraction of observations which will produce outliers in the analysis.

The extracted data were filtered using the following broad criteria:

- NDVI > zero;
- View zenith angle < 60°;
- Data produced at ideal quality in all image bands according to state flags.

The data was further filtered using the following NDVI spike detection filter:

$$\begin{aligned} &(NDVI_i - NDVI_{i-1}) < \tau \;\;\&\;\; (NDVI_i - NDVI_{i+1}) < \tau \\ &\qquad\qquad \text{or} \\ &(NDVI_{i-1} - NDVI_i) < \tau \;\;\&\;\; (NDVI_{i+1} - NDVI_i) < \tau \end{aligned} \qquad (3.1)$$

where i indicates the current time step, i-1 is the preceding epoch in the time series and i+1 indicates the subsequent epoch. The conservative threshold for τ of 0.15 was selected (e.g. Viovy et al., 1992 suggest a threshold

of 0.1) in order to retain a greater proportion of the original data. Pixel values detected using the spike detection algorithm are shown in blue in Figure 3.7.

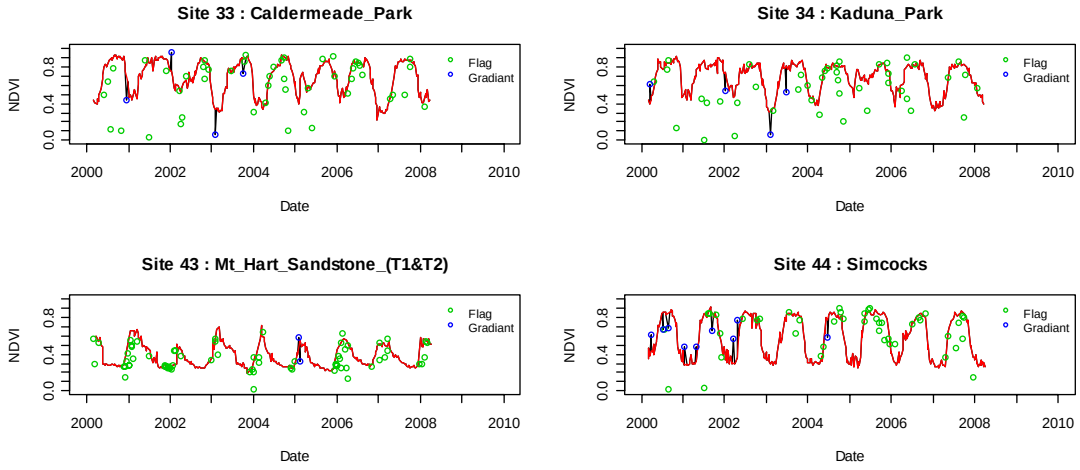

Figure 3.7: Example time series showing points removed using MOD09 state flags in green and points removed using spike detection in blue.

4 NDVI TIME SERIES METHODS

By far the most common basis for satellite-derived maps of vegetation properties is the NDVI. Although this index makes use of only two satellite bands (red and near infrared), NDVI serves well as a basis for comparison with previous studies that have investigated the estimation of curing using the AVHRR sensors. The NDVI also provides an established basis for the exploration of methods involving the analysis of long time series of satellite data.

This section begins by examining the spatial heterogeneity of 500m resolution MODIS NDVI data at the Australian field sites. The NDVI data is then used to assess the performance of the current south eastern Australian curing algorithm when extrapolated outside of Victoria. Alternative time series processing approaches are then investigated and each method assessed relative to the existing algorithm. These results provide a benchmark for extension of the methods in Section 5 to algorithms which utilise other spectral bands available via the MODIS sensor.

At the time of this analysis, MODIS data for New Zealand were not available in a consistent form to that for Australia. As such, analysis specific to New Zealand is dealt with in Section 6. Further, only sites where greater than 5 field measurements were recorded are considered in this section. The geographic distribution of these sites is shown in Figure 4.1, with further details given in Table 4.1. This dataset includes 25 individual sites where a total of 343 individual Levy Rod curing measurements had been recorded.

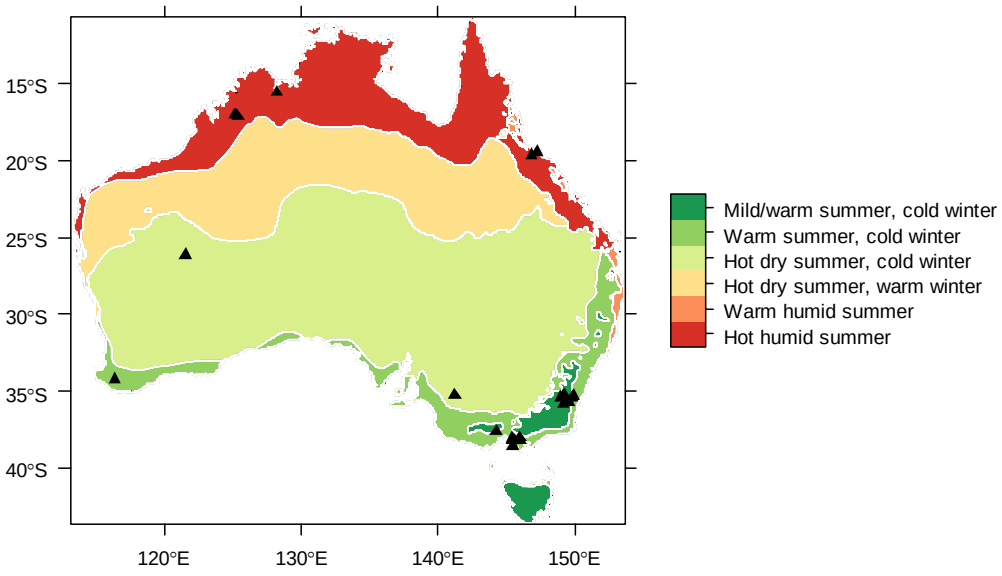

Figure 4.1: Geographic distribution of the 25 Australian field sampling sites (∫) used in Section 4 of the report, and their relationship to Bureau of Meteorology temperature and humidity climate zones.

Table 4.1: Field sites used in the NDVI time series component of the project. Grassland type codes: IP = improved pasture, NG = native grassland, MX = mixed native and exotic species. Climate zones codes as per Bureau of Meteorology temperature and humidity zones shown in Figure 4.1

Site Name	Region	Grassland Type	Latitude	Longitude	Climate Zone
Braidwood	NSW	MX	-35.4200	149.7932	5
Brooklyn	NSW	NG	-35.7198	149.5720	6
Durran Durra	NSW	NG	-35.3188	149.8735	5
Colinton	NSW	IP	-35.8500	149.1583	6
Majura	ACT	IP	-35.2777	149.1966	6
Monaro	ACT	IP	-35.3045	149.1700	6
Tidbinbilla	ACT	MX	-35.4191	148.9506	6
Ballan	VIC	IP	-37.6352	144.2213	6
Darnum	VIC	MX	-38.2136	145.9994	5
Kilcunda	VIC	IP	-38.5391	145.4560	5
Tooradin	VIC	IP	-38.2028	145.3820	5
Tooradin Nth	VIC	IP	-38.1645	145.3947	5
Caldermeade Park	VIC	IP	-38.2257	145.5633	5
Kaduna Park	VIC	IP	-38.0895	145.4307	5
Ryan's Farm / Calcium	QLD	NG	-19.6604	146.8140	1
Jerona / Bowling Green	QLD	NG	-19.4668	147.2211	1
Parry Lagoons	WA	NG	-15.5866	128.2338	1
Silent Grove Sandstone	WA	NG	-17.1309	125.3739	1
Silent Grove Black Soil	WA	NG	-17.0629	125.2609	1
Mt Hart Sandstone	WA	NG	-17.0297	125.1159	1
Simcocks	WA	IP	-34.2170	116.3831	5
Lorna Glen	WA	NG	-26.1629	121.5588	4
Murrayville Grass	VIC	NG	-35.2414	141.2247	4
Murrayville Wheat	VIC	IP	-35.2405	141.2152	4
Neerim South	VIC	MX	-38.0026	145.9549	5

4.1 NDVI CHARACTERISTICS FOR PROJECT SITES

The spatial resampling that is required in order to produce high-level MODIS products (such as MOD09) introduces an uncertainty in the ground coordinates of the pixel centre of 0.5 pixels. In the case of MOD09 with a spatial resolution of 500m, this equates to a pixel centre uncertainty of 250 m. As such, many studies (e.g. Yebra et al., 2008) that use high-level MODIS products choose to use mean reflectance values within three by three pixel windows to ensure that field validation sites truly fall within the satellite instantaneous field of view. However, the trade-off when comparing field data to a three by three pixel window is that field sites need to be representative of a larger homogeneous area; 1.5km by 1.5km in the case of MOD09. This assumption of homogeneity is often unjustified, particularly in more intensive land use areas of Australia and New Zealand.

The effect of using different sized pixel windows was investigated by assessing the correlation between NDVI and curing, assuming a linear relationship between these two variables. For smaller pixel windows, location uncertainty is expected to influence the correlation value, while the correlation for larger pixel windows is expected to be influenced by land cover heterogeneity.

NDVI values corresponding to field curing measurement dates were linearly interpolated using the neighbouring satellite observation dates, assuming a linear change in NDVI between successive observations. Here the satellite observation date refers to the date an individual pixel measurement was recorded by the MODIS instrument, as opposed to the date of the composite image production. It should be noted that for grassland sites, surface reflectance characteristics can change rapidly and erratically in response to curing and greening up caused by extreme heat or rainfall events. Consequently, although linear interpolation is the best approximation, it may lead to significant variations between the true NDVI at the time of the field measurement and the interpolated value.

Plots showing Levy rod measurements of curing versus mean interpolated NDVI for different pixel window sizes are shown in Figure 4.2. The highest correlation (r^2 = 0.427) between interpolated NDVI and field-measured curing was found using a single pixel window, with increasing window size resulting in decreasing correlations (r^2 = 0.414 for a three by three pixel window and r^2 = 0.388 for a five by five pixel window). This indicates that although there is significant spatial uncertainty in the pixel centre locations (±250m in the case of MOD09), degradation of the correlation due to spatial heterogeneity appears to dominate. Based on this result, further analysis in this section of the report deal only with the NDVI value derived from the central pixel directly centred on each field site.

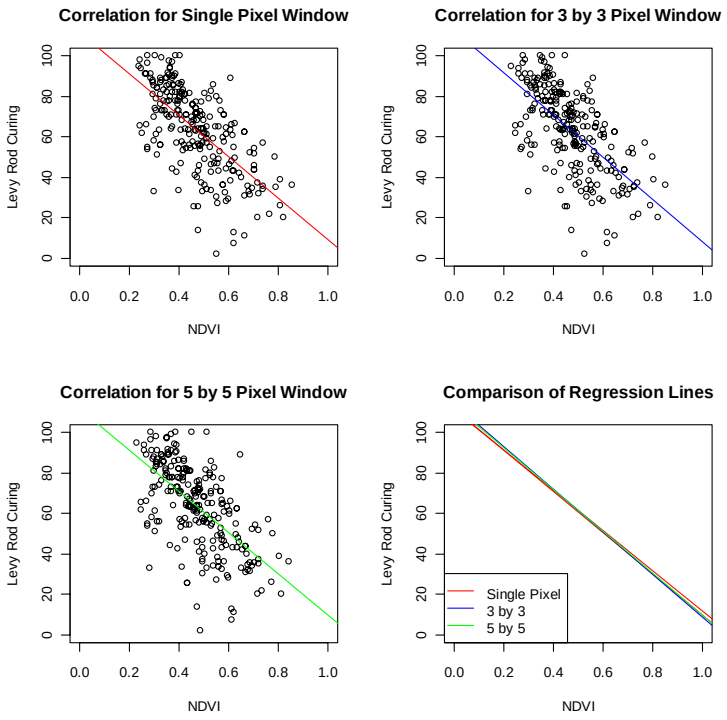

Figure 4.2: The relationship between Levy rod curing values and mean NDVI values for different pixel window sizes. Best fit lines are shown on each scatter plot and then on the same plot to illustrate their close correspondence of the relationship.

4.2 STATIC ALGORITHMS

Satellite data is often associated with land surface characteristics using some form of least squares regression. Commonly regression equations assume a linear relationship between a satellite-measured variable and the surface characteristic of interest. The current algorithm used by the Bureau of Meteorology to map curing in south-eastern Australia (Dilley et al., 2004) is a more complex non-linear least squares approach. However, the application of both linear and non-linear approaches to modelling the relationship between NDVI and curing are similar in term of their practical application, as they use pre-defined coefficients to derive curing estimates from satellite-derived NDVI. For this reason we describe such methods in the following section as static. In the following section, both the current non-linear approach and the simple linear modelling approach are used as a benchmark for investigating time series approaches which utilise historical variation in NDVI to adapt the relationship to local conditions.

4.2.1 Non-linear algorithm

As described in Section 1, the current algorithm used to estimate a grassland curing index (GCI) in south-eastern Australia is based on satellite NDVI and the exponential equation described by Dilley et al. (2004) as follows:

$$GCI = -19.1 + 218\exp\left(-\frac{NDVI}{0.434}\right) \qquad (4.1)$$

This equation was developed using field measurements from Victoria only. The Dilley et al. (2004) algorithm was based on AVHRR surface reflectance values generated with explicit atmospheric and angular corrections. The MOD09 surface reflectance in bands 1 and 2 (used to compute the NDVI) are expected to be approximately equivalent, since they derive from an explicit atmospheric correction, and a compositing process that implicitly reduces angular effects. The effect of differences between AVHRR and MODIS spectral bandpasses is expected to be secondary.

When applied to the interpolated NDVI values, the non-linear equation yielded a root mean square error (RMSE) of 17.1% for the Victorian portion of the curing dataset, while the application of the method to the complete Australian dataset produced a RMSE of 19.0%. It should be noted in Figure 4.3 that although there is little bias in the non-linear method, Victorian field data appears to be underestimated by the algorithm.

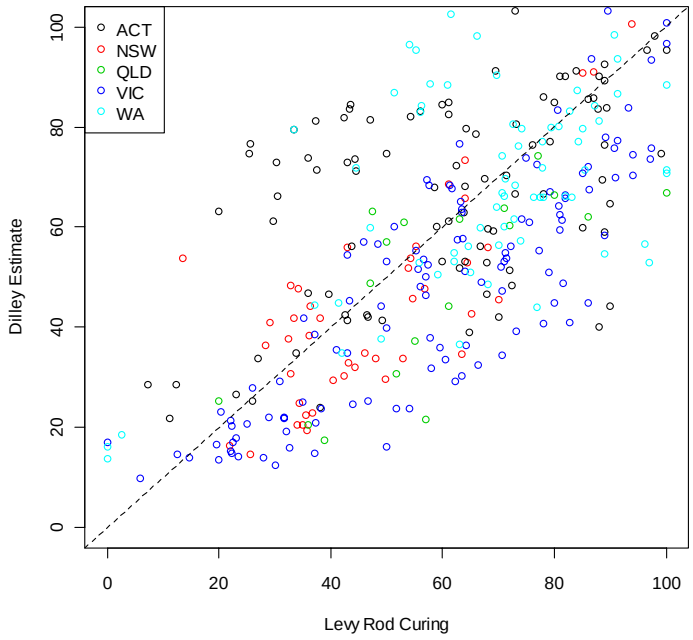

Figure 4.3: Relationship between the Dilley et al (2004) based non-linear estimate of curing and field measurements using the Levy rod method.

Using the current field dataset the non-linear model does not converge to a solution. However, it is possible to recalibrate the equation by calculating a new linear regression relationship between the non-linear algorithm estimates and the curing measurements. The application of these new linear coefficients to the full Australian dataset reduces the RMSE to 17.4%.

4.2.2 Linear Regression

Over all field sites, the ten year time series of filtered MODIS NDVI data ranged in value from 0.15 to 0.91. In the absence of any validation data, we might speculate that an approximate linear model could take the form:

$$GCI = (1 - NDVI) \times 100 . \quad (4.2)$$

Interestingly, even this speculative model performs better than the existing non-linear model with an RMSE of 18.30% over the 25 sites. If linear regression coefficients are fitted to the data then this error is reduced to 16.37, with the model taking the form:

$$GCI = (1.03 - NDVI) \times 108.11 \quad (4.3)$$

Figure 4.4 indicates that the model generally underestimates curing at levels greater than 80%. Throughout the mid-curing levels there is little perceptible bias for all states except the ACT, which appears to be generally overestimated.

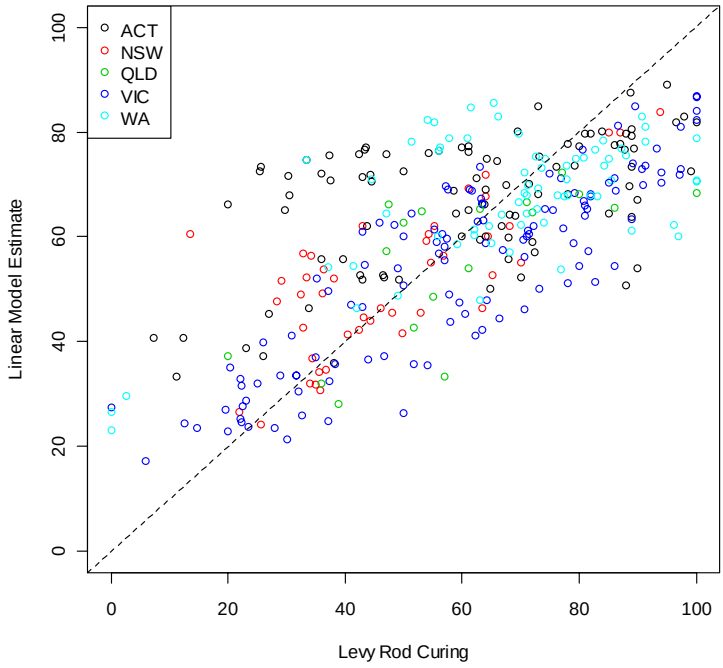

Figure 4.4: Levy rod curing data from 25 Australian sites plotted against the linear regression model estimate (r^2 = 0.5).

4.3 TIME SERIES NORMALISATION

Although the NDVI is useful in partially accounting for the effects of sensor degradation, variable atmospheric conditions, and variations in solar and view geometry, a large number of factors still influence any individual NDVI value. In the assessment of grasslands, a single NDVI measure will depend on many factors including:

1. The mixture of land cover types within the pixel;
2. Biomass per unit area;
3. The spectral characteristics of the soil;
4. The range and frequency of particular vegetation species;
5. Vegetation dryness and phenology expressed as chlorophyll content.

In the case of assessing grassland curing, we would ideally like to separate out NDVI variations in dryness irrespective of the proportion of grassland within a given pixel, their specific species composition, underlying soil type and biomass. This requires a different approach to normalisation which is not addressed by non-spatially explicit spectral indices.

4.3.1 Normalisation by NDVI range

Both North America (Burgan et al., 1998) and Europe (Sebastián López et al., 2002) have used a measure referred to as relative greenness in the assessment of fire potential. This places the NDVI in the context of the time series for that pixel using historical minimum and maximum values. In the case of Burgan et al. (1998), relative greenness of 100 equates to an NDVI measurement that is equal to the highest value ever measured for that pixel, while a relative greenness of 0 equates to a measurement equal to the lowest value ever measured at that pixel. This relative greenness measure is then used to partition the fuel load into live and dead proportions, each of which has its own fuel moisture model. In the absence of any field data, we might assume that relative greenness is the complement of curing and that as a first approximation could use the following equation to assess curing:

$$GCI_i = (1 - \frac{NDVI_i - NDVI_{\min}}{NDVI_{\max} - NDVI_{\min}}) \times 100 \,. \qquad (4.4)$$

where $NDVI_i$ is the current NDVI measurement, $NDVI_{min}$ is the minimum NDVI for that pixel and $NDVI_{max}$ is the maximum NDVI value for that pixel. The effect of using this approach is that it makes some attempt to normalise for spatial variations in the proportion of each pixel covered by grassland. The technique also addresses spatial variations in the contribution to the NDVI made by underlying soil. The assumption is that land cover proportions and vegetated biomass does not change within the pixel over the period in which the minimum and maximum values are being assessed. The setting of this period is therefore a compromise between adequately capturing the extremes of curing while not being influenced by longer term variations such as land use change or land degradation.

The full MOD09 dataset (February 2000 to December 2009) was used to derive estimates of $NDVI_{min}$ and $NDVI_{max}$ for each of the 25 field sites, which were then combined with the interpolated NDVI values for each measurement date in order to derive the relative greenness based estimate of curing. The resulting RMSE for the estimates was 17.5%, which indicates performance superior to the non-linear model, but inferior to the linear regression model.

An alternative approach, and one that is more compatible with the linear model, is to find the best fit linear regression model using relative greenness as a substitute for NDVI. This model produced an RMSE of 15.90% (r^2 = 0.52) and takes the form:

$$GCI_i = (1.24 - \frac{NDVI_i - NDVI_{\min}}{NDVI_{\max} - NDVI_{\min}}) \times 75.36 \,. \qquad (4.5)$$

As shown in Figure 4.5, the relative greenness model reduces the tendency of the model to underestimate curing at levels greater than 80% when compared to the linear model. However, this underestimation still appears to be a problem with the approach. Curing measurements from Western Australia tended to be underestimated by the approach while measurements in the ACT again were generally overestimated.

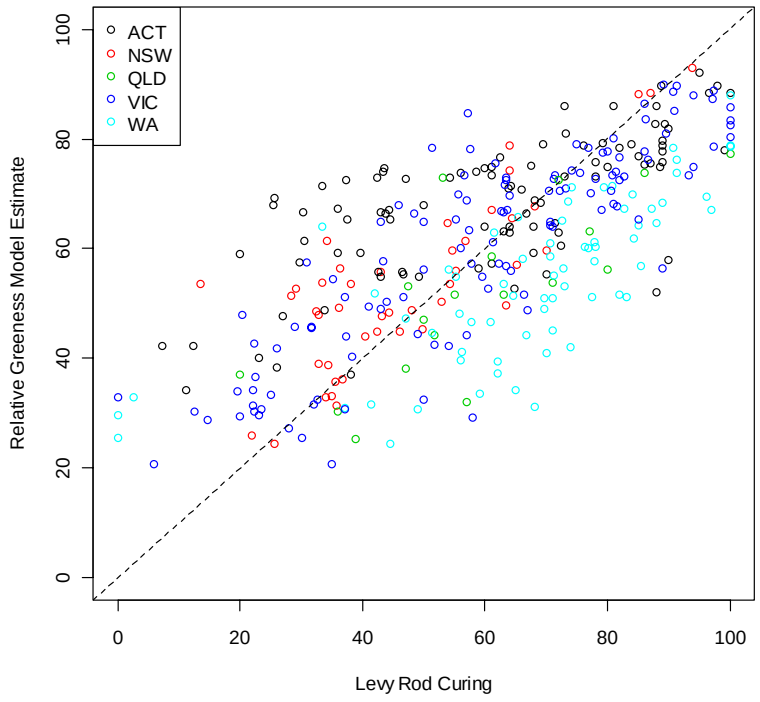

Figure 4.5: Levy rod curing data plotted against the relative greenness (min/max normalised) based estimate of curing (r^2 = 0.52).

As suggested previously, it is not necessarily appropriate to use the full time series to derive $NDVI_{min}$ and $NDVI_{max}$. This is due to the fact that the full time series may also be impacted by longer term changes that are not associated with curing, such as land use change, variations in grassland biomass, changes in species distribution, etc. It is prudent then to assess how the accuracy of the estimates changes as the period to find the minimum and maximum NDVI values is extended further back in time.

Figure 4.6 shows the impact on RMSE of using different time periods to derive $NDVI_{min}$ and $NDVI_{max}$. The relative greenness model shows a rapid decrease in the RMSE as the time period increases toward one year. From this point there is a more gradual decrease to a minimum at approximately 2.5 years, where the RMSE reaches 15.2%. Longer periods lead to an increase in RMSE, which stabilises at approximately 15.8%. Although the maximum benefit of using the relative greenness approach appears to be gained by considering a 2.5 year time series, the approach appears to out perform simple linear regression even if only a single year of data is considered.

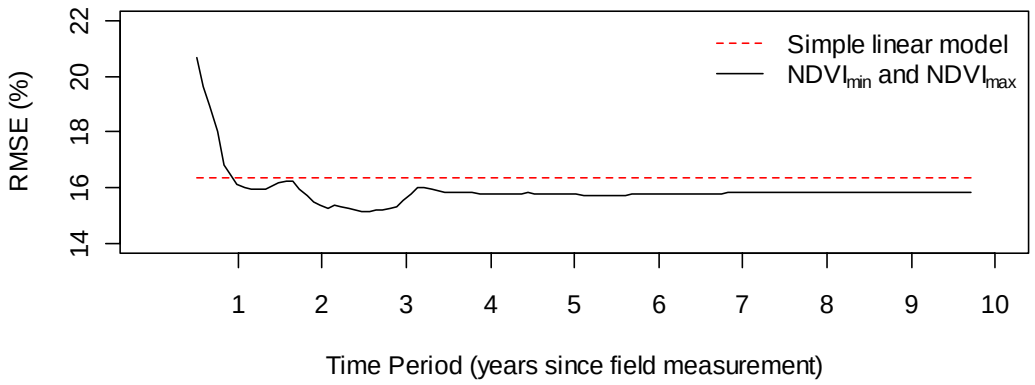

Figure 4.6: RMSE for the relative greenness model as the time period over which the minimum and maximum NDVI are assessed is increased. A constant RMSE of 16.4% for the simple linear model is shown as a red dashed line.

4.3.2 Normalisation with trend removed

Long-term trends in the NDVI may indicate changes in the fuel load in a region due to environmental or human influences. Changes in the species composition such as weed infestations may also influence the NDVI signal. Time series decomposition allows the separation of these longer-term trends from shorter-term changes such as seasonal curing cycles. There are a number of approaches used for time series decomposition. The simplest of these is to determine a trend component ($NDVI_T$) using a temporally broad moving average filter. This trend can then be removed (subtracted) and a seasonal component ($NDVI_S$) computed by averaging over all single year periods in the full time series. Once this seasonal signal is removed, the remainder ($NDVI_R$) shows the high frequency variations that are not attributable to either long-term trend or average seasonal variation. The original time series can be reconstructed through the summation of these individual components as follows:

$$NDVI(t) = NDVI_T(t) + NDVI_S(t) + NDVI_R(t)\,. \qquad (4.6)$$

One issue with this approach is that the trend component is truncated by half the width of the averaging filter. If we are interested in removing the trend at the current time step then it is possible to set up the averaging filter to only use previous values. However, this introduces a temporal lag in the trend component. Lu et al. (2003) suggest that Seasonal-Trend decomposition by LOESS (STL) developed by Cleveland et al. (1990) is a more appropriate method for the decomposition of NDVI time series since it is better able to deal with both noise and missing data. The approach uses a polynomial fit to the data with decreasing weights given to points as their temporal distance from the objective date increases. Extension of the trend to the edges of the time series is performed by a single-sided filter. However, the weighting of the filter means that the problem of lag introduced by single-sided averaging filters is minimised. An example decomposition of the Braidwood site using the STL approach with a one year filter width is shown in Figure 4.7.

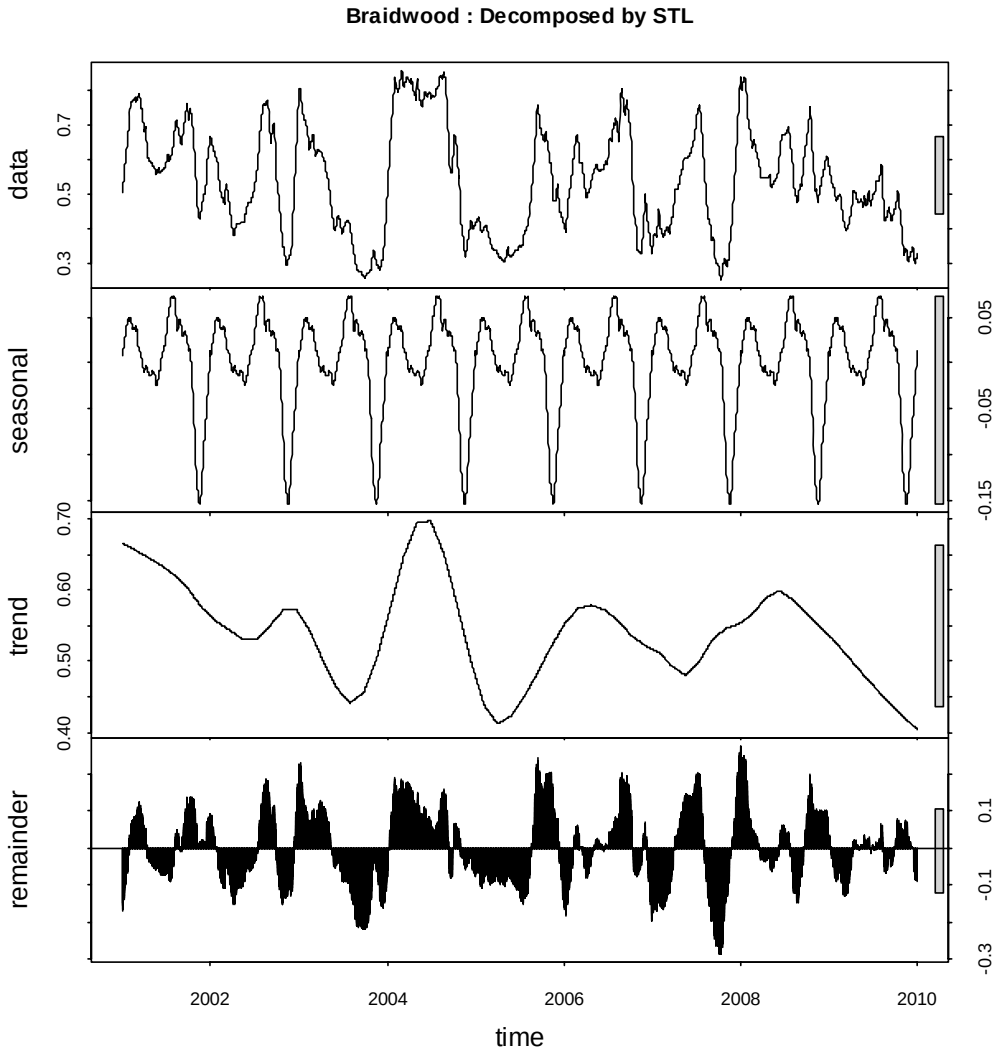

Figure 4.7: Decomposition of the NDVI time series for the Braidwood (NSW) site by the STL method with a filter width of one year.

The time series for each of the 25 sites were decomposed using the STL method and new time series constructed using the seasonal and remainder component as follows:

$$NDVI\_SR(t) = NDVI_S(t) + NDVI_R(t). \quad (4.7)$$

These data were then normalised using the relative greenness approach based on the minimum ($NDVI\_SR_{min}$) and maximum ($NDVI\_SR_{max}$) of this new trend-removed time series. Values from this new trend removed and normalised data corresponding to the dates of field measurement were then extracted to allow a regression against the Levy rod measurements. The resulting model produced a disappointing RMSE of 16.6% ($r^2 = 0.49$), which is an increase relative to the basic relative greenness approach. The pattern of the residuals (Figure 4.8) is similar to that of the relative greenness approach (see Figure 4.5) with a slightly exaggerated underestimation at higher curing levels.

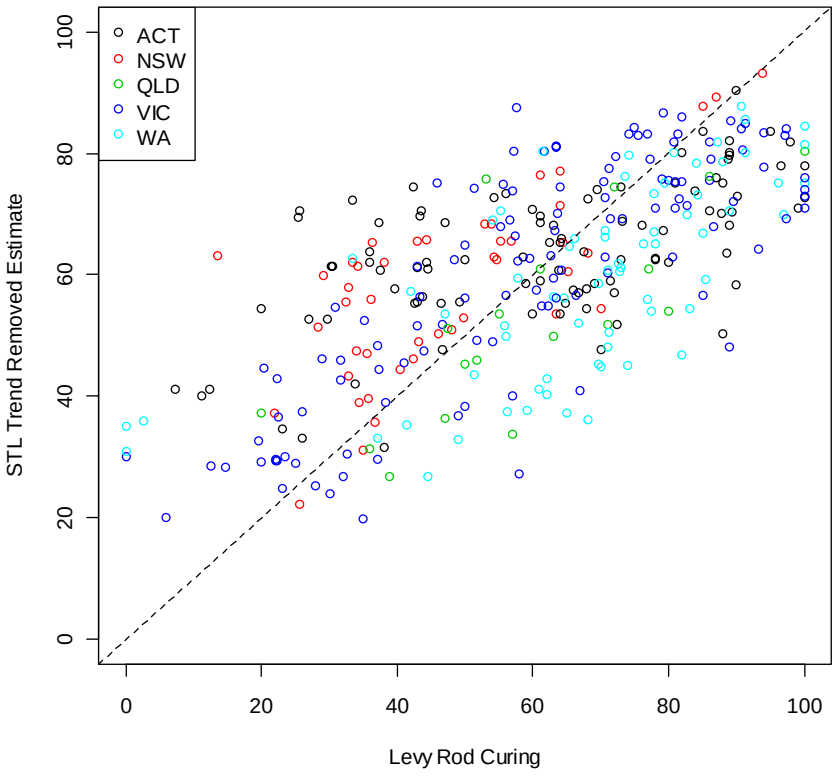

Figure 4.8: Levy rod curing data plotted against estimates derived from the trend removed time series data (r^2 = 0.49).

This may indicate that for our relatively short time series of ten years, the trend does contain information about the degree of curing and the approach may be more applicable in the case of longer time series over which land cover change is more pronounced.

4.3.3 Normalising by mean and standard deviation

The previous two sections deal with time series normalisation using minimum and maximum values, in the case of Section 4.3.1, from the time series itself and in the case of Section 4.3.2, from the sum of the seasonal and remainder components. The shortcoming of this approach is that a curing estimate becomes very sensitive to single minimum and maximum values, which may be subject to significant distortions due to undetected cloud or other atmospheric and sensor irregularities.

For the MOD09 dataset used here, every effort has been made to ensure that spurious values have been removed from each time series (see Section 3.2). However, it can be assumed that in an operational context, data errors will not always be detected automatically. It is prudent then to minimise the implications of these errors in the design and processing algorithm. The use of moments of the NDVI distribution, such as mean and standard deviation, has the effect of reducing the impact of data errors on the normalisation process. An error at the current time step will obviously have a dramatic effect on the curing estimate for that date, but the impact of such an error on subsequent curing estimates is limited to its contribution to the overall NDVI distribution, which in the case of a long time series is likely to be negligible.

Normalisation of the NDVI time series can be performed using the standard deviation of NDVI values in much the same manner as described by Eq. 4.4 for minima and maxima. In this case, in the absence of any validation data, we might assume that the mean NDVI for a time series (μ) corresponds to curing of 50% and that the extremes of curing occur at this mean value plus or minus three standard deviations (σ). In this case the equation for curing would take the form:

$$GCI = 100 \times \left(1 - \frac{NDVI - \mu + 3\sigma}{6\sigma} \right) + \varepsilon . \tag{4.8}$$

The constraint imposed by the assumption of a spread of exactly three standard deviations can be removed by introducing a fitted coefficient β_1 and that the mean NDVI equates to a curing of exactly 50% by introducing second coefficient β_2 as follows:

$$GCI = 100 \times \left(1 - \frac{NDVI - \mu - \beta_2 + \beta_1 \sigma}{2\beta_1 \sigma} \right). \tag{4.9}$$

This equation can be linearised as follows to allow linear least squares fitting of the coefficients:

$$GCI_{i,j} = 50 + \frac{\beta_2}{\beta_1} \left(\frac{50}{\sigma_j} \right) + \frac{1}{\beta_1} \left(\frac{50}{\sigma_j} (\mu_j - NDVI_{i,j}) \right) + \varepsilon_{i,j} , \tag{4.10}$$

where $GCI_{i,j}$ is the curing value for time step *i* at site *j*. Inversion of this equation using the field measured curing and MODIS NDVI yields the coefficients β_1 = 3.37 and β_1 = 0.07. However the RMSE for the model is only 18.91% which is less accurate than all previously discussed methods except the current operational non-linear model. Curing measurements from Western Australia and Queensland tended to be underestimated through the full range of curing, while measurements from the ACT, New South Wales and Victoria tended to be overestimated at low curing levels and underestimated at higher (>80%) curing levels.

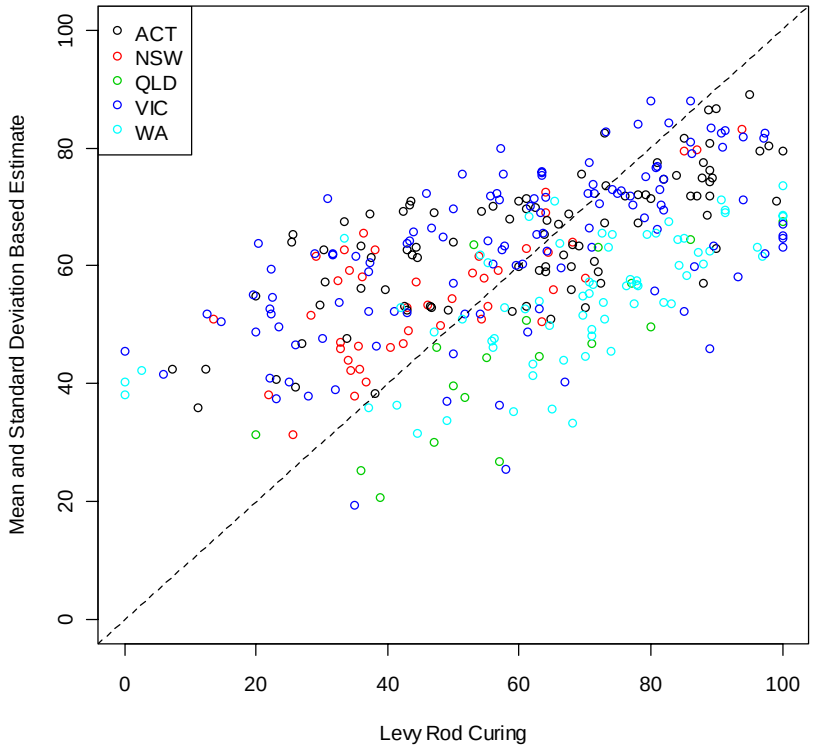

Figure 4.9: Levy rod curing data plotted against estimates based on the mean and standard deviation model.

4.4 NDVI TIME SERIES SUMMARY

This section has explored only a single spectral index (the NDVI) of the many that could be derived from the MOD09 product. The discussion illustrates some of the many ways that such an index could be treated in order to derive an estimate of curing. Results using the five methods discussed in this section are summarised in Table 4.2. These results indicate that when applied across our 25 field sites distributed across five states of Australia, the current operational non-linear curing algorithm performed least satisfactorily. However, all the methods tested suffer from a tendency to underestimate curing at high levels (> 80%). In contrast, despite greater uncertainty, the non-linear approach appears unbiased at these high curing levels.

Table 4.2: The root mean square error (RMSE) of curing estimates derived from several methods based on time series analysis of the NDVI.

Method	RMSE %
Non-linear model (Section 4.2.1)	18.97
Simple Linear model (Section 4.2.2)	16.37
Relative Greenness Regression (Section 4.3.1)	15.90
STL Trend Removed Regression (Section 4.3.2)	16.57
Mean and standard deviation model (Section 4.3.3)	18.91

The simple linear regression model is by far the easiest model to implement for operational mapping of grassland curing. However, this model also suffers from significant underestimation at curing levels greater than 80%, as shown by the mean error in Table 4.3.

Table 4.3: The errors of curing estimates for curing greater than 80%. RMSE gives an indication of the uncertainty in the estimate while the mean error indicates bias.

Method	RMSE (> 80%)	Mean Err (> 80%)
Non-linear model (Section 4.2.1)	19.62	-11.59
Simple Linear model (Section 4.2.2)	18.42	-16.19
Relative Greenness Regression (Section 4.3.1)	15.65	-12.66
STL Trend Removed Regression (Section 4.3.2)	17.63	-14.38
Mean and standard deviation model (Section 4.3.3)	21.23	-18.29

Normalisation of the data using historical minima and maxima for each satellite image pixel (referred to previously as relative greenness) produces a significant reduction in the overall error statistic relative to the non-linear model. Additionally, Table 4.3 shows that bias in the estimates at levels above 80% cured are slightly greater than that of the non-linear model but the certainty of the estimates at this level (random error) is significantly improved. This method does involve an increased computational overhead in an operational mapping system as, unlike the non-linear and simple linear modelling approaches, it requires access to and analysis of a time series of images. Empirical evidence indicates that that ideal length of this time series is of the order of two to three years.

Decomposition and removal of the trend component from the time series introduces significant computational overhead into the processing of data. As such, significant benefits would have to be shown to justify its inclusion in the operational system. The analysis here did not show an improvement in the overall accuracy of curing estimates from these methods over the basic relative greenness model.

The modified relative greenness approach developed in this section using mean and standard deviation of the NDVI did not result in a higher degree of accuracy in curing estimates. The model does reduce the sensitivity to single spurious measurements, which may be useful in an operational system, but the method requires more work to determine if the NDVI distribution can be adequately characterised using these parameters and over what period the distribution needs to be assessed.

The methods discussed in this section provide the basis for the extension of the analysis to other spectral domains and indices in the following section. Each of the methods discussed here can be applied to these other spectral domains with appropriate re-calibration to the field curing measurements. Clearly, the key methods to pursue in this analysis will be those that are operationally practical and provide increased accuracy relative to the existing non-linear model. Primarily these are the simple linear approach and the relative greenness approach using normalisation by pixel minima and maxima.

5. SPECTRAL METHODS

The measurement of spectral signatures (the variation of reflectance with wavelength) at a single time is a key remote sensing technique for characterising the nature and state of vegetation. While NDVI has been a common satellite-derived parameter for monitoring vegetation state, MODIS offers a broad suite of products that are sensitive to various aspects of plant physiology and have varying sensitivity to confounding effects such as bare soil and soil wetness. This section explores MODIS alternatives to NDVI that might better estimate curing. Such alternatives can be used with or without the temporal normalisation techniques developed in the previous section.

This section begins by outlining the spectral characteristics of vegetation and their response to senescence. It goes on to describe the response of field-measured spectra, MODIS multispectral reflectance and MODIS vegetation indices to variations in the degree of curing. The section concludes by recommending four candidate models for implementation in a pilot system designed to map curing over the landscape.

The background information, relevant literature and results presented in this section are presented in more detail by Martin (2010).

5.1 REVIEW OF SPECTRAL APPROACHES

The reflectance spectrum of green vegetation is characterised by low reflectance in the visible MODIS bands 1, 3 and 4 and short wave infrared (SWIR) bands 6 and 7, due to pigment and water absorption, and high reflectance in the near infrared (NIR) bands 2 and 5 due to significant scattering within the vegetation cell structure. The plant physiology behind these features and their response to curing is outlined here.

The low reflectance in the visible spectrum is due to leaf pigments, primarily chlorophylls. The leaves of vigorously growing plants are characterised by high chlorophyll concentrations, resulting in high absorption in the red and blue wavelengths (MODIS bands 1 and 3 respectively). As leaves cure, chlorophyll levels decline.

In the NIR (MODIS bands 2 and 5), there is little or no light absorbed by pigments, resulting in a region of high reflectance from 750 to 1300 nm. As curing commences, lack of moisture causes the internal leaf volume to decline and the number of cell interfaces to increase, resulting in a rise in NIR scattering and hence reflectance. In the later stages of senescence, the NIR reflectance eventually decreases, owing to the breakdown of cell walls. Vegetation water content generally controls the reflectance spectra in the SWIR wavelengths around 1450, 1950 and 2250 nm, influencing MODIS bands 6 and 7. Leaf reflectance in these bands is therefore inversely related to water content.

The development of satellite-based methods to characterise soil and vegetation has generally concentrated on the visible and NIR regions of the spectrum. A common and simple approach is to formulate a vegetation index, which is a combination of spectral bands designed to maximise sensitivity to a vegetation feature of interest while minimising the influence of confounding variables. The NDVI was one of the earliest indices used to assess vegetation amount and greenness. Other vegetation indices were subsequently developed to minimise secondary effects such as variations in soil background or the atmosphere. More recently, the richer spectral information

provided by sensors such as MODIS has stimulated the development of remote sensing approaches that are sensitive to a broader range of vegetation characteristics. In particular, the sensitivity of the MODIS SWIR bands to vegetation water content has been of interest.

5.2 FIELD SPECTROMETRY AND CURING

Field spectrometry was conducted at the Caldermeade and Kaduna sites over the 2007/08 summer in order to study the relationship between ground-measured reflectance spectra and curing. An ASD (Analytical Spectral Devices Inc. Boulder, CO, USA) Fieldspec 3 portable spectroradiometer was used, together with a Spectralon® white reference panel, to measure reflectance spectra over the wavelength range 350 to 2500 nm. Measurements were made roughly fortnightly, at multiple points along the same transects used for the Levy rod measurements.

Figure 5.1 shows that as curing progresses, reflectance tends to increase in the visible, decrease in the NIR, and increase in the SWIR. This follows the expected behaviour, based on the literature as:

- in the visible, chlorophyll content decreases as a result of curing and hence light absorption decreases;
- in the NIR, leaf internal structure breaks down as curing progresses, decreasing reflectance; and
- in the SWIR, leaf moisture content decreases with curing resulting in decreased absorption.

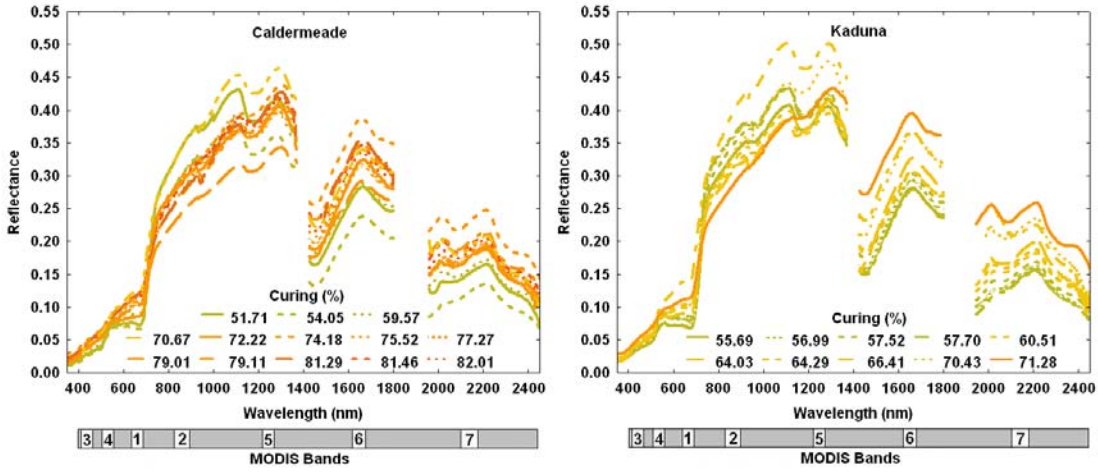

Figure 5.1: Reflectance spectra at Caldermeade and Kaduna recorded during the 2007/08 season. The colour and line style indicate the level of curing at the time of the measurement, as specified by the legend at the bottom. A bar across the bottom of the graph indicates the positions of the seven MODIS land bands.

To assess the sensitivity of the measured reflectance to curing, the ASD spectra were correlated with Levy Rod curing estimates at individual wavelengths from 350 to 2450 nm. Figure 5.2 shows the correlation coefficient at each measured wavelength, with the wavelength regions of significant correlations ($p < 0.05$) shaded in grey. The plots have gaps where data was removed at wavelength where atmospheric water causes very low signal to noise ratio. A spectral region around MODIS band 1 (red) is the only one that gives significant correlations at both sites. This is not surprising as it is the region most sensitive to chlorophyll.

Caldermeade also shows significant correlations with curing throughout the entire visible region (MODIS bands 3 and 4) and in the SWIR water absorption regions (MODIS bands 6 and 7). Kaduna shows significant correlation only in the visible red (MODIS band 1) and in a region from around 1150nm to 1200nm which is near a weak water absorption band and is not measured by any of the MODIS sensor bands. To summarise the results from these two sites:

- of the wavelength regions corresponding to MODIS reflectance bands, band 1 has the strongest and most consistent correlation to curing;
- although not significant (at the 95% confidence level) the other visible bands (3 and 4) generally show a strong positive correlation;
- the band 2 NIR region and the main SWIR water absorption bands 6 and 7 show positive correlations of variable strength;
- band 5 appears to have an inconsistent relationship to curing.

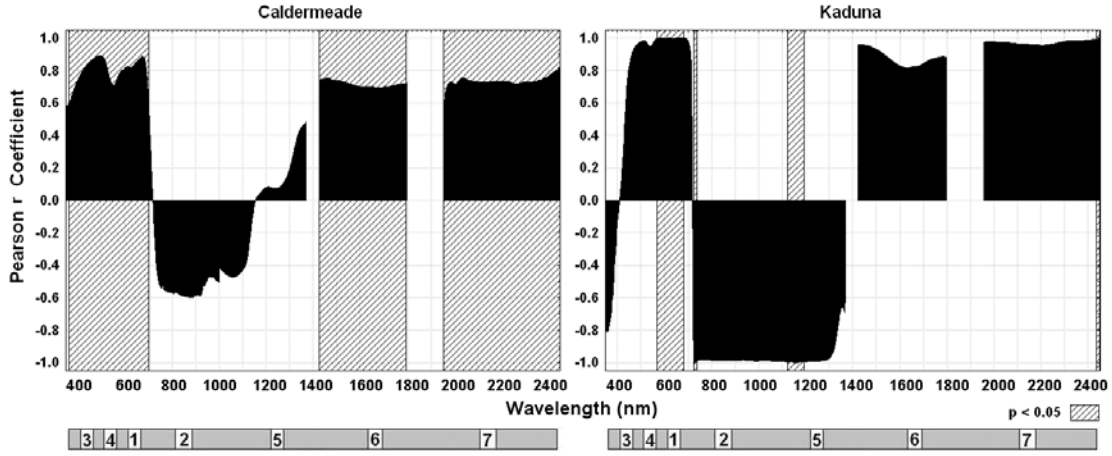

Figure 5.2: Correlation coefficients between Levy rod curing and field spectrometer based reflectance at wavelengths from 350 to 2500 nm. Grey shaded regions indicate significance ($p<0.05$). The locations of the MODIS land bands are indicated along the bottom.

5.3 SITE HOMOGENEITY AT THE MODIS SCALE

When relating satellite observations to field measurements, a recurring issue is the mismatch in spatial scale. In this project, Levy rod curing, destructive curing and spectrometer measurements are averages over two 20m transects, while MODIS pixels consider an area of 500m by 500m. Thus field sites need to be homogeneous over the scale of at least one MODIS pixel to ensure that the field measurements are representative of the satellite scale. A somewhat larger region will allow for an inherent uncertainty in the pixel location.

In a fragmented landscape, spatial uncertainty and the so called adjacency effect (Kaufman, 1982) can cause mixing of the reflectance signal between different land cover types. Some of the curing field sites were located in significantly fragmented landscapes. This section describes assessment of site homogeneity and selection of MODIS pixel locations for each field site that better represented the degree of curing in the region.

5.3.1 Site Homogeneity assessment by Landsat

To assess the homogeneity of each field site, a 30-m resolution Landsat NDVI image was analysed. These images were from the set collated for mapping of woody vegetation by the Australian Greenhouse Office, and tended to be on dates when grass was cured in order to maximise the contrast between trees and grassland/crop/pasture. This

timing suits the assessment of curing field sites, where trees are a key contaminant to be detected, along with bare soil, burned areas, water bodies and built areas. The images were taken from July 1999 to September 2000, and had been radiometrically and geometrically corrected.

On the basis of the Landsat NDVI images, a region 500 m × 500 m square of near uniform grassland near each ground sampling location was selected, where possible with a surrounding buffer of grassland of up to 500 m width. MODIS data from the single 500-m pixel nearest the centre of this location was then associated with the ground samples. While an average over a 3×3 pixel window is frequently used for satellite-ground comparisons to reduce the impact of geo-referencing errors (e.g. Yebra et al., 2008), the curing field sites used in this study showed considerable heterogeneity over this 1.5 km × 1.5 km area, and the NDVI correlations of Section 0 showed there is no significant benefit from using this expanded window.

The within pixel uniformity was quantified by calculating two measures from the Landsat images:

- within-pixel NDVI variation for a 500m square area, to quantify how representative a field site may be of the complete MODIS pixel and;
- between-pixel variation across a 3×3 set of 500-m pixels, where each pixel is the mean of the Landsat values within a 500-m square, to assess the impact of georeferencing variations on MODIS-scale measurements.

Variation is expressed using the coefficient of variation (CV); that is, the standard deviation divided by the mean. Figure 5.3 shows the Landsat image for Lakefield with the boundaries of a 3×3 window of 500-m pixels shown both centred on the field sampling location, and centred on the MODIS location adopted to avoid tree cover (as indicated by high NDVI). The within-pixel and between-pixel CVs for the Australian sites are given in Figure 5.4, as calculated for the pixel window after being centred on the field sampling location. For most field sites the within-pixel CV is around 10%, while the between-pixel CV is 5-10%.

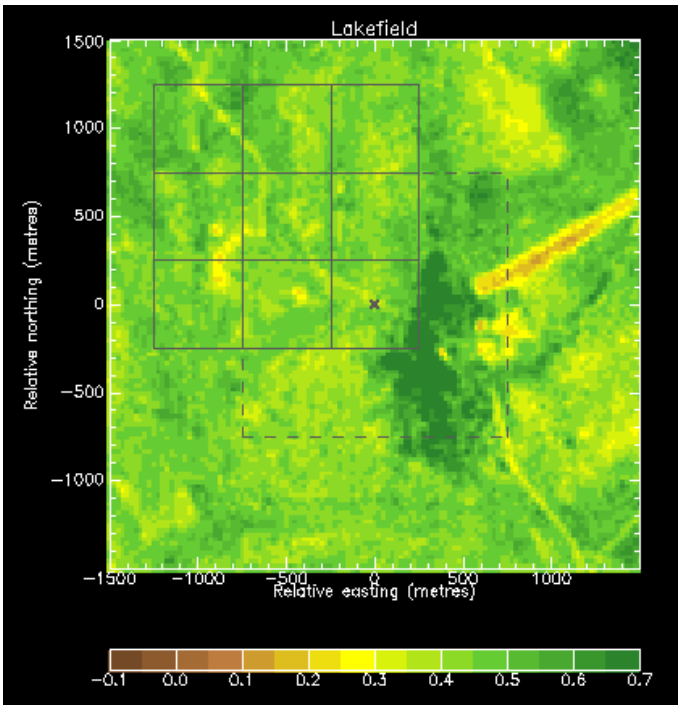

Figure 5.3: Landsat NDVI image for Lakefield. A cross at the centre marks the field sampling location. The solid grid is the 3×3 set of 500-m pixels centred on the adopted MODIS sampling location. The dashed lines mark the boundary of the grid when centred on the field sampling location.

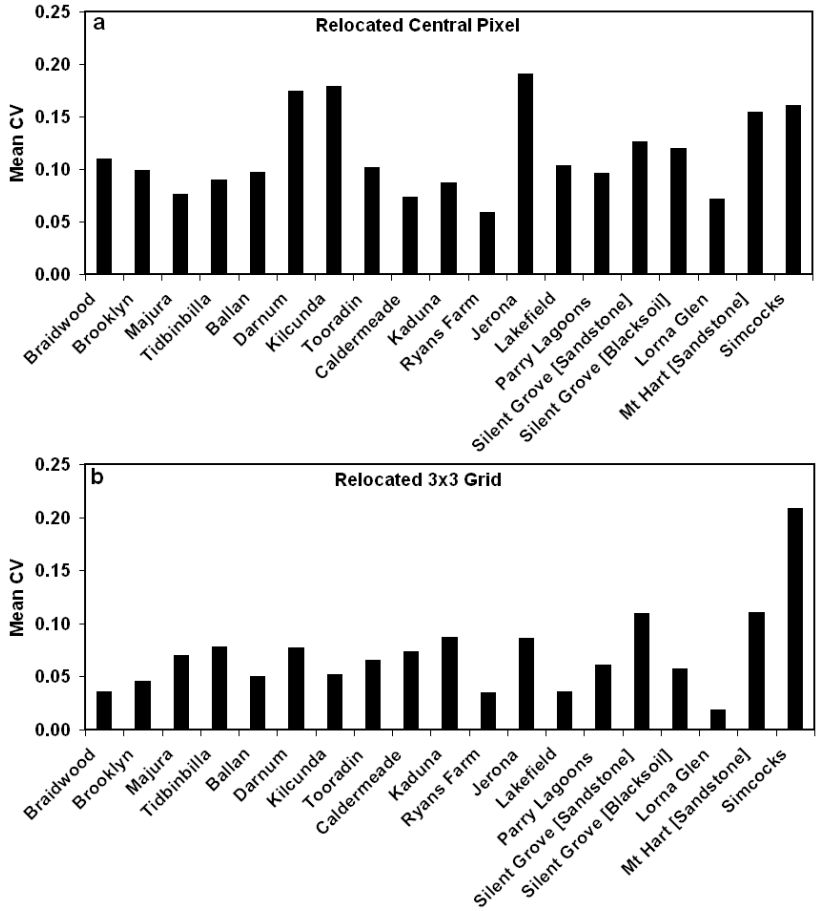

Figure 5.4: The coefficient of variation of the relocated central pixel and the coefficient of variation (across all nine pixels) of the relocated 3×3 pixel window at each Australian field site.

5.3.2 Site Homogeneity assessment by field spectra

The two sites at which ground based reflectance spectra were measured offered a second approach to assessing how representative field measurements were of corresponding MODIS observations. The ground-based spectra measured by the ASD spectrometer were resampled to the seven MODIS land bands using MODIS spectral response functions (Figure 3.3). These resampled reflectance data were compared to the closest date of MODIS data. The results (Figure 5.5) demonstrate a good agreement with little systematic or random errors apparent. This indicates that:

- MOD09, which is the result of an atmospheric correction, provides an accurate indication of surface reflectance;
- site homogeneity and the sampling methodology employed is adequate to overcome variations in the spatial scales of the measurements;
- by implication, the Levy rod curing measurements are representative of the MODIS scale, because they were taken along the same transects as the field spectrometer measurements.

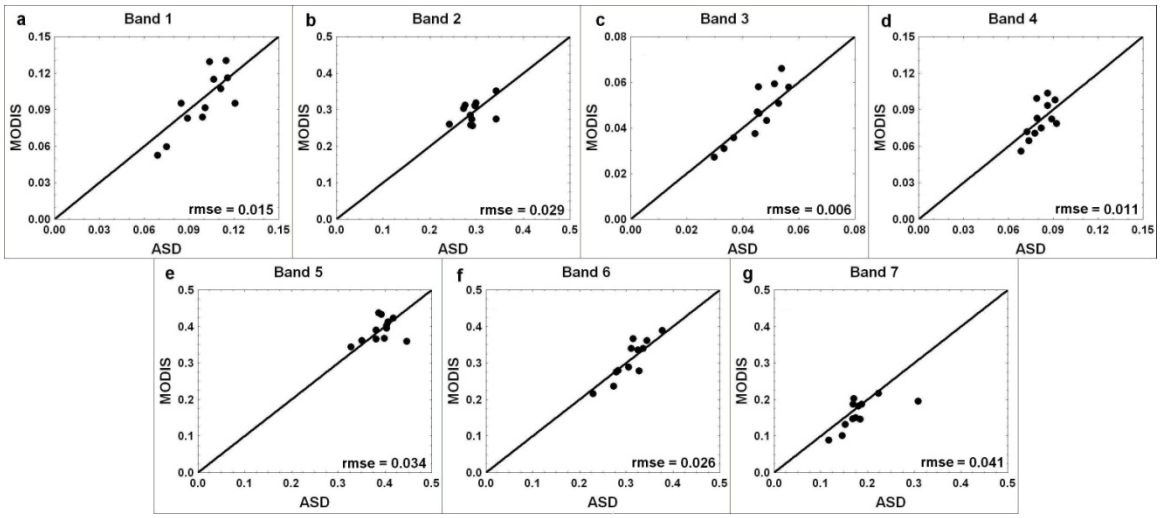

Figure 5.5: Comparison between the reflectance in each MODIS band (MOD09) and synthesised MODIS reflectance using field-measured ASD spectra at the Caldermeade site.

5.4 RELATIONSHIP BETWEEN MULTISPECTRAL MODIS DATA AND CURING

The method to estimate curing using the seven MOD09 bands was explored using single band correlations, vegetation indices and multiple regression relationships. Plots are shown here for one site, Tidbinbilla in NSW, as examples.

5.4.1 Correlation between reflectance and curing

The Levy rod curing estimates are plotted against the MOD09 reflectance in each band: for Tidbinbilla in Figure 5.6, and for all sites, grouped into four grass types, in Figure 5.7. The single Hummock grass site has been treated separately due to a clear distinction in its behaviour from other native grassland sites. As with the behaviour of the reflectance spectrum measurements at Caldermeade discussed in Section 5.2, the bands associated with chlorophyll (1, 3 and 4) and water (6 and 7) absorption were positively correlated with curing; band 2 associated with leaf internal structure, was negatively correlated, and band 5 showed no significant correlation.

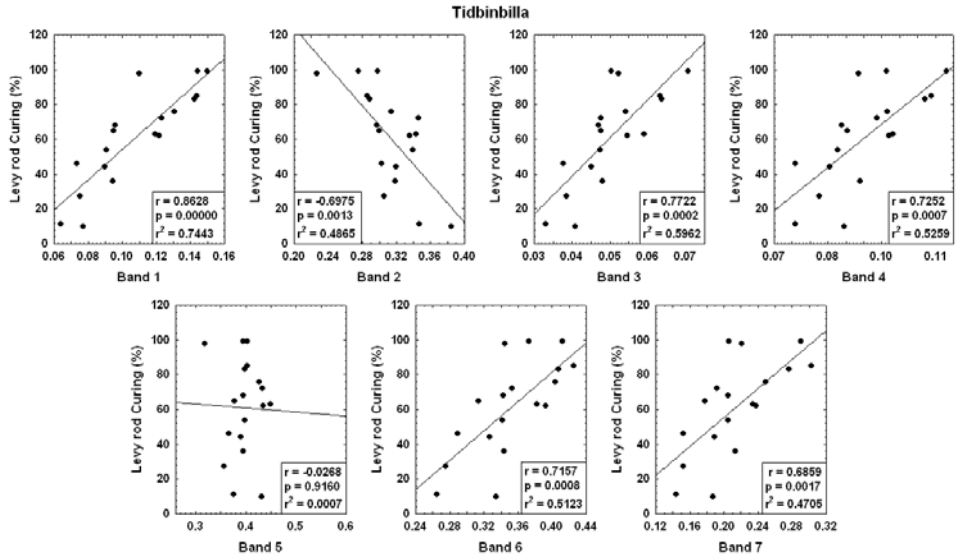

Figure 5.6: Comparisons of MOD09 bands with Levy rod curing at Tidbinbilla (ACT).

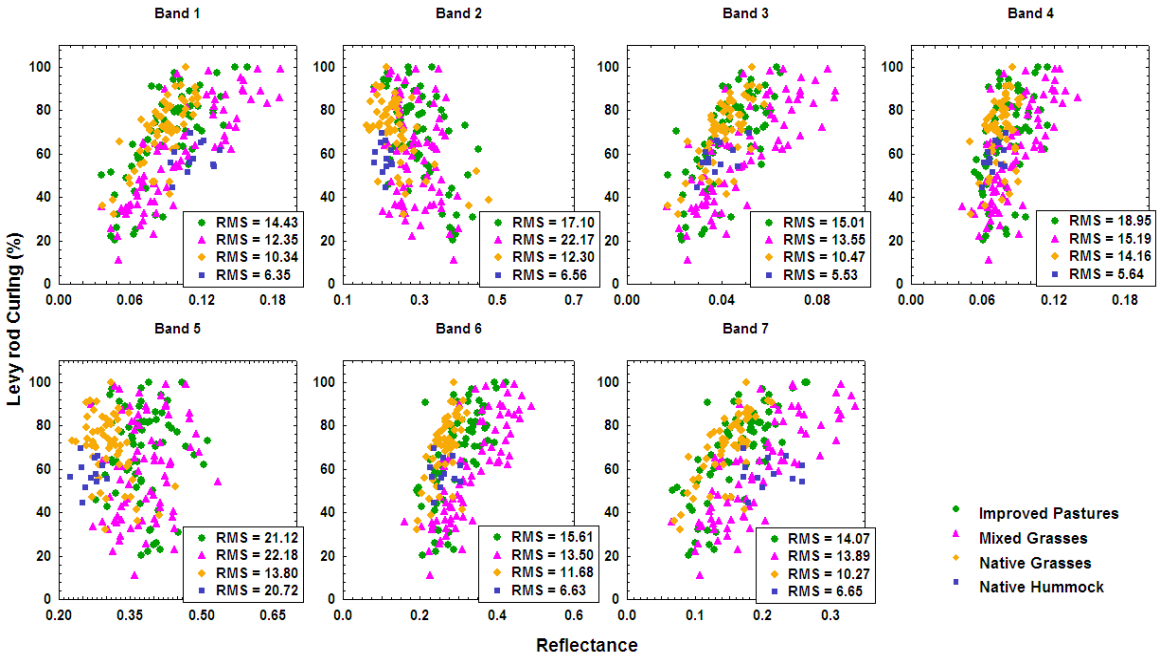

Figure 5.7: Comparisons of MOD09 bands with Levy rod curing for four grass types in all Australian sites.

All four grass types show similar behaviour, although their location within the Figure 5.7 plots differs. For instance, in band 3 and 6 mixed grasses separate out well across a wide range of curing levels.

5.4.2 Correlation between spectral indices and curing

A large number of spectral vegetation indices were computed from the MOD09 reflectance bands. After initial evaluation, the 25 indices defined in Appendix A were investigated for their correlation with curing. These indices generally fall into one of three groups: chlorophyll sensitive indices, soil adjusted indices, or water indices. Figure

5.8 illustrates the relationship between these indices and curing for all Australian sites, grouped by grass type. No index stands out as performing markedly better than the others, although many indices show stronger correlations than individual reflectance bands.

The lack of a clear preference for an index is borne out by similar analyses at individual sites (not shown). While some individual sites show preferences, the ranking is not consistent between sites and the interpretation is not straightforward. At sites where NDVI is not the best index, a soil-corrected or water index often performs well. This may be an indication of low biomass (or low grass cover proportion) at these sites, with little greening up being detectable by the MODIS instrument.

Figure 5.9 shows the RMSE for a regression over all Australian sites for each index. Because the single hummock grass site (Lorna Glen) generally stands apart in the plots of Figure 5.8, Figure 5.9 also shows the RMSE values calculated over all sites except Lorna Glen. Finally, in order to evaluate performance at high curing levels (the most critical range for operations), Figure 5.9 also shows RMSE values of the regressions on the sample subset with Levy rod curing exceeding 60%. This supports the observation that several indices have close to the best performance. As a reference value for later results, NDVI has an RMSE value of 11.8% over all sites except Lorna Glen and over the entire curing range, second only to the slightly better mNDVI.

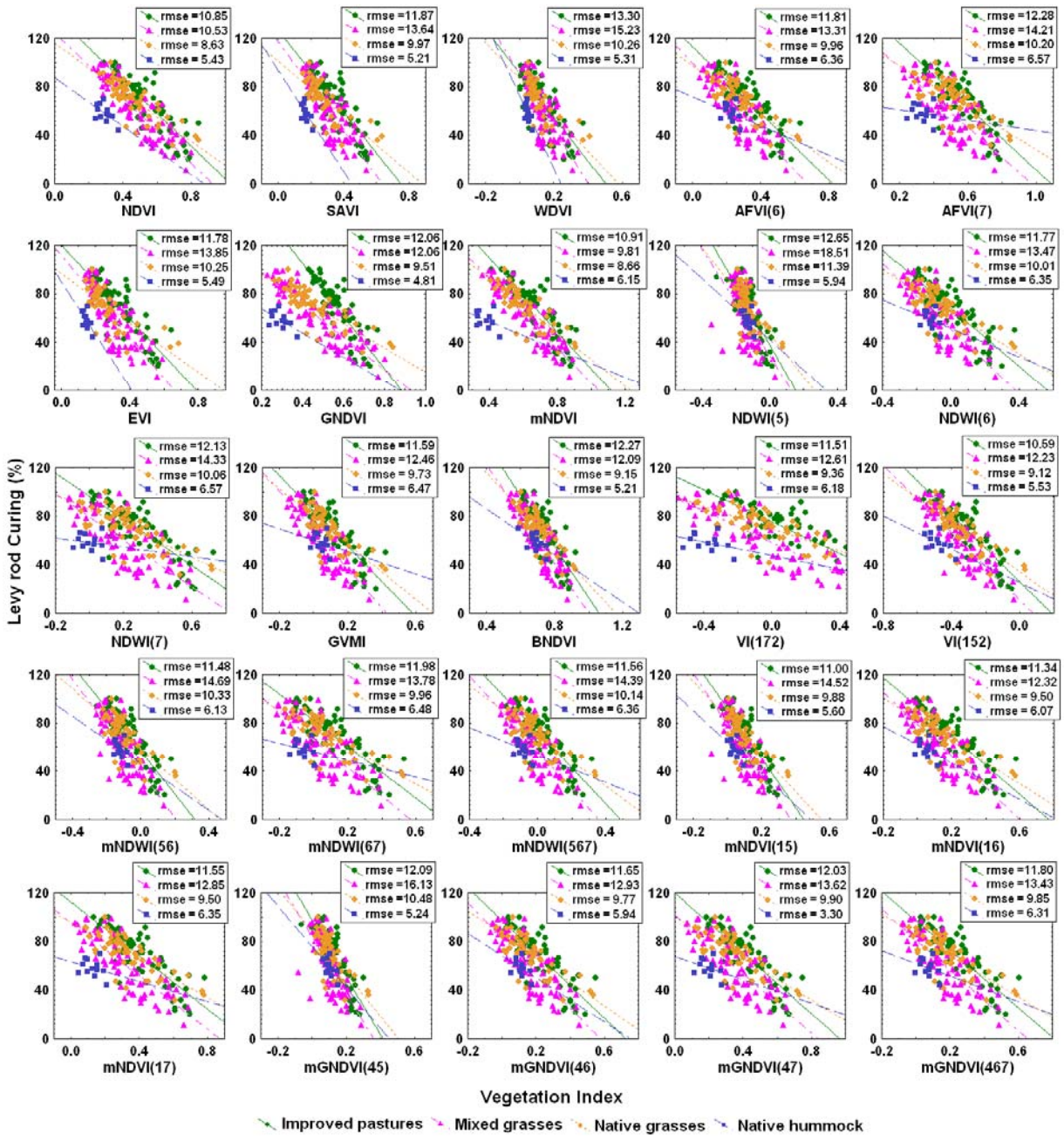

Figure 5.8: Relationship between Levy rod curing and 25 vegetation indices for four grass types in Australia.

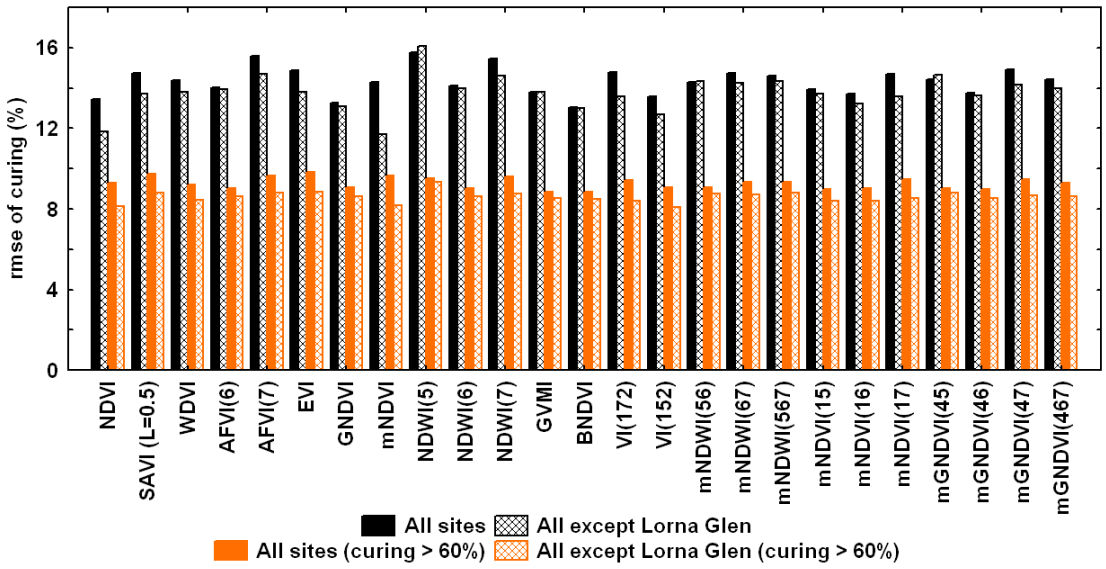

Figure 5.9: RMSE of Levy rod curing against 25 vegetation indices for all Australian sites, with and without Lorna Glen, and using either all data or only data relating to curing greater than 60%.

5.4.3 Correlation between normalised spectral indices and curing

The benefit of the temporal normalisation detailed in Section 4 was investigated for a small number of representative vegetation indices. A commonly used index was selected from each of three groups: NDVI for the simple chlorophyll-sensitive indices, SAVI for the soil adjusted indices, and NDWI(7) for the water indices. The Green NDVI (GNDVI) was also included because it performed the best by a significant margin for the single hummock grass site. The expressions for these vegetation indices, in terms of the MODIS surface reflectance R_i in bands i = 1 to 7, are:

$$NDVI = \frac{R_2 - R_1}{R_2 + R_1} \tag{5.1}$$

$$SAVI = \frac{R_2 - R_1}{R_2 + R_1 + 0.5} 1.5 \tag{5.2}$$

$$NDWI(7) = \frac{R_2 - R_7}{R_2 + R_7} \tag{5.3}$$

$$GNDVI = \frac{R_2 - R_4}{R_2 + R_4} . \tag{5.4}$$

As discussed in Section 4, the relative greenness approach is a method to place a spectral index in the context of the historical variation for a given pixel. It was show that this approach could be used to improve the accuracy of

curing estimates when applied to the NDVI. For each of the four indices shown above, a relative greenness variant was computed, based on the minimum and maximum values of the index from 3.5 years of cleaned MOD09 data at the site. The four basic indices and the four corresponding temporally normalised versions resulted in eight separate potential predictor variables that could be evaluated for their performance in predicting the field based estimates of curing.

Linear regression models were constructed using these eight indices for each of the four grassland categories (improved pasture, native, mixed, hummock). Further, aggregated models for all Australian sites were also produced. Scatter plots of Levy rod curing versus NDVI and normalised SAVI ("nSAVI") are shown in Figure 5.10 and Figure 5.11, while the RMSE for the eight indices and over each of the grassland categories is summarised in Table 5.1.

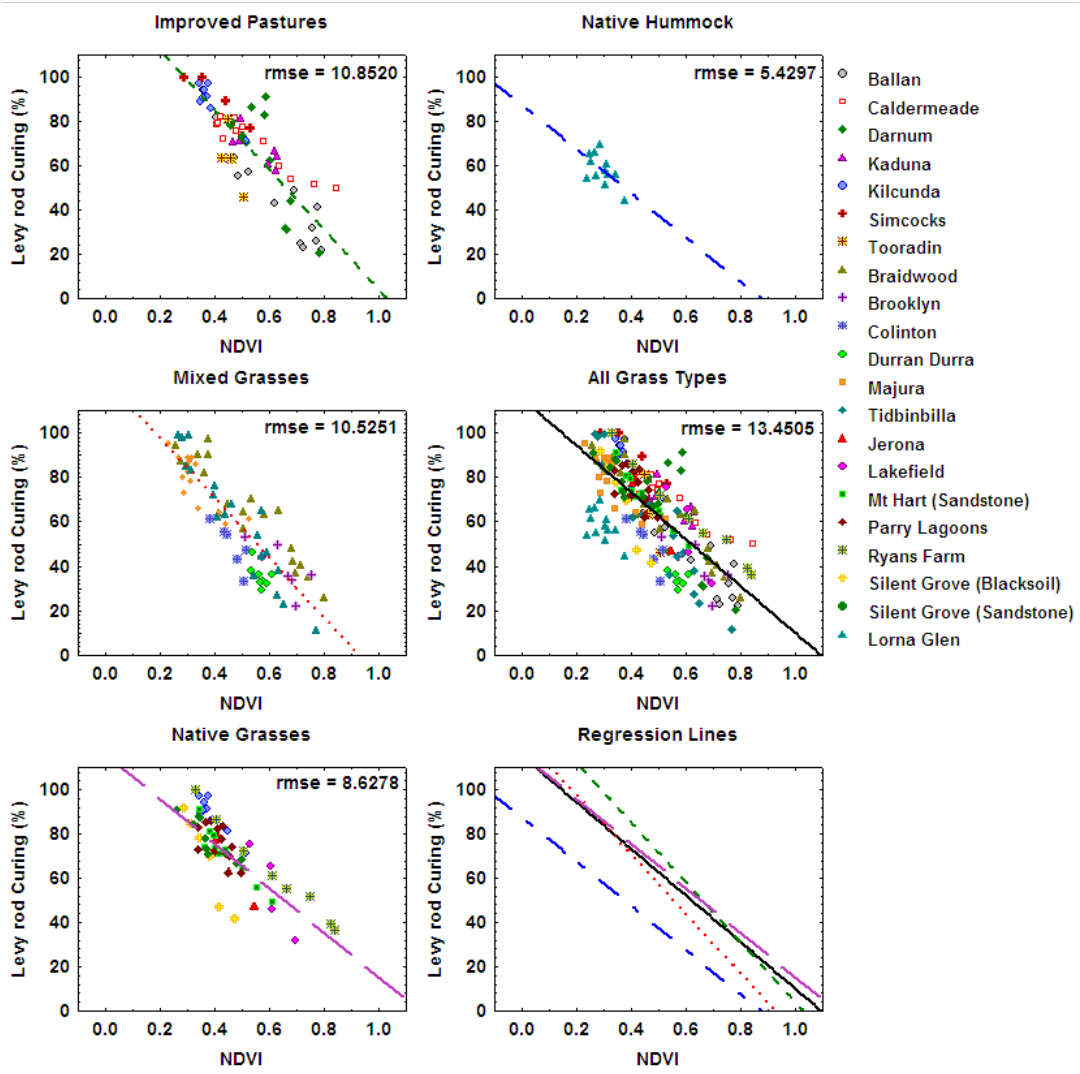

Figure 5.10: Regressions of Levy rod curing against NDVI for Australian sites grouped into four grassland categories, and all grass types together. The bottom-right panel overlays the regression lines from the other five panels for comparison.

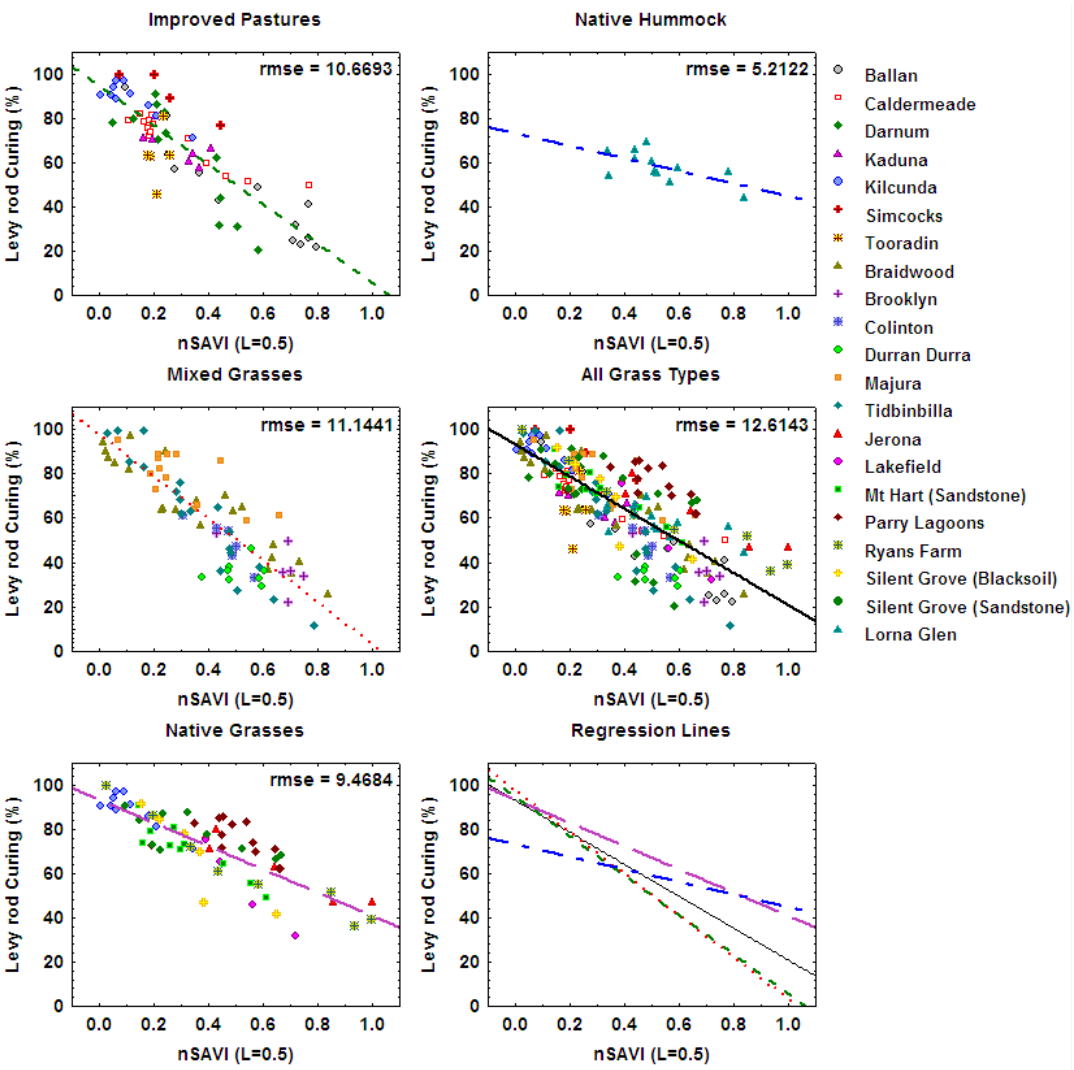

Figure 5.11: Regressions of Levy rod curing against normalised SAVI (L = 0.5) for Australian sites grouped into four grassland categories, and all grass types together. The bottom-right panel overlays the regression lines from the other five panels for comparison.

Table 5.1: RMSE values for curing predictions with four vegetation indices (original and normalised) for each grass type.

Vegetation Index	Improved Pastures	Mixed Grasses	Native Grasses	Native Hummock	All Grass Types
NDVI	10.85	10.53	8.63	5.43	13.45
nNDVI	11.28	9.81	9.10	5.43	12.90
SAVI	11.87	13.64	9.97	5.21	14.76
nSAVI	10.67	11.14	9.47	5.21	12.61
NDWI(7)	12.13	14.33	10.06	6.57	15.45
nNDWI(7)	12.14	14.07	10.27	6.57	14.22

GNDVI	12.06	12.06	9.51	4.81	13.29
nGNDVI	13.09	13.17	10.28	4.81	14.95

The relative greenness based nSAVI performed the best over the whole Australian dataset (RMSE = 12.6%) and particularly well in improved pastures (RMSE = 10.7%). NDVI was the best performer for native grasses (RMSE = 8.6%), and has a performance close to that of the best index for other grass categories. Although the NDVI performed slightly better in the native and mixed categories, the fact that the nSAVI was more broadly applicable may make it a stronger candidate for use in regions unrepresented by field data, given that the intention is to extrapolate over all of Australia and New Zealand.

5.4.4 Multiple linear regressions

The final analysis of this section examines the performance of combinations of raw reflectance bands and vegetation indices in predicting the degree of curing. Multiple linear regressions (MLRs) of Levy rod curing against 200 combinations of MODIS bands and indices were assessed. Increasing the number of parameters in the regression model invariably reduces the RMSE through the inclusion of random correlation but also increases the complexity of the predictive model. The regressions were ranked by the Bayesian information criterion (BIC) which balances these two factors. Figure 5.12 shows the RMSE values for the twenty MLR models with the highest BIC ranking. These models use no more than three parameters, exhibit low BIC scores, and predict curing with RMSE values under 11% for the complete time series and curing greater than 60%. Here, the exclusion of the Lorna Glen site from the complete time series does not significantly change the magnitude of the errors.

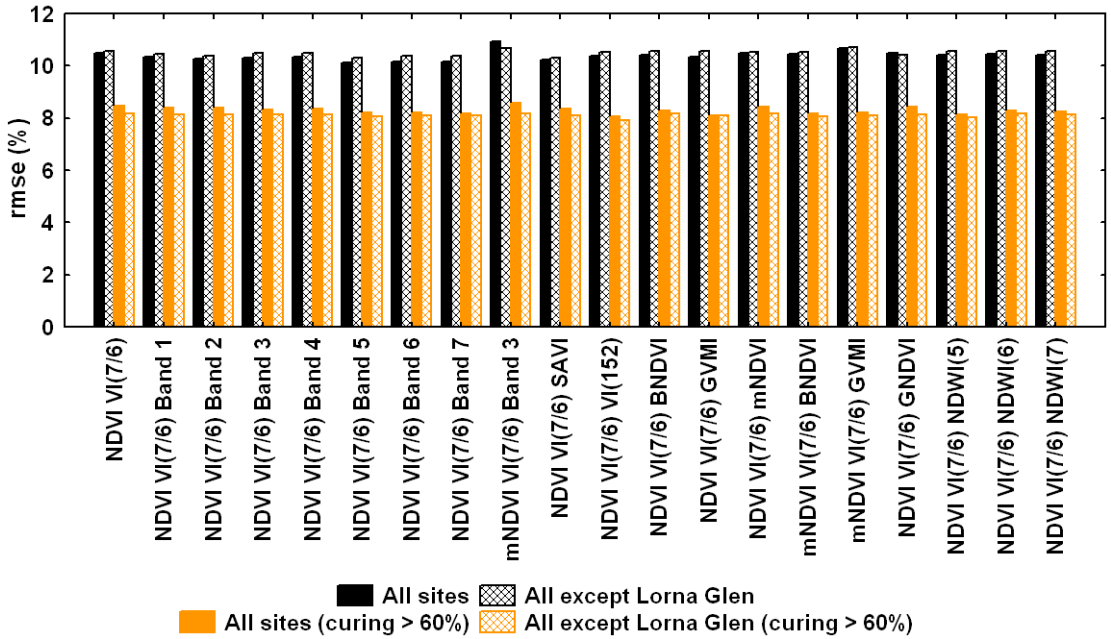

Figure 5.12: RMSE of twenty multiple linear regressions of Levy rod curing for all Australian sites, with and without Lorna Glen, and for the complete time series and the critical curing period. The groups of columns are labelled by the regression parameters: either two or three parameters.

The spectral vegetation index VI(7/6) which appears in each of the twenty best MLR models deserves special mention. CSIRO has developed a method to estimate the fractional cover of photosynthetic (green) vegetation (*PV*), non-photosynthetic (dead) vegetation (*NPV*) and bare soil (*BS*), using NDVI and the ratio of MODIS bands 7 and 6 (Guerschman et al., 2009). The ratio of bands 7 and 6 is designed to discriminate between dead vegetation and bare soil, which NDVI does not. Curing is effectively the ratio *NPV* / (*NPV*+*PV*), and Guerschman et al. (2009) tested their approach with Levy rod data from ten of the curing project field sites. While this estimate generally tracked the temporal variation of curing well, at several sites it showed systematic variations of up to 50%. Nevertheless, this demonstrated that the ratio of bands 7 and 6 is useful in assessing the live and dead vegetation fractions in at least some situations. This, along with the results shown in Figure 5.12 supports its inclusion in the further analysis.

5.5 FINAL AUSTRALIAN CURING MODELS

Four models to estimate curing from MODIS data were selected on the basis of the results in this section, which are in turn built on the results of previous sections. Regression against NDVI was selected because NDVI is the most established index of vegetation greenness, and its performance for curing prediction was close to the best for single vegetation indices. Temporally normalised NDVI was selected as the simplest use of temporal normalisation to mitigate the impact of non-curing related land cover variations. Normalised SAVI was selected as an additional normalised index that potentially offered better resistance to exposed soil than normalised NDVI. Finally, the multiple regression against NDVI and the ratio of bands 7 and 6 was selected as the best two-parameter multiple regression, with a performance almost as good as the best three-parameter multiple regression, and offering a spectral alternative to normalisation as a method for mitigating the effect of variations in land cover.

Thus the four models to predict grassland curing index (*GCI*) are:

A. linear regression against NDVI

$$GCI = 124.71 - 121.4 \times NDVI \tag{5.5}$$

B. multiple linear regression against NDVI and the ratio of bands 7 and 6

$$GCI = 237.308 - 190.139 \times NDVI - 142.655 \times \frac{R_7}{R_6} \tag{5.6}$$

C. linear regression against NDVI normalised using three years of NDVI data

$$GCI = 93.274 - 61.896 \times \frac{NDVI - NDVI_{\min}}{NDVI_{\max} - NDVI_{\min}} \tag{5.7}$$

D. linear regression against SAVI normalised using three years of SAVI data

$$GCI = 93.347 - 73.776 \times \frac{SAVI - SAVI_{\min}}{SAVI_{\max} - SAVI_{\min}} . \tag{5.8}$$

The two vegetation indices used are calculated from MODIS MOD09 surface reflectance as follows:

$$NDVI = \frac{R_2 - R_1}{R_2 + R_1} \tag{5.9}$$

$$SAVI = \frac{R_2 - R_1}{R_2 + R_1 + 0.5} 1.5 \ . \tag{5.10}$$

The temporal normalisation extremes $NDVI_{min}$, $NDVI_{max}$, $SAVI_{min}$ and $SAVI_{max}$ are the minimum and maximum of NDVI and SAVI respectively over this nearly four year period. The model coefficients are derived from regressions on the Levy rod and MODIS data falling within the period January 2005 to October 2008, combining all Australian sites except Lorna Glen. Table 0.2 lists the RMSE for these models.

Table 0.2: RMSE values for curing predictions from the four candidate models.

.Model	RMSE (%)
A	11.90
B	10.54
C	13.26
D	12.97

These four models are the recommended methods for estimating curing when performance is assessed using the data collected at the project field sites. However, the variety of landscapes sampled by the project is very limited. Considerable variation across the wider landscape is expected to influence these models to different degrees through effects such as species composition, cover fraction, and soil type. For this reason, landscape level validation is required in order to determine the best approach for an operational system to map curing using satellite data. Sections 7 and 8 describe a pilot trial conducted in collaboration with regional fire agencies designed to achieve this aim.

6. NEW ZEALAND CURING DATA ANALYSIS

The analysis of spectral methods for curing assessment in Australia concluded that a pilot system for mapping grassland curing should be developed and that four empirical models should be trialled. These models provide a best fit to field measurements of curing in Australia using:

A. linear regression against NDVI;
B. multiple linear regression against NDVI and the ratio of MODIS band 7 and 6;
C. linear regression against a temporally normalised NDVI; or
D. linear regression against a temporally normalised SAVI;

In this section we evaluate the performance of these Australian models using curing measurements recorded in New Zealand grasslands. We then compute new linear regression coefficients for these models specific to the New Zealand data and compare the estimates from both models.

6.1 NEW ZEALAND FIELD COLLECTION SITES

Ten field sites were set up specifically for grass curing satellite data calibration across both the North and South Islands of New Zealand. Over all sites, 194 Levy Rod measurements were recorded between 2005 and 2009. A longer history of destructive curing measurements was also available for these sites, along with two additional sites where Levy Rod measurements were not recorded. Destructive and Levy based measurements were integrated to give an enhanced dataset of 279 curing measurements. In cases where Levy and destructive measurements were recorded concurrently, the destructive measurements were considered to have precedence and the Levy rod measurement was ignored.

Table 6.1: Details of the 12 sites used in the New Zealand component of the analysis, including the New Zealand climate zone code and the grassland type (NG = native, IP = improved pasture and MX = mixture of native and exotic) and the number of Levy rod, destructive and combined (where destructive takes precedence over Levy) curing measurements.

Site Name	Latitude	Longitude	Climate Zone	Grass Type	Levy	Dest	Comb
Acheron	-42°06'03.60"	173°08'02.40"	C1	MX	11	0	11
Burnham	-43°36'18.00"	172°17'45.96"	F1	IP	17	5	17
Darfield	-43°29'33.00"	172°09'07.20"	F1	IP	12	41	50
East Taratahi	-41°00'29.52"	175°38'10.32"	C1	IP	23	0	23
Garston	-45°29'13.92"	168°41'49.20"	F2	IP	12	0	12
Godley Head	-43°35'12.84"	172°48'20.52"	C1	MX	33	22	45
Lake Lyndon	-43°19'51.24"	171°40'39.00"	F2	MX	35	9	35

Molesworth	-42°05'04.92"	173°15'53.64"	C1	MX	10	0	10
Mt. Biggs	-40°12'28.08"	175°27'31.32"	D1	MX	22	0	22
Wanganui	-39°48'15.48"	174°56'32.28"	D1	MX	19	0	19
Rangiora	-43°19'37.20"	172°36'14.40"	F1	IP	0	30	30
Martinborough	-41°15'11.52"	175°23'21.48"	C1	IP	0	5	5
Total					194	112	279

The final field curing dataset used in the satellite data analysis is summarised in Table 6.1 and the location of these sites is shown in Figure 6.1. The dataset includes six improved pasture sites, one native grassland site and five mixed grassland sites distributed across the North and South Islands of New Zealand.

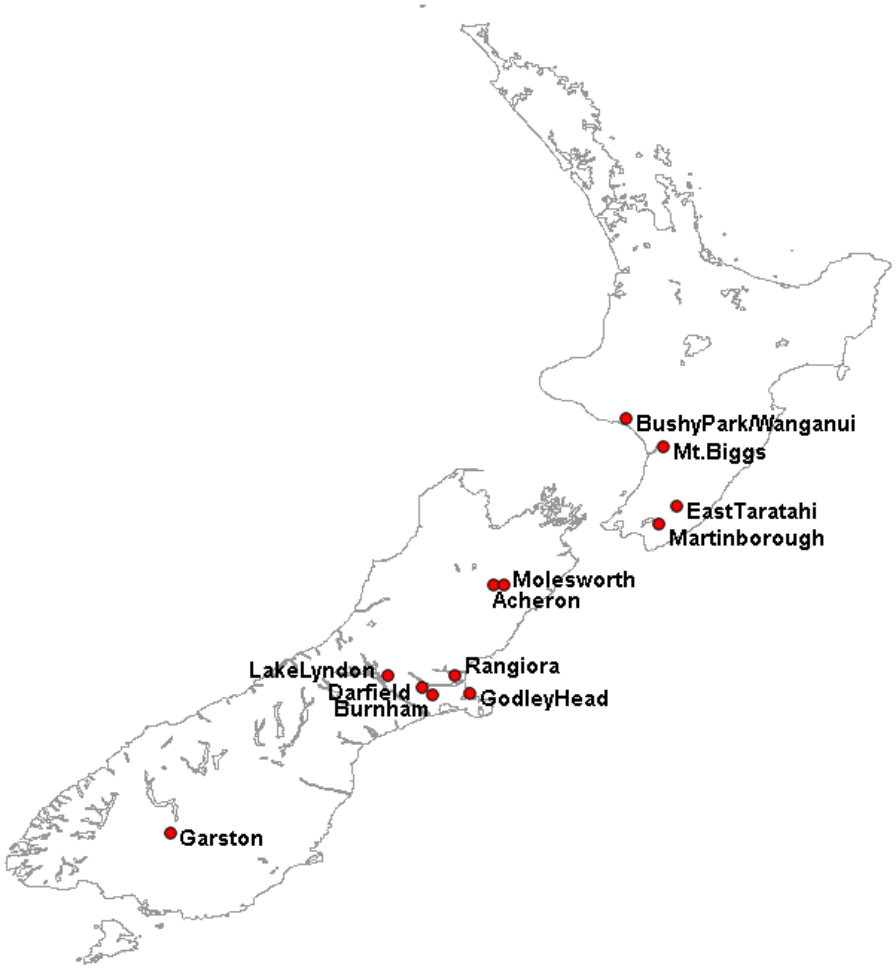

Figure 6.1: Location of field sites in New Zealand where curing measurements were recorded.

Preliminary analysis indicated that the correlations between field measurements and the satellite indices were lower than for Australia. Given the highly fragmented land cover and land use pattern in much of New Zealand, the ground coordinates for the MODIS data were adjusted from the field plot centres to be centred in nearby homogeneous areas of grassland. These new locations were determined on the basis of the performance of Australian models run over a 5 × 5 pixel window centred at the original plot location and further adjusted using qualitative assessment of Landsat scenes (as in Section 5).

Satellite data were pre-processed using the method applied to the Australian dataset (Section 3.2) as follows:

- Removal of any NDVI less than zero or recorded at a satellite view zenith angle greater than 60 degrees;
- Removal of measurements indicated as being retrieved with non-ideal quality according to the MODIS data quality flags;
- Filtering of spurious values using the spike filter.

6.2 APPLICATION OF AUSTRALIAN MODELS

Each of the models (A-D above) derived using the Australian dataset was applied to the New Zealand dataset and the residuals examined. Application of the model based on NDVI regression (model A) to the New Zealand field measurements (Figure 6.2) resulted in an RMSE of 15.4% and mean residual indicating underestimation of curing by 5%. Underestimation was more pronounced at higher curing levels (14% for curing levels greater than 80%). Two sites performed particularly badly using this method: Lake Lyndon with a mean residual of -16% and Martinborough with a mean residual of -17%.

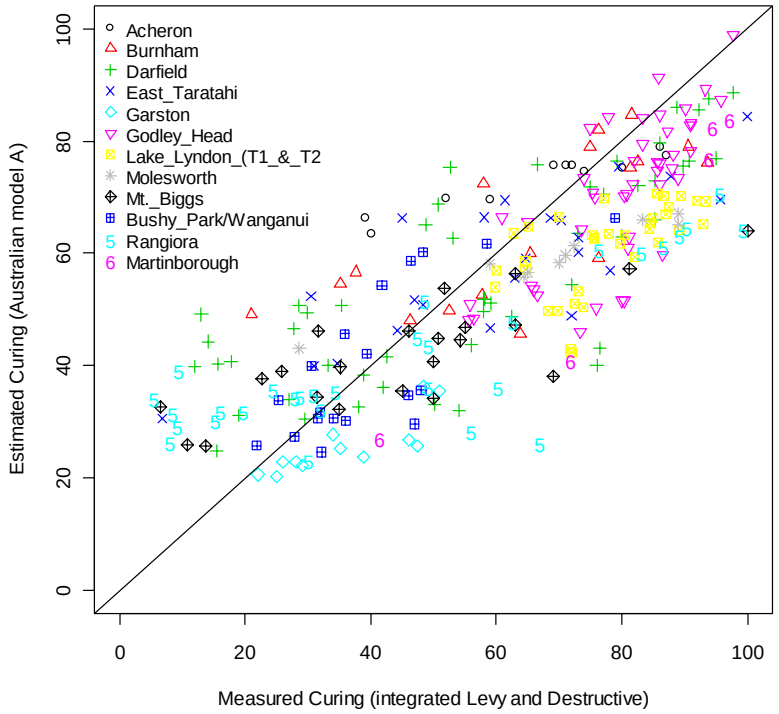

Figure 6.2: Plot of measured versus estimated curing for New Zealand data using the Australian model based on NDVI regression (model A) with coefficients based on the Australian dataset.

The multiple linear regression model (B) (Figure 6.3) provided a slightly better fit to the data with an RMSE of 14.3% and a bias of -4% (underestimation). Once again the underestimation was more pronounced at higher curing levels (-10% for curing levels greater than 80%) and the worst performing sites were Lake Lyndon and Martinborough.

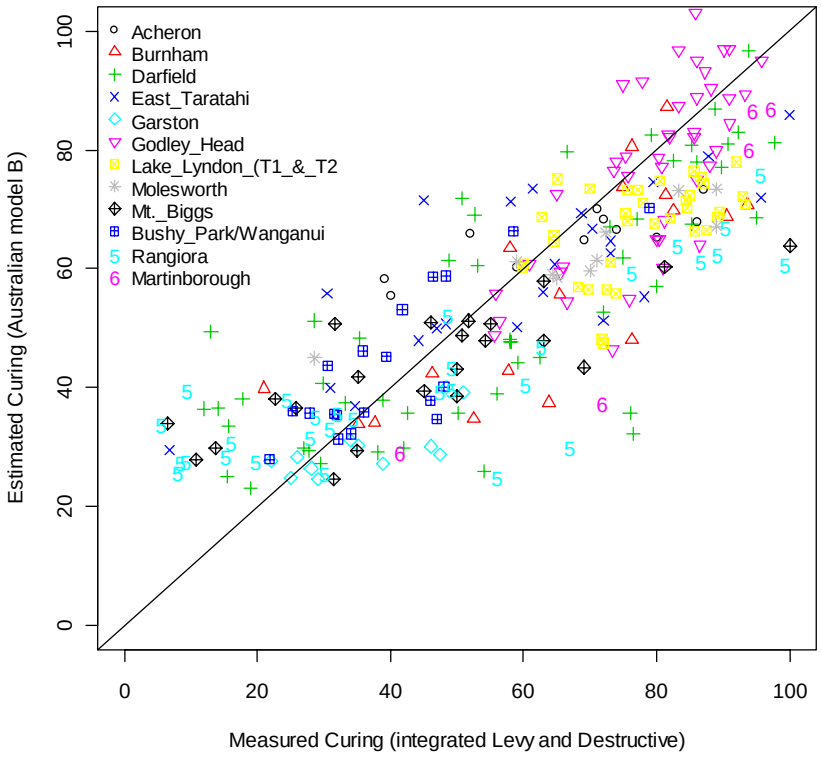

Figure 6.3: Plot of measured versus estimated curing for New Zealand data using multiple linear regression against NDVI and the ratio of MODIS bands 7 and 6 (model B) with coefficients based on the Australian dataset.

Model C is based on regression of the curing field measurements against NDVI which has been normalised by its historical minimum and maximum. Residuals using this model with coefficients derived from the Australian dataset (Figure 6.4) resulted in an RMSE of 18.2%, which indicates a poor prediction relative to models A and B. Bias in the residuals indicated an overall overestimation by 2%. However, for higher curing levels above 80%, the bias indicated underestimation by 13%. For this model, the worst performing sites were Lake Lyndon and Bushy Park/Wanganui, while the Martinborough site showed a mean residual of only 8%.

Model D is similar to Model C except that a normalised version of the Soil Adjusted Vegetation Index (SAVI) is used in place of the normalised NDVI. The RMSE for this model using the New Zealand data (Figure 6.5) was 19.6% but with less than 1% bias in the estimates. However, there was still a substantial underestimate of 16% for curing levels greater than 80%. In this case, the worst performing sites were Lake Lyndon and Bushy Park/Wanganui.

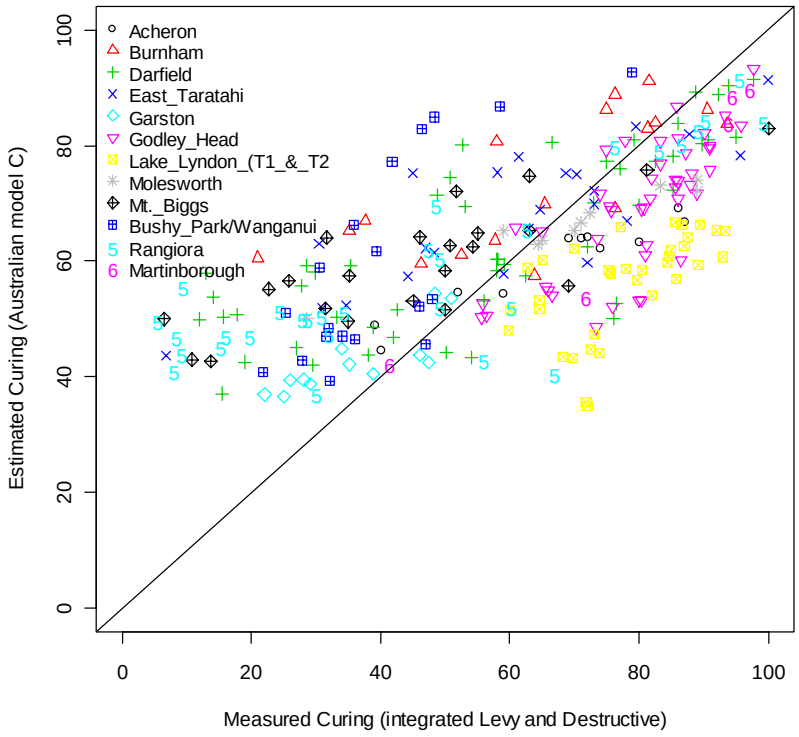

Figure 6.4: Plot of measured versus estimated curing for New Zealand data using linear regression against normalised NDVI (model C) with coefficients based on the Australian dataset.

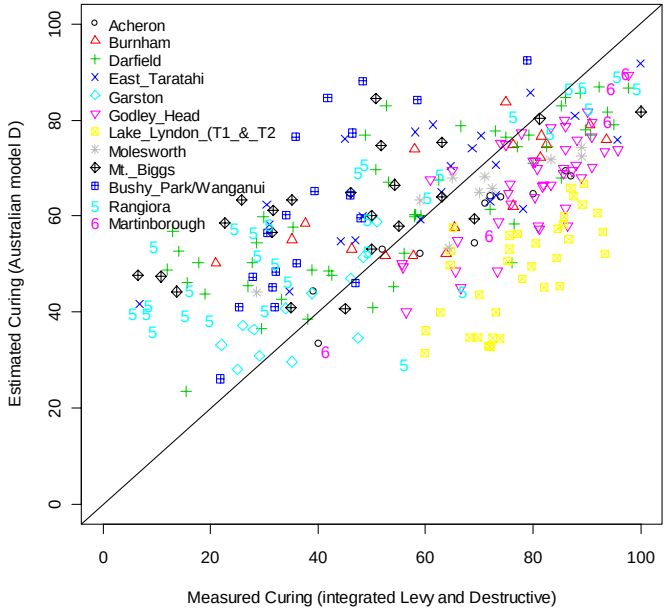

Figure 6.5: Plot of measured versus estimated curing for New Zealand data using linear regression against normalised SAVI (model D) with coefficients based on the Australian dataset.

6.3 CALCULATION OF NEW ZEALAND COEFFICIENTS

New coefficients for each of the four candidate models (A-D) were derived using the New Zealand data (Table 6.2). The use of linear regression eliminates any overall bias in the estimates but the RMSE and general distribution of errors are discussed.

Table 6.2: Comparison of model coefficients based on model-fitting to New Zealand rather than Australian curing data.

	New Zealand Coefficients			Australian Coefficients		
Model	**a**	**b**	**c**	**a**	**b**	**c**
A	137.70	-134.70		124.71	-121.40	
B	220.59	-183.36	-109.41	237.31	-190.14	-142.66
C	96.84	-72.73		93.27	-61.89	
D	92.61	-71.25		93.35	-73.78	

The model based on NDVI regression (model A) fitted to the New Zealand data (Figure 6.6) resulted in an RMSE of 14.4%, which represents an improvement of 1% over the Australian model. At higher curing levels the model tended to underestimate curing, with a mean error of -7%. Curing values at both the Lake Lyndon and Martinborough sites were again poorly predicted. However, the worst performing site in this instance was Acheron, with a mean error of 13%.

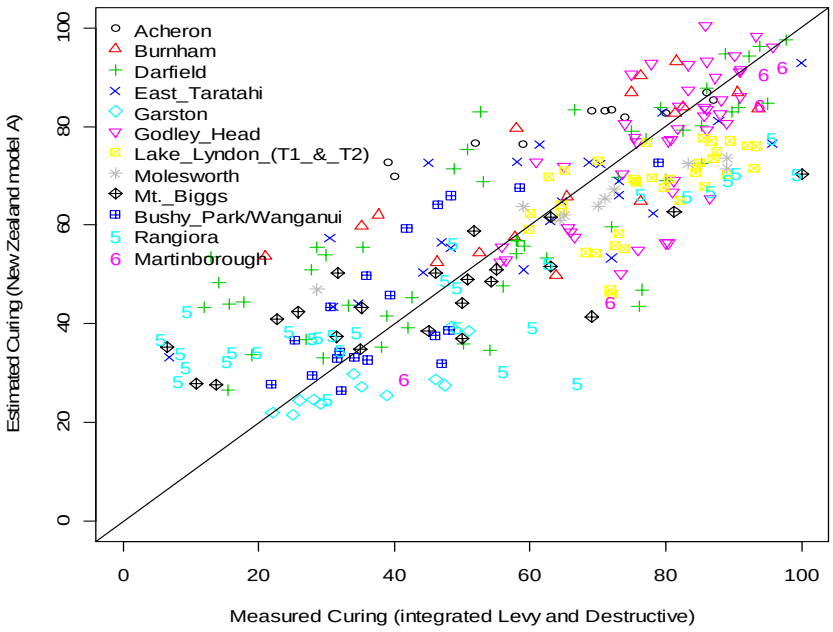

Figure 6.6: Plot of measured versus estimated curing using linear regression against NDVI (model A) with recomputed coefficients based on the New Zealand dataset.

Recalibration of Model B (multiple linear regression against NDVI and a ratio of MODIS bands 7 and 6) using the New Zealand data (Figure 6.7) resulted in an RMSE of 13.66%, which represents an improvement of less than 1% over the Australian model. At higher curing levels the model underestimated curing, with a mean error of 6%. Martinborough was the worst performing site with a mean error of 11%.

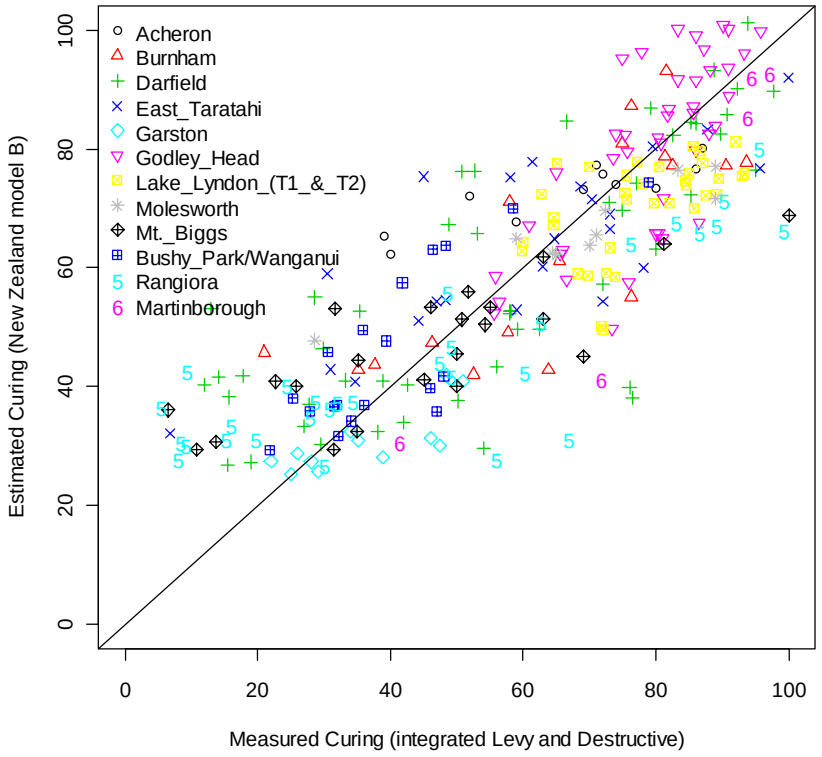

Figure 6.7: Plot of measured versus estimated curing using multiple linear regression against NDVI and the ratio of MODIS bands 7 and 6 (model B) with recomputed coefficients based on the New Zealand dataset.

Model C, based on the regression of New Zealand field data against NDVI normalised by the historical minimum and maximum (Figure 6.8), resulted in an RMSE of 17.9%. This is an improvement of less than 1% over the Australian model. Curing levels above 80% were again underestimated, in this case by 12% on average. For this model, the worst performing sites were again Lake Lyndon and Bushy Park/Wanganui.

There was no improvement in the RMSE for the similarly constructed model D based on a normalised SAVI that was recalibrated using the New Zealand data (Figure 6.9), with an RMSE equal to 19.5%. Once again there was a substantial underestimation (on average 16%) for curing levels greater than 80%. The worst performing sites were again Lake Lyndon and Bushy Park/Wanganui.

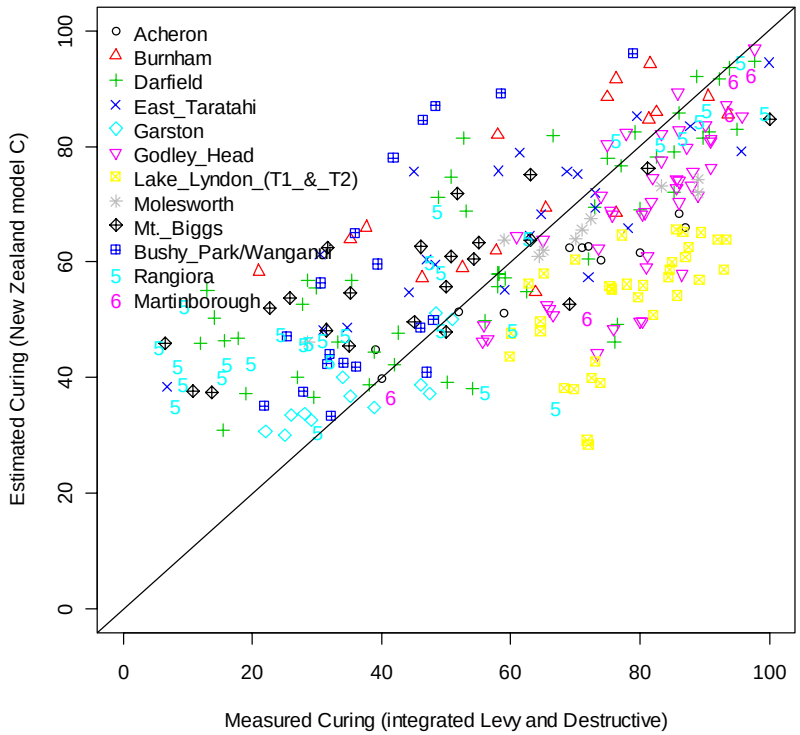

Figure 6.8: Plot of measured versus estimated curing using regression against normalised NDVI (model C) with recomputed coefficients based on the New Zealand dataset.

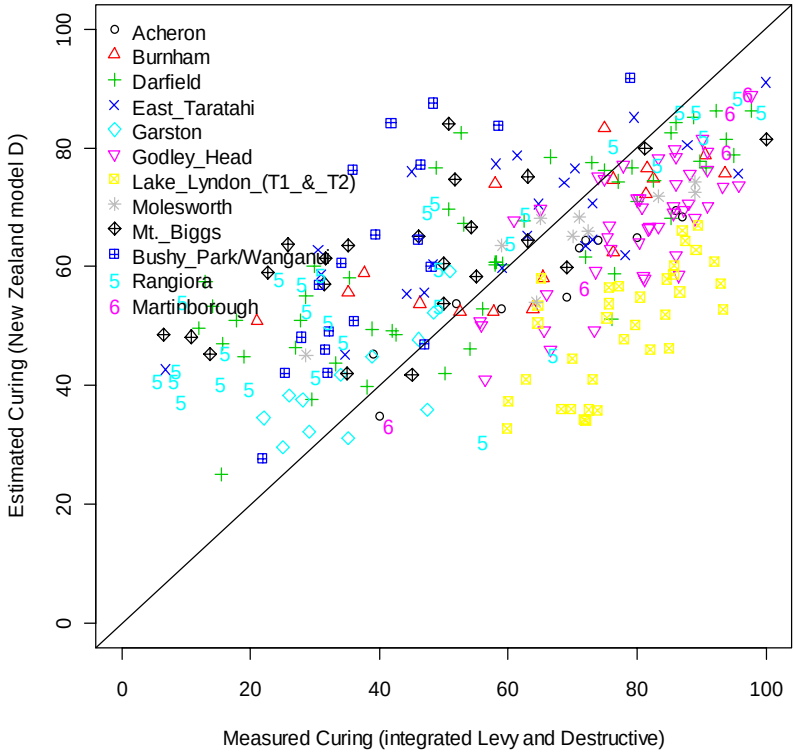

Figure 6.9: Plot of measured versus estimated curing using regression against normalised SAVI (model D) with recomputed coefficients based on the New Zealand dataset.

6.4 NEW ZEALAND MODEL SUMMARY

Comparison of the new models coefficients developed using the New Zealand data and those from the Australian data indicate only small differences (see Table 6.2). The New Zealand coefficients produced a reduction in error of not more than 1% in curing (Table 6.3).

Table 6.3: Summary of model performance for New Zealand curing measurements.

	Australian Coefficients			New Zealand Coefficients	
	RMSE	Mean Error	Mean Error Curing>80%	RMSE	Mean Error Curing>80%
Model A	15.4	-5.2	-14.6	14.4	-7.4
Model B	14.3	-3.9	-10.6	13.7	-5.9
Model C	18.2	1.8	-12.6	18.0	-12.2
Model D	19.6	-0.4	-15.8	19.5	-15.9

Models A and B were shown to underestimate the New Zealand data by 5% and 4% respectively. This offset appears to be consistent across the full range of curing as shown in Figure 6.10. In the case of model C, the Australian coefficients produce slightly higher estimates at low curing and slightly lower estimates at high curing, while model D produces almost identical estimates using both sets of coefficients.

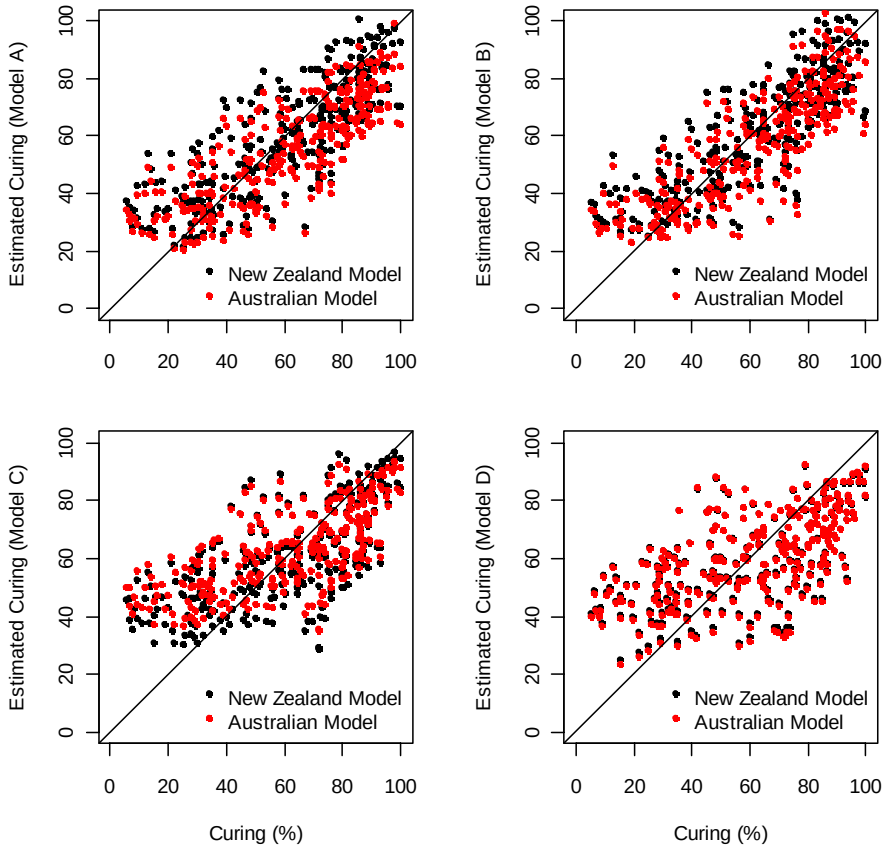

Figure 6.10: Comparison of curing estimates for the New Zealand field measurements using both New Zealand and Australian model coefficients.

Given the small reduction in error when the New Zealand coefficients are applied, it was concluded that the pilot trial for New Zealand should initially use the Australian coefficients and the New Zealand coefficients should be introduced if the bias in the models was supported by observations in the field. It should be noted that all eight of the curing models discussed in this section produce RMSE values lower than those measured for visual observation (Section 0), which was shown to be approximately 20%.

7. PILOT TRIAL DESIGN

The results from the previous three sections indicate that satellite estimates based on linear models for MODIS consistently outperform both ground-based visual estimates and the older non-linear satellite algorithm developed for the AVHRR. However, the dataset used to develop the models represents a very small sample of grasslands across Australia and New Zealand. It is difficult to fully account for the many influences on the satellite indices used (NDVI, SAVI, etc.). These include the influences of:

- grass cover or biomass, which influences the proportions of vegetation and soil viewed from above;
- grass species, which may have different spectral characteristics for a given level of curing;
- soil types, which have a distinct spectral signature;
- patterns of land use, such as grazing, which may influence the retention of dead plant material; and
- topography and the related influence on directional reflectance.

Adequate ground sampling is an inherent problem with the development of remote sensing methods. During 2009, the project team put a proposal to regional fire agencies to run pilot trials of a curing map system for Australia and New Zealand which could be used to extend the validation of the maps outside the curing validation sites. The pilot trial was conducted in three phases:

1. Consultation to determine system requirements (March 2009);
2. Pilot trial run for Southern Australia (September to December 2009);
3. Pilot trial for New Zealand (January to March 2010).

The project schedule meant that it was not possible to run a pilot trial to coincide with the key period for grassland curing in northern Australia. Details of the consultation process and the pilot curing map system developed are given in this section of the report. Feedback from the two pilot trials is then summarised in Section 0.

7.1 USER CONSULTATION

A questionnaire was prepared to determine end user priorities and preferences for specific aspects of the pilot mapping system and ultimately a new operational system. This survey was intended for key data managers and staff in all relevant state agencies and was distributed in March 2009. A list of agencies responding to the survey is given in Table 7.1. The survey covered:

1. the current and projected manner in which curing data will be used in the end user's organisation;
2. the preferred format and distribution centre for new curing data products (e.g. Bureau of Meteorology, Geoscience Australia);
3. additional information that should be included with the curing data;
4. the appropriate spatial and temporal scale and timeliness for the curing data.

Table 7.1: Agencies who provided feedback on the design of the pilot mapping system.

Region	Agency
ACT	ACTPCL
NSW	FNSW
NSW	NSWRFS
Qld	QFRS
Qld	QPWS
SA	SACFS
Tas	TFS
Vic	CFA
Vic	DSE
WA	FESA
Aus	BoM
NZ	NZNRFA

Currently the predominant method used to assessing curing across Australia and New Zealand is via visual estimations. The Tasmanian Fire Service (TFS) was the single agency currently not measuring curing for input to fire danger ratings. The Queensland Fire and Rescue Service (QFRS) identified aerial photo interpretation as a source of data that augmented their visual estimates, while fire agencies from Western Australia (DEC and FESA) use a combination of visual estimates and curing maps produced by Landgate and based on the existing non-linear curing algorithm (see Section 4.2.1) to determine curing levels.

Feedback indicated that weekly updates of curing percent were required. The preferred spatial resolution ranged from 250m pixels to regional assessments, with a large number of preferred image formats suggested. In general, an ESRI compatible format was the preferred option. A delay between the satellite measurement and the availability of curing maps of less than 7 days was preferred. Access to images without masking of non-grassland was considered the best option in the pilot phase of the project as there is some subjectivity in the definition of pure grassland, and the degree to which the curing maps might be applicable in areas of mixed woody vegetation and grass cover was considered of interest to potential users.

7.2 BASE DATA

The pilot system required satellite data with an acceptably small delay after acquisition. MODIS data was used in the pilot system principally because the algorithm development was based on MODIS, and continuing with the same satellite instrument avoided the need to consider the effect of any potential changes in data characteristics on the curing estimates. Access to conveniently post-processed products via CSIRO, as well as procedures such as cleaning,

were also in place as a result of the research phase. While using the AVHRR data that is collected in near-real-time by the Bureau of Meteorology would have minimised the time lag between satellite data capture and delivery of curing maps, AVHRR lacks the spectral bands needed for Map B, has poorer spatial resolution (1 km compared to 500 m for MOD09) and is less radiometrically stable due to the lack of onboard calibration. At the time of the pilot trial, the Bureau was putting in place infrastructure to enable near-real-time access to MODIS data. This was not available at the time of the pilot trial, but its imminent availability as a potential data source for an operational system was another motivation to use MODIS in the pilot trial.

7.3 PROCESSING STEPS

Implementation of the pilot grassland curing mapping system involved the following:

- Download of 8-day composites of MOD09 Australian and New Zealand mosaics from the CSIRO WRON data archive in Canberra. These mosaics are produced using MOD09 image tiles processed at the Land Processes Distributed Active Archive Center (LP DAAC) located at the US Geological Survey centre in Sioux Falls, South Dakota.

- Filtering of satellite observations using MOD09 quality control flags so that only surface reflectance values produced at ideal quality were retained.

- Calculation of the NDVI and SAVI indices and their normalised variants, with the normalisation performed using the pixel specific 4^{th} and 97^{th} percentiles assessed over the previous three years of data to avoid any minimum and maximum values that might be distorted by anomalous data.

- Application of curing model coefficients to produce four different curing maps for evaluation by agencies.

The removal of spurious satellite observations (for example, cloud and cloud shadow) has been detailed in Section 3.2 and has involved the testing of MODIS data quality flags and empirical filtering. This procedure was followed in the pilot system using the same MODIS flags. The empirical test implemented in Section 3.2 used NDVI values either side of a given date to determine if the value is spurious or valid, and could not be applied when filtering the current time step of data.

Normalisation was shown in Sections 4 and 5 to improve the relationship between certain spectral indices and curing. The simplest of these normalisation methods uses a temporal minimum and maximum for the index, and assumes that these correspond to 0% and 100% curing. An issue highlighted in Section 4 is the compromise in the period over which minimum and maximum are found. If the search for minimum and maximum values is over too long an interval, it becomes more likely that the time series includes land cover change as well as the phenological cycle. If the search period is too short then the true extreme values of the curing will not be captured. Section 4 has shown that three years before any measurement date provides an adequate compromise between these considerations.

Curing maps were made available to agencies via FTP download from the Bureau of Meteorology in GeoTIFF format at a spatial resolution of 500m. GeoTIFF offers the advantage that it can either be viewed as a simple image with common image viewing applications, or ingested into a GIS system using embedded georeferencing information. Maps were generally made available three to four days after the end of the eight day compositing period. However, there were a number of occasions when delays occurred at the LP DAAC which caused delays of up to 2 weeks. Agencies were asked to assess the accuracy and operational utility of each product across their own state.

7.4 CURING MODEL SUMMARY

Four curing maps were produced every eight days (corresponding to an eight-day MOD09 compositing period). The four models are detailed below. This set of models is based on Australian coefficients and was used for both the Australian and New Zealand phases of the trial.

Map A = Linear Regression (NDVI)

Curing map A was a linear regression of curing as measured at specific test sites against the Normalised Difference Vegetation Index (NDVI), derived from MODIS surface reflectance (MOD09). NDVI is a well known measure of greenness and as such, product A assumes that the level of greenness varies inversely with curing according to the equation:

$$GCI = 124.71 - 121.4 \times NDVI$$

Map B = Multiple Linear Regression (NDVI, R_7/R_6)

Curing map B used a multiple regression of field-measured curing against MOD09 NDVI and an additional parameter which is the ratio of reflectance in MODIS bands 6 and 7 (R_7/R_6). The weightings of the two indices in this multiple linear regression are biased toward NDVI in a ratio of approximately 4:3. The inclusion of the Band 7 to Band 6 ratio is designed to discriminate dead biomass from bare soil within the sensor field of view. However, it is also sensitive to any water content of soil and vegetation.

$$GCI = 237.308 - 190.139 \times NDVI - 142.655 \times \frac{R_7}{R_6}$$

Map C = Normalised Regression (nNDVI)

Curing map C is a linear regression of field-measured curing against temporally normalised MOD09 NDVI. Normalisation converts the NDVI from an absolute measure of greenness to a value which reflects where the current NDVI falls relative to its range of variation over a three year history of the index for that particular pixel. The 4th and 97th percentiles were used as normalising factors to ensure that spurious NDVI values were not used in the normalisation. The resulting map could be considered a relative (rather than absolute) measure of brownness/greenness for that pixel.

$$GCI = 93.274 - 61.896 \times \frac{NDVI - NDVI_{\min}}{NDVI_{\max} - NDVI_{\min}}$$

Map D = Normalised Regression (nSAVI)

Curing map D uses the same approach as map C, except that a Soil Adjusted Vegetation Index (SAVI) is used. This index is reported to reduce the impact of soil brightness variations on the greenness measurement, which is particularly important where there is low biomass and more exposed soil. Maps C and D generally showed very similar patterns of curing.

$$GCI = 93.347 - 73.776 \times \frac{SAVI - SAVI_{\min}}{SAVI_{\max} - SAVI_{\min}}$$

8. PILOT TRIAL RESULTS

Regional fire management agencies were asked to assess the accuracy and operational utility of each or the four curing maps across their own state. Feedback was coordinated by a single agency contact, drawing on visual assessments made by regional and district staff within their state. Feedback was generally based on visual assessments made as part of standard operational curing assessment. Although this project has shown that visual estimates generally underestimate curing and have a larger mean error than satellite estimates, the ability to assess the patterns of curing across the landscape and relate this back to patterns shown in the satellite maps was regarded as valuable validation of the four models, particularly in cases where the four maps diverged or in regions with land cover different from the field sites.

Feedback was sought on key usability and accuracy issues, such as determining if:

- delivery mechanisms were appropriate and easy to use;
- the data format is easily integrated into existing fire hazard assessment systems; and
- the data being delivered was accurate to a level acceptable by the agency.

8.1 SOUTHERN AUSTRALIAN PILOT TRIAL

Validation of the pilot curing system for southern Australia was conducted during the period from September to December 2009. Example curing maps from two dates in the trial are shown in Figure 8.1 and Figure 8.2.

Key agency contacts were responsible for downloading curing maps from the Bureau of Meteorology FTP site and providing a summary of the accuracy and utility of the maps at the state level. This feedback was generally documented on standardised feedback forms that were uploaded to the FTP site for review by the project research team. Key contacts also coordinated distribution of the maps to regional and district staff for local scale assessments where applicable. These regional staff conducted local validation based on visual assessments and their expert knowledge of the distribution of curing in their area. This information was then communicated back to the main agency contact for the trial and included in their summaries. The feedback from each state, which varied in level of detail depending on local circumstances, is summarised in the following subsections.

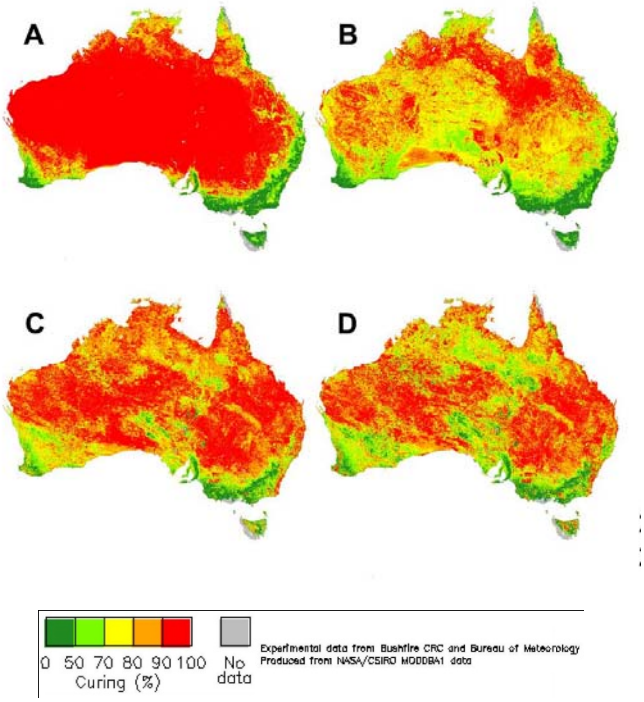

Figure 8.1: Four variants of satellite curing maps (A through D as described in Section 7.4) for the satellite compositing period from October 16th to October 23rd, 2009.

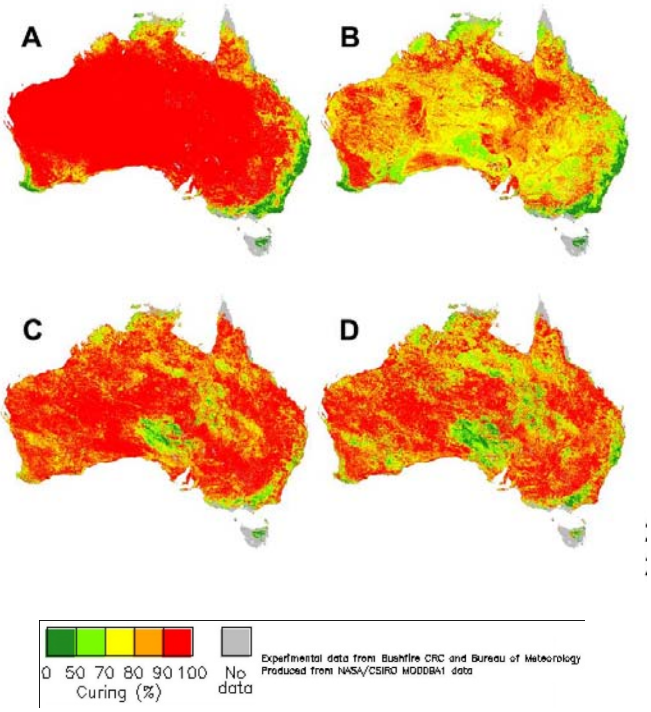

Figure 8.2: Four variants of satellite curing maps (A through D as described in Section 7.4) for the satellite compositing period from December 3rd to December 10th, 2009.

8.1.1 Victoria

The Victorian Country Fire Authority (CFA) currently produces manually interpolated maps of curing derived from visual estimates provided by regional staff. These maps were used as the primary source of validation data for the satellite maps. It is assumed that both the visual estimates and the interpolation process introduce significant uncertainty into this validation. Mr. Martin Bonwick (Project Officer at the CFA) provided detailed state wide assessment summaries for six satellite compositing periods between October 24th 2009 and February 2nd 2010:

For the period 24/10/2009 to 31/10/2009, generally the satellite maps overestimated curing relative to interpolated maps derived from the visual observation network. This was particularly true for the spatial extent of the 80-100% cured region. Overall the correspondence was best for map D, followed by C, B and then A. Map B was the only map that tended to underestimate curing, particularly in the north of Victoria.

For the period 26/11/2009 to 02/12/2009, satellite maps A, D and C corresponded with the interpolated curing maps equally well. However, all overestimated curing relative to the visually interpolated values by around 10–20 %. Satellite map B was less accurate, with a slightly better performance in areas of lower curing. Satellite maps A and D correspond best with the interpolated maps at the higher curing levels. However, map C showed the best fit for the 90–100% curing level. It was noted that satellite maps show a more detailed spatial pattern of curing than interpolated maps due to the sparse visual observer network.

For the period 03/12/2009 to 10/12/2009, satellite map A correlated best with the interpolated map, particularly at the 90–100% curing level, followed in decreasing correlation by C and B. The maps showed a higher level of variation in curing than past periods, presumably due to recent rain. However, map B showed a very noisy response that did not appear to correspond to curing levels. Generally the maps overestimated curing except for map B which showed a general underestimation.

Due to inconclusive feedback from Victoria and strong support for map B in Western Australia, during the later part of the trial, the CFA was directed by the project research team to concentrate assessments on Map B. For the period from 11/12/2009 to 18/12/2009 and from 19/12/2009 to 26/12/2009, map B showed lower curing levels in the north of Victoria by around 10 to 15% than indicated by visual observation and around 20% lower than that observed in the region of Melbourne Airport. In the central and east of Victoria, the results were mixed with Map B tended to overestimate curing by around 20% around Macedon, Cardinia and Bass, while underestimating relative to the interpolated maps at Sale and Mt Moornappa.

For the period from 25/01/2010 to 02/02/2010, Map B showed good agreement with the interpolated maps through the central parts of the state. However, there were large areas of the state where curing was consistently lower than the interpolated maps such as:

- In the north along the Murray River from Mildura, through Swan Hill to Shepparton.
- Along the south coast in the west from Portland to Anglesea and in the east from Bass shire to Lakes Entrance.
- In the alpine areas.

As many of these areas include significant areas of forest, it is assumed that tree cover has contributed to a general underestimation in curing that might best be addressed by masking of the curing maps.

In addition to the CFA feedback, Dr. Kevin Tolhurst and Mr Derek Chong from Melbourne University Department of Forest and Ecosystem Science have conducted detailed assessments of the curing maps based on their knowledge of fire behaviour during the Black Saturday fires of February 2009. Their assessments were based on the use of the maps as inputs to the Phoenix Fire behaviour model (Tolhurst et al., 2008) and focussed on two key areas; near Kilmore north of Melbourne and Bunyip Ridge to the east of Melbourne. Both Map A and B were judged to provide plausible assessments of curing at the time of the fires. The use of Map C in Phoenix resulted in more realistic fire behaviour in the Kilmore area, with Map B underestimating the extent of curing and generally not reproducing the fire extent known to have occurred during the event. For Bunyip Ridge, the use of Map B provided a better representation of the fire behaviour, with Map C generally being too high and producing a greatly overestimated rate of spread and resulting fire extent.

8.1.2 Western Australia

The Western Australian Department of Environment and Conservation (DEC) rely heavily on their network of ground observers to monitor curing across the state. However, this information is supplemented with curing maps provided by the Western Australian Government agency Landgate, which are based on the non-linear curing model (Section 0) developed for Victoria by Dilley et al. (2004). The four new satellite based curing maps developed in this project were distributed to regional staff by Paul Rampant from DEC and feedback summaries coordinated by Josie Dean.

Lack of masking of the satellite curing maps caused some concern for DEC regional staff. Forested areas are generally interpreted in the satellite maps as low curing, while bare ground, burnt areas, water bodies and man-made surfaces are generally interpreted as highly cured. Paul Rampant began applying a non-grassland mask over the maps later in the trial. However, the development and validation of such masks will be an operational consideration that has not been dealt with in the project.

There was not an accepted consensus across all regions regarding the best satellite maps to capture the observed curing levels. Rankings recorded by regional staff are shown in Table 8.1, with 1 representing the most preferred and 4 the least preferred. The ranking total over all regions and all dates provides a summary statistic which helps to indicate the preference of regional staff in Western Australia. By this measure Map B, with a total of 24, was the most preferred. Map A was the next most preferred at 37, then map C at 51 and map D the least preferred at 58. Map B was also noted as showing more spatial detail in the curing relative to Map A. Map C and D were often thought to overestimate the degree of curing relative to ground observations.

Table 8.1: Preferences for each of the map products recoded by regional staff at DEC during the pilot trial numbered from 1 (most preferred) to 4 (least preferred).

Region	Observer	Ranking	A	B	C	D
South West	Lachie McCaw	30-Sep	2	1	3	4
		16-Oct	2	1	3	4
		24-Nov	2	1	3	4
		2-Dec	2	1	3	4
		26-Dec	2	1	4	3
Mid West	Dave Atkins	30-Sep	1	3	2	4
Swan	Rob Towers	30-Sep	2	1	4	3
		16-Oct	2	1	3	4
		1-Nov	2	1	3	4
Wheatbelt	Graeme Keals	16-Oct	4	2	1	3
		9-Nov	1	2	4	3
		17-Nov	1	2	4	3
Goldfields	Ryan Butler	1-Nov	4	1	2	3
		9-Nov	4	1	2	3
		17-Nov	4	1	2	3
South Coast	Greg Broomhall	9-Nov	1	2	4	3
		17-Nov	1	2	4	3
		Total	37	24	51	58

8.1.3 New South Wales

New South Wales Rural Fire Service currently carries out visual observations at around 50 regional sites on a weekly basis during the fire season. A subset of these observers was asked to assess how well the satellite-based curing maps conformed to their field observations of curing for their region. Assessments were performed from September to December 2009 and reported back to Peter Kinkead, who collated results for the research team.

For the first two months of the trial, assessments were only performed at the regional level with no synopsis at the state level. These indicated preferences that were evenly distributed between the four satellite map products. From mid October, an overall assessment was made by Peter Kinkead at the state level. His assessment showed a preference for satellite map B, followed closely by map A, with C and D being equally less preferred.

8.1.4 Australian Capital Territory

Assessment of the satellite based curing maps across the ACT was performed by Stephen Wilkes from the ACT Department of Parks, Conservation & Lands. All assessments ranked the maps from best to worst as B, C, D and A. However, all products were thought to be overestimating lower curing levels, while C, D and A underestimated the highly cured areas. Map A appeared to be the best at characterising low curing but worst at high curing. Products B and C appeared to track well against the relative trajectory of curing as described by field observations.

Both of models based on relative greenness (maps C and D) underestimated high curing and overestimated low curing, indicating that additional variance not associated with the curing cycle is being captured in the satellite data. Such variance might include sensor errors, undetected cloud or soil moisture changes; all of which can impact apparent reflectance values and the derived indices.

8.2 NEW ZEALAND PILOT TRIAL

The second phase of the pilot trial was conducted in New Zealand during the period from January 2010 to April 2010. There was a concern that cloud cover would be a more significant issue for the spatial and temporal continuity of estimates in New Zealand and this did prove to be a problem in many of the maps produced (see Figure 8.3 and Figure 8.4). Regional staff often defaulted to the previous image as a reference for current assessments. A protocol to deal with this issue needs consideration if an operational system is to be put in place.

A tally of the rankings placed on the four maps (1st being considered the most accurate) by all New Zealand respondents is shown in Table 8.2. Feedback seemed to contrast with that from Australia, with preferences heavily biased towards the normalised relative greenness models (C and D). These two approaches are very similar in terms of both the methods used in their derivation (see Section 7.4), and in the spatial pattern that they tend to produce when applied over the landscape (Figure 8.3 and Figure 8.4). Only one end user response assessed map A as being the most accurate, which was for the region east of Queenstown in late March. The small number of preferences for map B also originated from the South Island around Otago and Canterbury. It was suggested that the diversity of vegetation in these areas may have influenced the greater range of feedback and preferred maps (pers. comm. Mike Grant, Southern Rural Fire Authority).

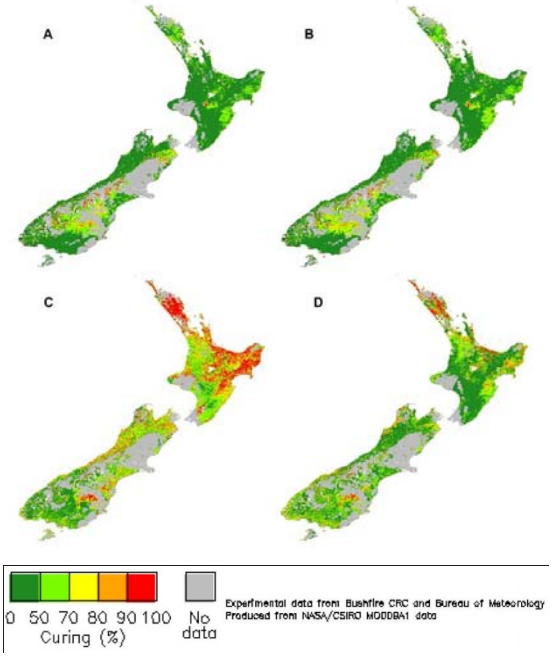

Figure 8.3: Four variants of satellite curing maps (A through D as described in Section 0) for the satellite compositing period from January 9th to January 16th, 2010.

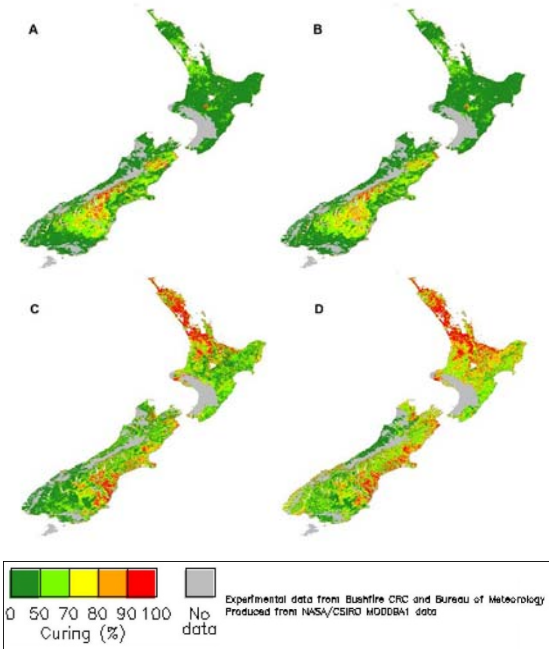

Figure 8.4: Four variants of satellite curing maps (A through D as described in Section 0) for the satellite compositing period from March 7th to March 14th, 2010.

Table 8.2: Tally of rankings from New Zealand curing observers; Rankings (1st to 4th) indicates the preferred model (A-D) for an observer in a given region at a given time.

Map	1st	2nd	3rd	4th
A	1	8	13	18
B	8	5	17	10
C	24	18	6	1
D	22	16	1	8

Consistent with the Australian feedback, it was suggested that maps A and B tended to underestimate curing while C and D tended to over estimate curing throughout the trial. Consideration was given to changing the map coefficients to the New Zealand specific ones described in Section 6.3. However, the tendency of maps A and B to underestimate curing (as suggested by observer feedback) would be exacerbated by the use of these new coefficients. A change in coefficients for maps C and D was not considered likely to be significant enough to affect curing observer responses.

8.3 GENERAL SUMMARY OF FEEDBACK

The clearest conclusion drawn from the feedback across both Australia and New Zealand was that maps A and B tended to underestimate curing and that maps C and D tended to overestimate. This should be considered in the context of the validation approach, commonly visual observations by trained regional staff. Early work on this project has shown that these visual observations tend to underestimate curing by an average of 11% relative to benchmark destructive measurements (Section 3.1). We might then expect an accurate satellite map to be judged to overestimate curing in a subjective assessment.

Maps A and B tended to be the preferred option by Australian agencies. Although often the preferred option, it was noted in Victoria that map B produced a noisy result after a rainfall event. Although this was mentioned only once during the pilot trial (pers. comm. Martin Bonwick, Victorian Country Fire Authority), it may be an important observation given the band 7 to band 6 ratio used in the map. These bands are at the longer wavelength end of the short wave infrared region (Figure 3.3), which is sensitive to the amount of vegetation matter or biomass. However, this region is also sensitive to any liquid water present in the form of internal leaf water, water droplets on the vegetation surface and soil moisture. As such, spatial variations in drying after rainfall events are likely to have an effect on map B, independent of the curing state.

Although maps C and D did not receive a high rating in the southern Australian pilot trial, they were the preferred option in the New Zealand trial. The processing methodology for these two maps is very similar, with both based on a temporal normalisation of a greenness index (NDVI and SAVI respectively). This similarity is reflected in the spatial patterns produced in the Australian and New Zealand curing maps, as well as in the feedback provided. Of these two, the more commonly preferred option in the pilot trial was map C, particularly in New Zealand.

9. CONCLUSIONS

Project A1.4 has shown that MODIS satellite data can be used to map the degree of curing in grasslands across Australia and New Zealand throughout the fire season. The accuracy of these maps, as measured at 39 sites in Australia and 16 sites in New Zealand, was shown to be superior to that of visual assessments.

The testing of various approaches and models indicated that spectral indices which target the assessment of greenness, such as the Normalised Difference Vegetation Index (NDVI) and Soil Adjusted Vegetation Index (SAVI), showed consistently better results than those that used other spectral regions with their sensitivity to other aspects of plant physiology such as moisture content. However, when combined with NDVI, a ratio of MODIS bands 7 and 6 did improve the accuracy of estimates. It is presumed that this is tied to the intended purpose of the index to account for differences in the amount of vegetation matter between sites.

Normalisation of indices by their historical maximum and minimum for a given pixel was also intended to account for between site variations. Although improvements in accuracy for the validation sites were not large, the benefit of this type of normalisation may be best exposed when extrapolating models across the landscape where variations in the amount, structure and species distribution of vegetation are encountered.

A pilot system was set up to produce eight-day updates of curing maps using four approaches which had shown particular promise in estimating the degree of curing at the project validation sites. These approaches were:

A. Simple regression against NDVI;
B. Multiple regression against NDVI and a ratio of MODIS bands 7 and 6;
C. Regression against temporally normalised NDVI; and
D. Regression against temporally normalised SAVI.

These maps were made available to end users and feedback has been collated and summarised in the preceding sections of this report. User feedback was collated during the period from September to December for southern Australia and January to March for New Zealand to coincide with the major period of curing in each region. Unfortunately the system pilot was not in place in time to conduct a similar trial for the northern Australian curing cycle.

Although there was encouraging feedback from the trial for the maps in a general sense, the user feedback did not consistently support any one approach of the four trialled. In the southern Australian trial, there was greater support for maps A and B, while in the New Zealand trial, Maps C and D received greater praise. These groupings (A and B versus C and D) are not surprising, as maps A and B are similar in that they provide a best estimate for the current epoch of satellite data in isolation, while C and D use information from the time series of measurements to adjust the current measurement before providing a best estimate. One consistent message from the trials was that relative to visual estimates, maps A and B tended to underestimate curing and maps C and D tended to overestimate. It should be noted that visual estimates were also shown to underestimate curing relative to destructive measurements.

9.1 LEGACY DATASET

The project has compiled a dataset of curing measurements recorded in the field. The dataset includes:

- 25 field validation sites in Australia
- 16 field validation sites in New Zealand
- Sites categorised by grassland type and climate zone
- 607 visual estimates of curing
- 580 Levy rod curing measurements
- 251 destructive curing measurements
- 290 fuel moisture content measurements

This dataset has potential benefit beyond the life of this project and should be made available to the fire research community and fire management agencies. Research projects such as the one described in this report have limited time and resources to build up new field datasets. As such, these data could form an important basis for future measurements in projects that might seek to recalibrate existing curing models, to test new approaches and to evaluate the performance of various methods for specific regions. However, the dataset does not have value in its own right and it is only through its use in new research that value can be extracted.

9.2 COMPARISON OF SATELLITE MODELS

All four of models used in the pilot trial have shown significant improvements over visual curing assessments recorded by trained staff using standard operational procedures. Not only have the satellite mapping approaches used in the pilot trial provided higher accuracy curing estimates than generally achievable with visual estimates, but the measurement is objective, efficient and spatially continuous, requiring low ongoing investment in system maintenance and staff training.

Although feedback indicated that all four methods used in the curing map pilot trials produced promising results, the maps show dramatically different characteristics over some regions when applied over the varied landscapes of Australia (see Figure 8.1 and Figure 8.2) and New Zealand (Figure 8.3 and Figure 8.4). Spatial patterns in the maps lead to a tendency for end users to prefer either maps A and B or maps C and D. These pairings are not surprising given that there are distinct similarities between the methods used to generate each pair of maps.

Maps A and B were the preferred maps in the southern Australian pilot trial. Map A is the simplest possible approach upon which to base a curing map using MODIS data. This linear regression against NDVI has the advantage that the index is well understood and the regression equation can be recalibrated easily for specific regions or when new data become available. The limitation of the approach is that there is no attempt to account for variations in land cover characteristics. For this reason, Map A will always appear fully cured in regions of low vegetation cover, while the presence of evergreen vegetation will cause the map to indicate a low level of curing.

Map B uses the ratio of MODIS band 7 and 6 to account for variations in the amount of vegetation present. This approach has appeared successful, as it quantitatively outperformed Map A at the field sites, and feedback from the southern Australian pilot trial indicated the highest preference for this approach. Map B also resolved spatial detail in curing estimates more consistently across the landscape, without the large areas of saturation present in the

semi-arid inland regions of the map A images. For these reasons, Map B is the recommended method for adoption in Australia.

In early 2010 the *Ground cover monitoring for Australia* project was established, lead by the federal Bureau of Rural Sciences. This program will collect field data on cover fraction (PV, NPV and BS) across Australia for the purpose of validating and developing the Guerschman et al. (2009) approach to estimating cover fractions with MODIS. The data will be collected by a method that is similar to the Levy Rod method, but which measures only the uppermost element of cover at each sample point rather than the composition over the full vertical extent of the vegetation. Despite the difference in the measured parameter, this field data might be useful to further validate the curing algorithm, particularly in sparsely vegetated regions such as rangelands, which will be emphasised by the ground cover project. The project may also improve the methodology for estimating cover fractions, which may in turn suggest improvements to the approach of Map B. Any new MODIS curing algorithms can be retrospectively assessed with the existing field curing data. Thus the outcomes of the ground cover project should be monitored for possible use in improving satellite-based curing estimates.

Curing estimates produced using Maps C and D result in almost identical spatial patterns across the landscape. This similarity is primarily due to the normalisation procedure used, where the current value of the vegetation index is placed in the context of a three year minimum and maximum for any given pixel. Feedback received during the pilot trial indicated that these two models were preferred for New Zealand. There was, however, very little to support the adoption of one over the other. Of these two maps the NDVI used in Map C is the more established index. Given no obvious advantage of the SAVI index used in Map D, Map C is our recommended method for adoption in New Zealand. It should be noted that the feedback on which this decision is based resulted from a pilot trial that ran from January to April 2010, which includes only the latter part of the New Zealand fire season. It is recommended that further validation be carried out over the full curing cycle to ensure that the preferred map product remains consistent.

There are a number of possible reasons for differences in the preferred algorithm between Australia and New Zealand. Foremost are the degree of fragmentation and the climatic disparity. At the scale of the spatial resolution for MODIS data (500m for MOD09) areas of uniform grassland without partial tree cover are more difficult to find in New Zealand than in Australia. This is likely to lead to a preference for the time series normalisation approach of Map C. However, the generally drier and hotter climate of Australia also means that grasslands often exist with lower biomass and fractional cover. Map B is well equipped to account for these types of variations due to its use of the band 7 over band 6 ratio.

In summary, Map A gives a simple and reliable indication of “brownness”, which in the map A equation is almost the complement of the NDVI greenness index. However, Map A essentially assumes full vegetation cover. In simple terms, the lower the amount of vegetation the more bare soil that is observed by a satellite sensor and the greater the estimated curing. This means that high fuel loads may lead to underestimated curing, while low fuel loads may lead to overestimated curing. Map B makes an attempt to account for these variations in fuel load by incorporating an index sensitive to the amount of vegetation present, while map C does similarly using information derived from the historical variation in greenness for each pixel. Both the spectral (Map B) and temporal (map C) normalisation of site characteristics have merits for adoption in an operational curing map system.

Map B requires a single satellite image. As such the assessment of vegetation amount is valid for the current assessment of curing. However, the method is likely to be more sensitive to the presence of surface water. Map C

requires a three-year history of satellite data to derive the historical context for the current measurement. This means that if land cover changes have occurred, such as fire, species composition changes or environmental degradation, the historical measurements may not be an appropriate indictor of the current state of the fuel present.

9.3 OPERATIONAL CURING MAP SYSTEM

Users have an urgent need and an enthusiasm for accurate satellite-based curing maps. The most direct and rapid implementation of the project results for operational use is to continue the pilot map generation system, fully automating it to optimise its timeliness and reliability. To summarise the pilot system:

- CSIRO Marine and Atmospheric Research in Canberra automatically downloads eight-day composites of MODIS surface reflectance data (MOD09 product) from the United States Geological Survey (USGS) Land Processes Distributed Active Archive Center (LPDAAC)
- CSIRO processes these data to separate Australian and New Zealand mosaics
- Once mosaics are complete, the data is downloaded by the Bureau of Meteorology in Melbourne and processed to curing maps which are placed onto the Bureau's FTP site.

While the pilot system could be automated for routine operation with minimal effort by the Bureau, several immediate alternatives and enhancements could be considered.

9.3.1 Timeliness and processing agency

The issue of timeliness is linked to the choice of base MODIS data product, the choice of processing agency, and the availability of processing software. In many cases, satellite measurements collected over a number of days are processed into single composite images (e.g. 8 days composites for MOD09), which become available after a latency period. Thus curing maps could be based on satellite measurements as old as the length of the composite period total plus the processing latency period.

During the pilot trial, maps were typically available 4-7 days after the end of the compositing period, most of the delay coming from the latency of the LP DAAC data. However, neither the LP DAAC nor the CSIRO processing system are intended to be operational systems, and anomalies in one of these systems can cause additional delays by as much as one week.

The Bureau has recently installed a network of X-band satellite reception stations, with the last station due to be commissioned mid to late 2010. This network, in combination with stations operated by Bureau partner agencies, gives the Bureau a direct downlink for MODIS data (so called "direct readout") that can be processed in near real-time. This facility will be compatible with the US operational satellite systems (NPP and JPSS) scheduled to replace MODIS in the coming years. In principle, the direct readout data could be processed to curing within a few hours of the satellite observation. However, the capacity of communications links between the reception stations and the Bureau's Head Office will be a consideration. Also, while most of the software to produce a real-time clone of the pilot products is available, a key gap at present is the lack of 8-day compositing software. In order to use the

Bureau's direct readout MODIS data in the context of the present availability of processing software, three ways forward are apparent:

1. Write 8-day compositing software. This might require a modest effort, but its feasibility requires investigation. An advantage is that a rolling 8-day window (resulting in daily composite images) could be implemented.
2. Use uncomposited single-orbit MOD09 data. Curing maps could be produced daily from this product, but would be more susceptible to "noise" due to variability in atmospheric and angular effects, and by data gaps caused by cloud cover.
3. As an alternative to MOD09, produce the MCD43 product every 16 days or a daily product using a 16 day rolling window. The 16-day window will minimise gaps due to cloud, but will increase the effective latency between observation and map availability compared with the 8-day MOD09. Also, the decreased temporal resolution may not adequately track the most rapid curing changes. These issues should be investigated for periods and regions of rapid curing change before adopting any 16 day composite product.

Geoscience Australia in Canberra and Landgate in Western Australia currently produce versions of the MCD43 product from direct readout data, using software they developed before the availability of an internationally standard MCD43 processing package. The Landgate product is produced daily using a variable length window, while the Geoscience Australia product is updated every four days and is available approximately three days after the end of the data collection window.

A suitable development path would be to convert the current pilot map generation system in the Bureau to automated routine operation, and then investigate the options above to generate the base MODIS product used by the system from the direct readout data available to the Bureau.

9.3.2 Gap filling

Atmospheric influences such as cloud and smoke, as well as sensor and data processing errors can cause gaps in the existing pilot system maps. A reliable and accurate method of filling these gaps needs to be addressed in an operational curing map system. Longer compositing periods than 8 days are undesirable due to the rapid nature of curing in some parts of the country and the tendency for compositing such as used for MOD09 to retain the lowest estimate of curing (highest NDVI). This gap filling might best rely on such indicators as the:

- previous acceptable satellite observation;
- trajectory of satellite estimates prior to the data gap;
- trajectory of satellite estimates in surrounding regions;
- mean seasonal cycles of curing derived from satellite time series.

Initially, gap filling using the previous acceptable satellite observation and providing information on the age of each observation is recommended for its simplicity of implementation and ease of interpretation. Prolonged periods of cloud, such as occur in northern Australia in the build up to the wet season and in parts of New Zealand, may remain a particular challenge. Such cases stand to benefit from the development of grass growth model based approaches being developed by another stream of research within Project A1.4.

9.3.3 Masking

A major concern for some end users during the pilot trial was the lack of masking of non-grassland cover types in the curing maps. There was a conscious decision not to mask any areas of the maps as feedback on the performance of the maps in areas of mixed land cover was considered of interest by both the researchers and agencies. An operational system will require some form of masking so that forested areas, recent burn scars, water bodies and non-vegetated areas do not lead to the production of misleading curing estimates. Possible sources of such data include the Landsat-based woody cover map held by the federal Department of Climate Change and Energy Efficiency, or land cover datasets available through state land management agencies.

9.3.4 Formats

Integration of the satellite curing maps into the broadest range of existing information systems will require consideration of a range of data formats. One such system will be the Bureau of Meteorology's Next Generation Forecast and Warning System, which is undergoing a phased roll out across Australia. Given an approved satellite-based curing data as input, along with meteorological inputs, this system has the potential to produce and distribute spatially contiguous gridded GFDI.

Another information system that requires consideration is the Phoenix fire behaviour simulation system being run by the University of Melbourne. These applications typically need daily updates of data at a resolution coarser than 500 m, so both the input satellite data and spatial aggregation procedures need to be assessed.

9.4 FUTURE DEVELOPMENT

The MODIS algorithm development described has been based on the restricted range of landscape types sampled by the project field sites. The project was unable to obtain field samples in some land cover types that are important for fire management but potentially offer challenges for satellite-based assessment, such as wooded grasslands, which are exemplified in western New South Wales. While the recommended satellite approaches attempt to adapt to landscape variations, their evaluation in these areas has been limited to a single season of qualitative user feedback during the pilot trial. Thus the project strongly recommends that agencies seeking the demonstrated reliability of satellite-based curing in regions of their state not sampled during the project continue objective field measurements in upcoming curing seasons, and that the Levy Rod method be used where possible to provide an adequate balance of accuracy and efficiency. To this end, the Levy Rod sampling instructions and reporting sheets are appended to this report (Appendix B). The immediate use of these measurements would be to expand the region of quantitative evaluation for the satellite curing map, and possible evaluation of alternative mapping approaches. Expansion of the existing database of curing field measurements to increase the geographic and temporal coverage, would increase its value as a lasting national resource for future research and refinement of the satellite-based mapping system. Besides archiving the existing database, any future objective curing measurements made by agencies should be archived in a nationally accessible way.

In the longer term, continuous evaluation and improvement of the operational curing map system could be supported by, for instance, a web based interface that would allow users to submit new ground-based measurements of curing. Such a system, if resourced, might generate reports (for example, Figure 9.1) of the

performance of the nominal and alternative mapping approaches at the ground-measured sites for distribution to users and those responsible for its maintenance and development.

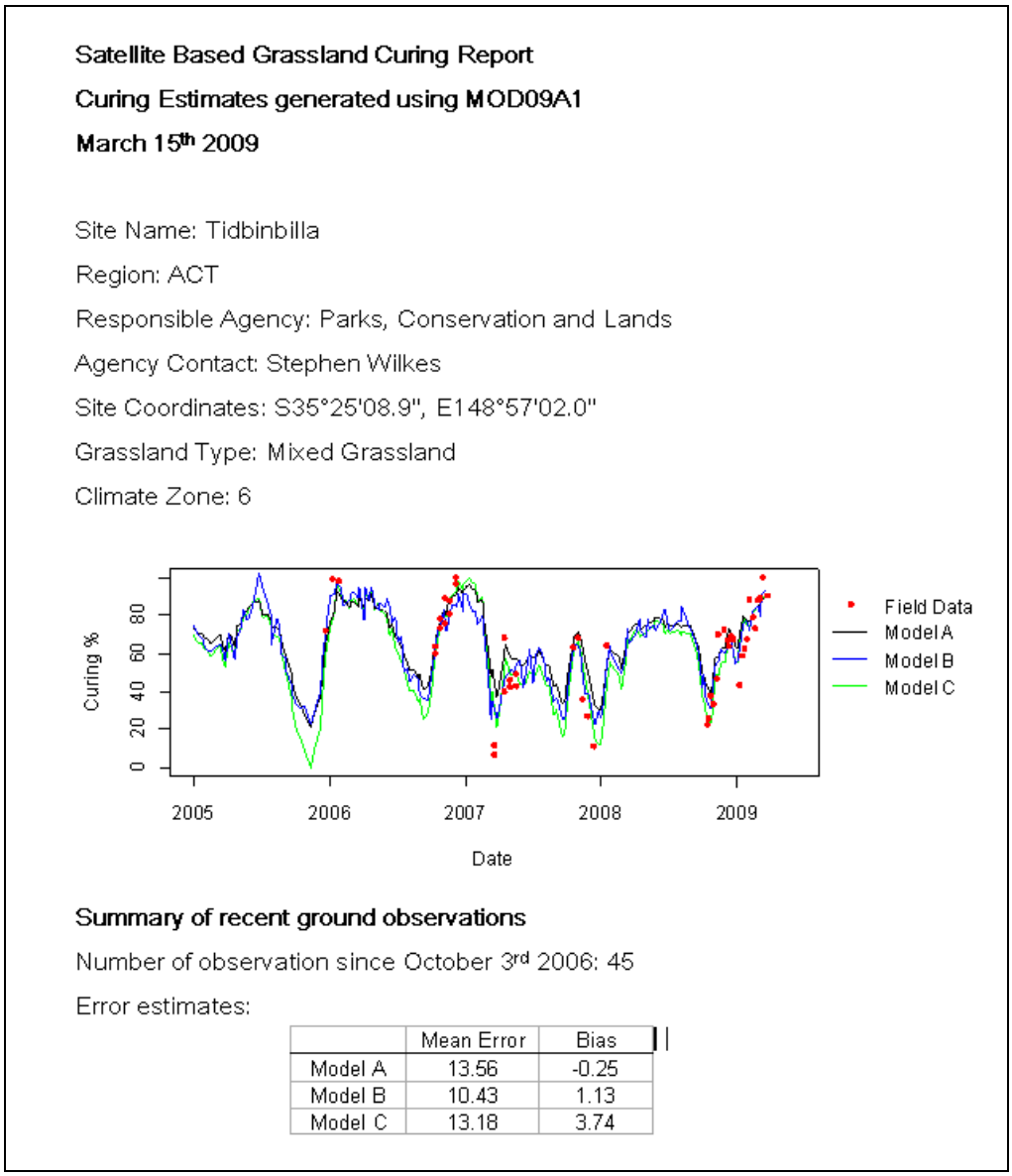

Figure 9.1: Example auto-generated report indicating the relationship between ongoing ground-based measurements of curing and satellite estimates.

9.5 IMPACT ON APPLICATIONS

Despite the perceived benefits of adopting satellite-based estimates of curing as a basis for grassland curing assessment, ultimately the performance of the proposed system may be judged on the basis of its reliability as an input to grassland fire danger indices and in providing additional spatial detail to fire spread models. The impact of the proposed satellite methods is untested in this regard. Given the current reliance on visual observations and the tendency of such estimates to understate the degree of curing (relative to destructive measurements), integration

of satellite-based curing estimates may require careful management of potential impacts on these downstream systems.

9.6 SUMMARY OF RECOMMENDATIONS

The project makes the following recommendations.

1. Routine satellite-based monitoring of a grassland curing index (GCI) across Australia should commence using MODIS satellite data by means of the relations

$$NDVI = \frac{R_2 - R_1}{R_2 + R_1}$$

$$GCI = 237.308 - 190.139 \times NDVI - 142.655 \times \frac{R_7}{R_6}$$

where R_i is the surface reflectance value for MODIS band i.

2. Grassland curing should be routinely mapped across New Zealand from MODIS data, initially using the relation

$$GCI = 93.274 - 61.896 \times \frac{NDVI - NDVI_{\min}}{NDVI_{\max} - NDVI_{\min}}$$

where $NDVI_{\min}$ and $NDVI_{\max}$ are the minimum and maximum values of NDVI over the preceding three years.

3. The routine production and distribution of spatial curing data products be done by an operational agency with capability to produce satellite data products in near real-time. The Australian Bureau of Meteorology, where the current prototype system has been implemented, could, for example, put a suitable data processing system in place.

4. Fire management agencies should be made aware of the basis for the satellite curing maps and the assumptions and limitations underpinning the products. End users should use the new product cautiously and continue to evaluate its accuracy. Users should particularly be aware that some regions and land cover types were not well represented by the project field sites.

5. A further pilot trial should be considered in New Zealand over the full 2010/11 curing season. This is in light of the late start to the 2009/10 pilot trial. Scion could collate Levy Rod measurements made by agency staff. Particular focus should be given to the South Island where feedback was less conclusively weighted towards the recommended Map C.

6. Agencies should undertake further validation and calibration within their jurisdictions to ascertain the accuracy and reliability of the maps and the suitability of these data for integration into their own fire danger rating and fire behaviour systems. Researchers, data providers and fire management agencies should continue to work together to refine the recommended methods, where possible based on objective field measurements.

7. Where a need for further model development is identified, agencies should collect objective field measurements using the Levy Rod method developed by the project. This applies particularly to regions that have not previously been sampled and regions where the recommended model is found to perform poorly. Agencies should be aware that the project has developed alternative methods to estimate curing in variable landscapes.

8. The Ground Cover Monitoring Project led by the Australian Government's Bureau of Rural Sciences should be monitored for the potential to improve the satellite estimation of curing.

REFERENCES

Alexander, M.E. (2008). Proposed revision of fire danger class criteria for forest and rural areas in New Zealand. Second edition (reprint with corrections). *Wellington and Christchurch: Nat. Rural Fire Authority, Wellington, New Zealand. Circular, 2*, 73

Allan, G., Johnson, A., Cridland, S., & Fitzgerald, N. (2003). Application of NDVI for predicting fuel curing at landscape scales in northern Australia: Can remotely sensed data help schedule fire management operations? *International Journal of Wildland Fire, 12*, 299-308

Anderson, S.A.J. (2005). Forest and rural fire danger rating. *Forestry handbook. Edited by M. Colley. New Zealand Institute of Forestry Inc., Christchurch*, 241–244

Anderson, S.A.J., Anderson, W.R., Hines, F., & Fountain, A. (2005). *Determination of field sampling methods for the assessment of curing levels in grasslands*. unpublished report: Bushfire CRC Project A1.4, Melbourne, Australia

Anderson, S.A.J., & Pearce, H.G. (2003). Improved methods for the assessment of grassland curing. In, *3rd International Wildland Conference*. Sydney, Australia

Barber, J. (1990). *Monitoring the curing of grassland fire fuels in Victoria, Australia with sensors in satellites and aircraft. A Country Fire Authority study in Remote Sensing*. Melbourne: CFA

Barber, J.R. (1979). Remote sensing in fire prevention planning: Monitoring the curing of grasslands by means of sensors in satellites and aircraft. In, *Environmental Science*. Clayton: Monash University

Barber, J.R. (1989). Remote sensing strategies for monitoring grassland fire fuels. In, *School of Environmental Planning*. Melbourne: The University of Melbourne

Burgan, R.E., Klaver, R.W., & Klaver, J.M. (1998). Fuel Models and Fire Potential from Satellite and Surface Observations. *International Journal of Wildland Fire, 8*, 159-170

Ceccato, P., Gobron, N., Flasse, S., Pinty, B., & Tarantola, S. (2002). Designing a spectral index to estimate vegetation water content from remote sensing data: Part 1: Theoretical approach. *Remote Sensing of Environment, 82*, 188-197

Chen, D., Huang, J., & Jackson, T.J. (2005). Vegetation water content estimation for corn and soybeans using spectral indices derived from MODIS near- and short-wave infrared bands. *Remote Sensing of Environment., 98*, 225-236

Cheney, P., Gould, J.S., & Catchpole, W.R. (1998). Prediction of fire spread in grasslands. *International Journal of Wildland Fire, 8*, 1-13

Cheney, P., & Sullivan, A. (2008). *Grassfires: fuel, weather and fire behaviour*. Collingwood, VIC: Commonwealth Scientific and Industrial Research Organisation Publishing

Chladil, M.A., & Nunez, M. (1995). Assessing grassland moisture and biomass in Tasmania: The application of remote sensing and empirical models for a cloudy environment. *International Journal of Wildland Fire, 5*, 165-171

Cleveland, R.B., Cleveland, W.S., McRae, J.E., & Terpenning, I. (1990). STL: A Seasonal-Trend Decomposition Procedure Based on Loess. *Journal of Official Statistics, 6*, 3–73

Dilley, A., Millie, S., O'Brien, D., & Edwards, M. (2004). The Relation between Normalized Difference Vegetation Index and Vegetation Moisture Content at three grassland locations in Victoria, Australia. *International Journal of Remote Sensing, 25*, 3913 - 3928

Gao, B.-C. (1996). NDWI: A Normalized Difference Water Index for remote sensing of vegetation liquid water from space. *Remote Sensing of Environment, 58*, 257-266

Gitelson, A.A., Buschmann, C., & Lichtenthaler, H.K. (1999). The Chlorophyll fluorescence ratio F735/F700 as an accurate measure of the chlorophyll content of plants. *Remote Sensing of Environment, 69*, 296-302.

Guerschman, J.P., Hill, M.J., Renzullo, L.J., Barrett, D.J., Marks, A.S., & Botha, E.J. (2009). Estimating fractional cover of photosynthetic vegetation, non-photosynthetic vegetation and bare soil in the Australian tropical savanna region upscaling the EO-1 Hyperion and MODIS sensors. *Remote Sensing of Environment, 113 (5):*, 928-945

Hosking, R. (1990). Grassland Curing Index - a district model that allows forecasting of curing *Mathematical and Computer Modelling, 13*, 73 - 82

Huete, A., & Didan, K. (2004). MODIS seasonal and inter-annual responses of semiarid ecosystems to drought in the Southwest U.S.A. In, *Geoscience and Remote Sensing Symposium* (pp. 1538-1541)

Huete, A.R. (1988). A Soil-Adjusted Vegetation Index (SAVI). *Remote Sensing of Environment, 25*, 295-309

Huete, A.R., Justice, C., & Van Leeuwen, W. (1999). *MODIS Vegetation Index (MOD 13) - algorithm theoretical basis document*. unpublished report: University of Arizona, Arizona

Karnieli, A., Kaufman, Y.J., Remer, L., & Wald, A. (2001). AFRI - aerosol free vegetation index. *Remote Sensing of Environment, 77*, 10-21

Kaufman, Y.J. (1982). Solution of the equation of radiative-transfer for remote sensing over nonuniform surface reflectivity. *Journal of Geophysical Research-Oceans and Atmospheres, 87*, 4137-4147

Levy, E.B., & Madden, E.A. (1933). The point method of pasture analysis. *New England Journal of Agriculture, 46*, 267-279

Lu, H., Raupach, M.R., McVicar, T.R., & D.J, B. (2003). Decomposition of vegetation cover into woody and herbaceous components using AVHRR NDVI time series. *Remote Sensing of Environment, 86*, 1-18

Luke, R.H., & McArthur, A.G. (1978). *Bushfires in Australia*. ACT: Australian Government Publishing Service

Martin, D.N. (2010). Development of satellite vegetation indices to assess grassland curing across Australia and New Zealand. In, *School of Mathematical and Geospatial Sciences*: RMIT University, Melbourne, Australia

McArthur, A.G. (1966). *Weather and grassland fire behaviour*. unpublished report: leaflet No. 100, Department of National Development, Forestry and Timber Bureau, Forestry Research Institute., Canberra

Millie, S., & Adams, R. (1999). Measures of grassland curing: a comparison of destructive sampling with visual and satellite estimates. In, *Australian Bushfire Conference* (pp. 1-8). Albury: School of Ecology and Environment, Deakin University, Rusden

Paget, M.J., & King, E.A. (2008). MODIS land data sets for the Australian region. *electronic resource* http://www.cmar.csiro.au/e-print/open/2008/Pagetmj_a.pdf, *last accessed* June 3, 2010, CSIRO Marine and Atmospheric Research, Canberra, Australia

Pairman, D., Barnes, E.J., & Fogarty, L.G. (1995). Initial evaluation of satellite derived NDVI to estimate the degree of curing and composite fuel moisture content in grasslands. *NZ FRI Project Record, 4805*

Pairman, D., Fogarty, L.G., & Barnes, E.J. (1996). Estimating fire danger parameters in New Zealand using NDVI. *NZ FRI Project Record 5291 (unpublished report): New Zealand Forest Research Institute, Rotorua.*

Paltridge, G.W., & Barber, J. (1988). Monitoring grassland dryness and fire potential in Australia with NOAA/AVHRR data. *Remote Sensing of Environment, 25*, 381-394

Paltridge, G.W., & Mitchell, R.M. (1990). Atmospheric and viewing angle correction of vegetation indices and grassland fuel moisture content derived from NOAA/AVHRR. *Remote Sensing of Environment, 31*, 121-135

Qi, J., Chehbouni, A., Huete, A.R., Kerr, Y.H., & Sorooshian, S. (1994). A Modified Soil Adjusted Vegetation Index. *Remote Sensing of Environment, 48*, 119-126

Rouse, J.W., Haas, R.W., Schell, J.A., & Deering, D.H. (1973). *Monitoring vegetation systems in the great plains with ERTS. Third ERTS Symposium, NASA SP-351, Vol. 1*. unpublished report

Sebastián López, A.S., San-Miguel-Ayanz, J., & Burgan, R.E. (2002). Integration of satellite sensor data, fuel type maps and meteorological observations for evaluation of forest fire risk at the pan-European scale. *International Journal of Remote Sensing, 23*, 2713–2719

Sims, D.A., & Gamon, J.A. (2002). Relationships between leaf pigment content and spectral reflectance across a wide range of species, leaf structure and development stages. *Remote Sensing of Environment, 81*, 337-354

Stocks, B.J., Lawson, B.D., Alexander, M.E., Van Wagner, C.E., McAlpine, R.S., Lynham, T.J., & Dube, D.E. (1989). Canadian Forest Fire Danger Rating System: an overview. *Forestry Chronicle, 65*, 258-265

Tolhurst, K., Shields, B., & Chong, D. (2008). Phoenix: development and application of a bushfire risk management tool. *Australian Journal of Emergency Management, The, 23*, 47

Viovy, N., Arino, O., & Belward, A.S. (1992). The Best Index Slope Extraction (BISE): A method for reducing noise in NDVI time-series. *International Journal of Remote Sensing, 13*, 1585-1590

Wotton, B.M., Alexander, M.E., Taylor, S.W., & Great Lakes Forestry, C. (2009). *Updates and Revisions to the 1992 Canadian Forest Fire Behavior Prediction System*: Information Report GLC-X-10 Great Lakes Forestry Centre, Sault Ste. Marie, Ontario

Yebra, M., Chuvieco, E., & Riano, D. (2008). Estimation of live fuel moisture content from MODIS images for fire risk assessment. *Agricultural and Forest Meteorology 148*, 523-536

APPENDIX A - FORMULAE FOR VEGETATION INDICES

The following vegetation indices were used in the analysis described in Section 0. Indices without references were created in the course of the research reported here. Averaging is denoted by μ such that $\mu(R_1,R_2)$ is the average of band 1 and 2. In the original development of WDVI, A is the slope of the soil line, but here A is the slope of the linear regression of R_2 on R_1.

Vegetation Index	Reference
$NDVI = \frac{R_2 - R_1}{R_2 + R_1}$	(Rouse et al., 1973)
$SAVI = \frac{R_2 - R_1}{R_2 + R_1 + L}(1+L)$, where L = 0.5	(Huete, 1988)
$WDVI = R_2 - A(R_1)$	after Qi et al. (1994)
$AFVI(6) = \frac{R_2 - 0.5R_6}{R_2 + 0.5R_6}$	after Karnieli et al. (2001)
$AFVI(7) = \frac{R_2 - 0.5R_7}{R_2 + 0.5R_7}$	
$EVI = 2.5\left(\frac{R_2 - R_1}{R_2 + 6(R_1) - 7.5(R_3) + 1}\right)$	(Huete et al., 1999)
$GNDVI = \frac{R_2 - R_4}{R_2 + R_4}$	(Gitelson et al., 1999)
$mNDVI = \frac{R_2 - R_1}{R_2 + R_1 - 2R_3}$	(Sims and Gamon, 2002)
$NDWI(5) = \frac{R_2 - R_5}{R_2 + R_5}$	(Gao, 1996)
$NDWI(6) = \frac{R_2 - R_6}{R_2 + R_6}$	(Chen et al., 2005)
$NDWI(7) = \frac{R_2 - R_7}{R_2 + R_7}$	(Chen et al., 2005; Huete and Didan, 2004)
$GVMI = \frac{(R_2 + 0.1) - (R_6 + 0.02)}{(R_2 + 0.1) + (R_6 + 0.02)}$	(Ceccato et al., 2002)
$BNDVI = \frac{R_2 - R_3}{R_2 + R_3}$	
$VI(172) = \frac{R_1 + R_7 - R_2}{R_1 - R_7 - R_2}$	

$VI(152) = \frac{R_1 + R_5 - R_2}{R_1 - R_5 - R_2}$	
$\text{mNDWI}(56) = \frac{R_2 - \mu(R_5, R_6)}{R_2 + \mu(R_5, R_6)}$	
$\text{mNDWI}(67) = \frac{R_2 - \mu(R_6, R_7)}{R_2 + \mu(R_6, R_7)}$	
$\text{mNDWI}(567) = \frac{R_2 - \mu(R_5, R_6, R_7)}{R_2 + \mu(R_5, R_6, R_7)}$	
$mNDVI(15) = \frac{R_2 - \mu(R_1, R_5)}{R_2 + \mu(R_1, R_5)}$	
$mNDVI(16) = \frac{R_2 - \mu(R_1, R_6)}{R_2 + \mu(R_1, R_6)}$	
$mNDVI(17) = \frac{R_2 - \mu(R_1, R_7)}{R_2 + \mu(R_1, R_7)}$	
$mGNDVI(45) = \frac{R_2 - \mu(R_4, R_5)}{R_2 + \mu(R_4, R_5)}$	
$mGNDVI(46) = \frac{R_2 - \mu(R_4, R_6)}{R_2 + \mu(R_4, R_6)}$	
$mGNDVI(47) = \frac{R_2 - \mu(R_4, R_7)}{R_2 + \mu(R_4, R_7)}$	
$mGNDVI(467) = \frac{R_2 - \mu(R_4, R_6, R_7)}{R_2 + \mu(R_4, R_6, R_7)}$	

APPENDIX B - FIELD ASSESSMENT METHODOLOGY

Carry out Levy Rod assessment and fuel moisture collection at a minimum frequency of once per fortnight for each site.

Site selection criteria

Sites selected for assessment should meet the following criteria:

- Level terrain.
- Continuous cover of grass fuels (as far as is practically possible).
- Sites should be no smaller than 500m x 500m. Homogenous areas of sites where data is to be used for remote sensing applications should be as large as possible since the satellite image has a 1km x 1km pixel size (ideally a 3km x 3km area should be used if at all possible). Alternatively, ensure that the area is as large as possible and consists mainly of grass cover (i.e. a minimum of trees, shrubs, roads, waterways, etc.).
- Sites should not be irrigated.

Assessment procedure

1. The sampling area should consist of two 20 or 50[1] metre transects, laid out at right angles to each other. This distance may be simply paced out whilst sampling, or the end-points of the transects may be permanently marked with pegs/stakes (depending on the location). Ensure the transects are located at least 15m away from roadsides or other breaks in the grass fuel cover, and in areas generally representative of the surrounding grasslands.
2. Complete the first (relevant) sections of the field sampling cover sheet, including taking Kestrel weather readings prior to the start of sampling.
3. Using a digital camera, take 1 photograph of the general sampling area. Include a whiteboard with location, date and time displayed in the photograph. Try to avoid excessive glare from the sun on the board.
4. At the first metre/pace mark of the first transect, strike the Levy Rod vertically into the earth, ensuring that the sample area is not compromised (trampled) by the observer. Ideally the observer should always walk on one side of the transect/measuring tape and strike the Levy Rod in the opposite side.
5. Count the number of touches of live and dead vegetation on the rod separately. Start at the top of the rod and work your way down the rod. To be counted, the vegetation MUST be touching the rod. Tally all of the live and all of the dead touches from the top to the bottom of the rod[2]. If thick and dense thatch is present, count down as far as is practically possible. Record this tally of live and dead touches on the Levy Rod Field Sheet.
6. Move to the following metre/pace interval and repeat the process, continuing for the length of each transect.
7. At a minimum of three points along transects take a downward-looking digital image. The image should look straight down onto the grass fuels, and include a ruler for scale. Refer to the sheet "Guidelines for downward-looking digital photographs". If combined fuel moisture samples are collected, take downward-looking digital images of the area to be sampled.
8. Collect a total of 10 fuel moisture samples from within the general sampling area: 5 dead grass only, and 5 combined (live and dead grass mixed). Refer to the fuel moisture content sampling methodology sheet.
9. Using a digital camera, take a second photograph of the general sampling area. Make sure the grass sampling board (or a whiteboard with location, date and time displayed) is included in the photograph.
10. Complete the remaining sections of the field sampling cover sheet, including repeating kestrel weather readings following the completion of sampling.
11. Refer to the fuel moisture content methodology sheet for fuel moisture sample processing and data entry instructions.
12. Enter Levy Rod tallies into the spreadsheet, which will automatically calculate curing percentage.
13. Periodically (2-3 times during the season) additional destructive samples will be collected to allow validation of Levy Rod curing assessment rather than fuel moisture assessment. Refer to the destructive sampling methodology field sheet for instructions.
14. Download digital photographs and label and archive accordingly.

[1] Length of transect will depend on grassland type, and will be determined at the time of assessing the area.
[2] In most cases, it will be easy to distinguish whether a blade of grass touching the rod is live or dead. However, in some instances, part of the grass blade or sheath may be dead and the remainder live. In this case, record exactly what is touching the Levy Rod.

Important

- It is important that the Levy Rod is as close to perpendicular with the earth as possible to ensure an accurate representation of the vertical profile of the grass.
- When driving the Levy Rod into the ground at the sample points, the operator should not directly look at the area to be sampled. This eliminates operator bias.
- Transects can either be fixed (marked out permanently) or paced out on each sampling occasion.
- To avoid trampling the site during repeated sampling sessions, the transects can be rotated through 30° around a fixed point on consecutive sampling runs (e.g. the first transects can be laid out at compass bearings 0° and 90° the next fortnight, the transects can be laid out at compass bearings 30° and 120° etc.)

Equipment:

- Levy rod: a steel rod 1.3 metres in height, 3.5mm – 5mm in diameter, with the tip fashioned into a point. A handle may be mounted to allow ease in operational use.
- Booking sheets, including:
  - Grass Curing Field Sampling Cover Sheet
  - Grass Curing Field Sampling – Levy Rod Field Sheet
  - Fuel moisture content sampling methodology sheet (see Anderson et al., 2005)
  - Guidelines for downward-looking digital photographs (see Anderson et al., 2005)
- Small sampling tins x 10 (if sampling combined- and dead fuel moisture content)
- Tape (30-50m length)
- Grass shears/secateurs
- Digital camera
- Ruler
- Grass sampling field board/whiteboard and erasable marker pen
- Permanent marker pen
- CFA curing guide
- Kestrel or psychrometer for weather observations (if available)

GRASS CURING FIELD SAMPLING

COVER SHEET

LOCATION: **DATE:**

OBSERVERS: **START TIME:**

FINISH TIME:

Weather (Kestrel)		
	Start	Finish
Time Temp RH Wind speed		

Visual estimation of grass curing along transect:

Comments:

Pasture Type (circle one)

Cultivated	Improved pasture	Native grass

Fuel Condition (circle one)

Ungrazed	Grazed	Eaten out

Growth Phase (circle one)

Flowering	Curing	Fully cured	New growth

Sampling details

Method	**Y/N**	**Comments**
Levy rod		
Fuel moisture		
Destructive		
Other		

Average grass height:

Comments:

(grass species present, soil type, grazing, etc.)

Photography

2 x overview photographs (1 at start, 1 at end)	
3 x downward-looking photos from transects	

bushfire CRC

GRASS CURING FIELD SAMPLING – LEVY ROD SHEET

Assessors: _____ **Date:** _____

Location: _____

	1	2	3	4	5	6	7	8	9	10	11	12	13	14	15	16	17	18	19	20
TOTAL LIVE																				
TOTAL DEAD																				

GRASS CURING FIELD SAMPLING – LEVY ROD SHEET

Assessors: _____ **Date:** _____

Location: _____

	1	2	3	4	5	6	7	8	9	10	11	12	13	14	15	16	17	18	19	20
TOTAL LIVE																				
TOTAL DEAD																				